DISSERTATION

APPLICATIONS OF LC-QQQ FOR QUANTIFICATION OF SMALL MOLECULES IN BIOLOGICAL MEDIA

Submitted by

Madeline Christine Roach Schwarz

Department of Chemistry

In partial fulfillment of the requirements

For the Degree of Doctor of Philosophy

Colorado State University

Fort Collins, Colorado

Spring 2025

Doctoral Committee:

Advisor: Melissa Reynolds

Alan Van Orden
Jean Chung
Sue VandeWoude

ABSTRACT

APPLICATIONS OF LC-QQQ FOR QUANTIFICATION OF SMALL MOLECULES IN BIOLOGICAL MEDIA

Liquid chromatography triple quadrupole mass spectrometry (LC-QQQ) is a popular instrumental technique with rising popularity in research and clinical laboratories. LC-QQQ allows for high analytical specificity due to specific biomarker detection, along with high analytical sensitivity due to the trace amounts of substances being accurately quantified. Due to these specific advantages, LC-QQQ is gaining popularity for clinical diagnoses to determine the extent of an infection or disease, leading to better informed treatment, or to determine the metabolic rate at which a drug moves through the body. Small molecules (<1000 Daltons) can be used as biomarkers for both clinical diagnosis and metabolomic studies and are detected at extremely low levels using LC-QQQ. This work endeavors to utilize LC-QQQ for two primary applications: first, for the detection of a biomarker for the purposes of diagnosing pulmonary fungal infections, second, for the detection of cannabinoids in plasma during their metabolism.

Pulmonary fungal infections such as invasive pulmonary aspergillosis (IPA) have increased in incidence over the last decade due to the increased number of immunocompromised individuals. This increase is especially problematic when considering mortality rates associated with IPA are upwards of 70%. This mortality rate, in part, is due to the length of time it takes to diagnose a patient with IPA. When diagnosed early, mortality rates of IPA decrease by as much as 30%. Chapter 1 discusses current technologies employed in both medical and research laboratories to diagnose IIPA, including culture, imaging, polymerase chain reaction, peptide

nucleic acid-fluorescence *in situ* hybridization, enzyme-linked immunosorbent assay, lateral flow assay, and liquid chromatography mass spectrometry. For each technique, Chapter 1 discusses both promising results and potential areas for improvement with each technique, paying special attention to liquid chromatography mass spectrometry as a potential diagnostic method.

Due to the demonstrated need for diagnostic methods that decrease time-to-diagnosis for IPA, Chapter 2 discusses the development and implementation of a method for the quantification for low levels of glucosamine from *Aspergillus* species using LC-QQQ. The limit of detection in the final method used on samples of *Aspergillus* was calculated to be 0.020 ± 0.001, with a limit of quantification of 0.061 ± 0.004 ng/mL. The method described in Chapter 2 also has a high internal repeatability ($R^2 = 0.9996$) and does not require a derivatization step for specificity. This allows for ease of translation to a clinical setting. The method was applied to several pathogenic species of *Aspergillus*, including *Aspergillus fumigatus*, which causes more than 90% of cases of IPA.

Due to the reduced sample prep and run time, high analytical sensitivity, and high specificity the developed glucosamine detection method discussed in Chapter 2 was applied to samples of biological media relevant to clinical diagnosis of IPA in Chapter 3. Artificial sputum medium and artificial bronchioalveolar lavage fluid were used to determine the matrix effects of clinical samples on the developed method. The FDA's bioanalytical method development standards were applied, and it was determined that the artificial media cause extremely strong and inconsistent matrix effects. Separation methods were also tested to remove the glucosamine from the artificial media but were unsuccessful. These results show that the method requires further validation before it can be implemented on clinical samples.

Chapter 4 delves into a method to detect CBD, Δ^9-tetrahydrocannabinol, and their major metabolites using LC-QQQ. Cannabinoids and their metabolites are of major interest to the medical community due in part to their recent decriminalization. Chapter 4 details the LC-QQQ method developed, as well as the endeavors to account for matrix effects. Several protein precipitation methods were tested in an attempt to reduce sample preparation time and increase throughput. Unfortunately, the separation methods developed did not lead to quality control samples that met FDA standards, so more work is needed before the method can be applied to clinical samples.

While the methods described are not fully realized for clinical sample testing, the research described provides valuable insights into a few areas. First, it is the first work to describe LC-QQQ detection of glucosamine derived from several fungal species. The work also provides insight for future method optimization work. Finally, this work demonstrates the effect that matrices can have on method development and some of the problem-solving steps that are required to bring a method from the research lab to a clinical setting.

ACKNOWLEDGEMENTS

Dr. Melissa Reynolds
Dr. Alan Van Orden
Dr. Jean Chung
Dr. Sue VandeWoude
Dr. Chuck Henry
Dr. Kate McMahon
Dr. Alex Moskaluk
Dr. Josh Daniels
Dr. Chris Allison
The Reynolds Group, past and present
Panacea Life Sciences
My friends and family

DEDICATION

To my husband, Charles:

You are my best friend and the most encouraging partner – thank you for believing in me, celebrating every victory with me, lamenting missed opportunities and failed experiments with me, and listening even when you don't understand what I am saying. I love you – pinkie promise.

To my advisor, Melissa:

Your guidance and encouragement have been invaluable during my work. Thank you for everything – I could not have asked for a more personable and caring advisor.

To my sister, Ava:

Thank you for reminding me to laugh through everything with a continuous supply of memes, funny videos, and bad jokes.

To the gal pals:

Thank you for encouraging texts, brunches, hangouts, shared highs and lows, and constant reminders that it is okay to be human.

And to my parents, Mia and Joe:

Thanks for always believing in me and pushing me to strive for my best in all my endeavors. Mom - you can stop nagging me about writing now.

TABLE OF CONTENTS

CHAPTER 1[1]

Introduction

1.1 *Aspergillus*

Humans are exposed to fungal spores daily. Globally, the average abundance of spores in the air ranges between 10^3 – 10^4 spores per cubic meter.[1] Infections from airborne fungal spores mainly occur invasively.[2] Despite their low occurrence rates, a study performed in 2017 estimated that fungal infections result in the death of more than 1.5 million people per year. This is similar in scale to the mortality rate of tuberculosis, and three times greater than malaria.[3] One common disease-causing genus of fungi is *Aspergillus*. *Aspergillus* is often associated with spoilage and mycotoxin production in food, but also a cause of an array of infectious and allergic human and animal diseases.[4] In this review, we discuss *Aspergillus* including associated human diseases and diagnostic techniques available, with a focus on diagnosis of pulmonary aspergillosis.

1.1.1 Morphology and Growth of Aspergillus

Aspergillus belongs to the *Trichocomaceae* family under the order Eurotiales and phylum Ascomycota. The genus *Aspergillus* contains more than 250 species grouped into eight subgenera and species complexes.[5] The subgenera include *Aspergillus*, *Circumdati, Cremei, Fumigati, Nidulantes*, and *Polypaecilum*.[6] Important and medically relevant species complexes include *Aspergillus fumigatus, Aspergillus flavus, Aspergillus terreus, Aspergillus niger, Aspergillus nidulellus,* and *Aspergillus ustus*.[5] *Aspergillus* was first described in 1729 by Micheli

[1] Chapter 1 sections 1-3 are adapted from a manuscript published in the *Journal of Fungi* with coauthors Alex E. Moskaluk, Joshua B. Daniels, Sue VandeWoude, and Melissa M. Reynolds. doi: 10.3390/jof10120829

who named it for the brush used for sprinkling holy water in churches.[5,7] Aspergillosis, the name for the invasive infection by *Aspergillus* species, was first described by Reaumur in 1749 in birds. The pathogenic *Aspergillus candidus* was detected in an air sac lesion of a bullfinch by Rayer and Montagene in 1842.[5] The first time "Aspergillosis" was used to describe a respiratory disease was in 1863 when *A. fumigatus* was detected in the lung of a great bustard.[5] The first description of a human disease caused by *Aspergillus sp.* was recorded by Sluyter in 1847.[7]

Aspergillus is a widespread fungal genus that has both pathogenic and beneficial species. It is commonly found in soil, air, water, in vegetables, and in feed as saprophytes.[5,8] Due to its concentration in air (between 0.2 and 15 conidia/m^3 and up to 10^7 conidia/m^3 in some settings), *Aspergillus* can be considered a common laboratory contaminant.[5] Some species can be identified based on their microscopic morphological appearances. Generally, and as shown in Figure 1.1, its mycelia are composed of septate hyphae with dichotomous branching. The primary branch that originates from the vegetative portion of the thallus is called the "foot cell". This is branched into conidiophores that contain flask-shaped vesicles. The part of the vesicle positioned away from the connecting point (distal half) is covered with a single series of phialide that arrange upwards paralleling the axis of the conidiophore. Asexual spores originate from these phialides. In tissue samples, only the mycelia are observed, while conidiophores are found in body cavities that contain air.[5]

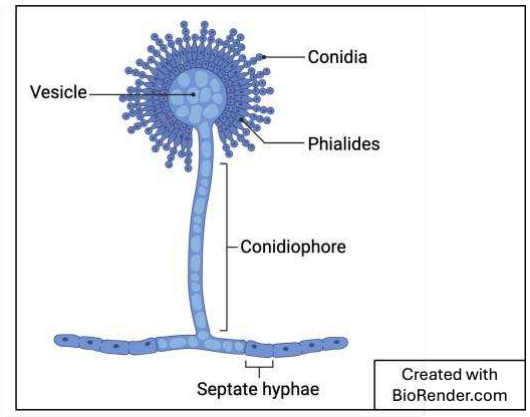

Figure 1.1: Generic structure of *Aspergillus* species

Aspergillus can be isolated on Sabouraud dextrose agar (SDA) or Czapek Dox agar (CDA), among others, to observe visual characteristics between the major human pathogens.[5,9] *A. fumigatus* colonies are a white cottony mold, which becomes velvety or granular with green coloration after several days. *A. niger* colonies are white in color when they begin to grow, but later become black as growth continues. *A. terreus* colonies start white as well, but later become cinnamon-colored with a "sugary texture".[5] *A. flavus* has spreading yellow-green colonies that have phialides over their entire surface, while *A. nidulans* has a brown pigment that helps it blend in with the soil where it commonly grows.[9]

1.1.2 Diseases caused by Aspergillus Species

Aspergillus species are associated with a spectrum of respiratory diseases in both humans and animals, affecting areas including nasal cavities, sinuses, airways, and lung tissues and cavities. The diseases associated with *Aspergillus* range from allergy of variable severity to invasive infections with high mortality rates in humans.[10] Rates of infection and mortality are elevated in immunocompromised individuals and patients on immunosuppressive therapies.[11-13] *Aspergillus*-induced diseases can be broadly classified according to their characteristics: chronic

colonization, allergic diseases, and systemic diseases. It is important to note, however, that any given clinical condition may fall into two or more classifications, rather than just one.[7,9]

1.1.2.1 Chronic Colonization

Chronic colonizations are broadly classified as fungal infections that do not cause tissue damage, meaning they grow inside the body but do not directly damage tissue. Bronchopulmonary colonization refers to the infestation of airways, but without invasion of tissue. In its most uncomplicated form, this colonization is not technically an infection. However, chronic colonization has been shown to have a high incidence in patients with other pulmonary infections such as chronic bronchitis, primary ciliary dyskinesia syndrome, and cystic fibrosis. Some patients suffer from adverse immune system effects from *Aspergillus* antigens, such as skin reactivity.[7]

An *Aspergillus*-specific chronic colonization is called an aspergilloma. Also known as a fungus ball, aspergillomas are proliferations of the fungus in a poorly drained lung space. If an intrathoracic cavity communicates with the bronchial tree and does not drain, it can become colonized by an *Aspergillus* species and the colony can grow for months or years. Patients who have contracted pulmonary tuberculosis with healed cavities and chronic pulmonary sarcoidosis with cystic spaces are prime breeding grounds for fungal balls.[7,9,10]

1.1.2.2 Allergic Disease

Aspergillus species can also contribute to a variety of allergic diseases including allergic asthma, allergic rhinitis, allergic sinusitis, extrinsic allergic alveolitis (also called hypersensitivity pneumonitis (HP)), and allergic bronchopulmonary aspergillosis (ABPA). Most allergic airway diseases are managed in general practice and testing for fungus as an etiology is not common until the disease progresses.[14]

Allergic asthma induced by fungal spores is characterized by higher responsiveness of the tracheobronchial tree to stimuli, potentially causing chronic respiratory symptoms of variable severity, that can lead to patients requiring corticosteroids.[14] Interestingly, corticosteroid administration can be a contributing factor for fungal infections in immunocompromised individuals.[15] Patients with mold sensitivities, like those with compromised immune systems, develop asthma slowly but persistently and have other symptoms similar to a cold followed by coughing and wheezing.[7,10]

Allergic rhinitis describes a nasal allergy and is commonly called hay fever. This condition develops because of interactions of allergens, like molds, with immunoglobulin E antibodies on the nasal mucosa epithelium.[7,10]

Allergic sinusitis, or sinus disease, includes fungal ball production and allergic fungal sinusitis. The fungal balls produced differ considerably from aspergillomas as the fungus does not invade tissues, but chronically affects multiple sinuses.[7,10]

HP is caused by the exposure to multiple organisms by inhalation. *Aspergillus* species are commonly associated with HP. If chronic HP goes untreated, it can cause irreversible lung damage. Continuous exposure to the antigen causing HP can result in an intense inflammatory reaction in the lungs.[7,10]

ABPA is one of the most commonly contracted diseases associated with *Aspergillus*, usually by asthmatic patients in the hospital and rhinitis and/or cystic fibrosis patients. ABPA is the result of hypersensitivity to *Aspergillus* antigens in patients with long-standing asthma triggered by an allergen. While ABPA begins as an easily reversible asthmatic syndrome, it can progress to a more difficult-to-manage asthmatic state with any substance denser than air, such as spores from *Aspergillus*, lingering in the parenchyma of the lungs. A strong sensitivity to the

antigen produced by the body when *Aspergillus* is present can also develop, leading to a diagnosis of ABPA.[7,10]

1.1.2.3 Systemic Diseases

The final classification for conditions caused by *Aspergillus* species is systemic dis-eases. Invasive pulmonary aspergillosis (IPA) is primarily an infection of immunocompromised patients but can also occur in patients with chronic diseases like diabetes and some cancers or as a postoperative complication. IPA can also evolve to a superinfection following antibiotic therapy.[7,8,16,17] In the last decades, the incidence of IPA has increased due to an upsurge of immunocompromised patients.[18] IPA also has an associated mortality rate of 70% if diagnosis is delayed, making it the deadliest form of disease caused by *Aspergillus* species.[19,20] However, with early diagnosis, mortality rates for IPA may decrease to as low as 30%.[19] Due to this, the development of fast and accurate detection methods for this disease are vital to improving patient outcomes. Current clinical and proposed laboratory detection methods for IPA along with methods in the research stage will be the focus of the remainder of this chapter.

1.2 Current Detection Methods for Pulmonary Aspergillosis

1.2.1 Clinical Specimens

If a patient is suspected of having a fungal pulmonary infection, several sample types can be collected. The diagnostic standard for IPA is culture of tissue, which is collected using either fine needle aspiration or open biopsy.[10] In the absence of tissue specimens, blood samples may be collected. Fluid samples may also be collected from the lower respiratory tract using a collection technique called bronchoalveolar lavage (BAL).[5,8,21] Other non-sterile samples, like sputum, can also be examined.[8,21-23]

1.2.2 Fungal Culture

The most basic and primary method for diagnosing IPA is fungal culture. Fungal culture has been the standard for detection of IPA since definitions were proposed by the European Organization for the Research and Treatment of Cancer/Mycoses Study group (EORTC/MSG).[24] When taken from a sterile site, a positive culture provides proven diagnosis of IPA.[24,25] Culture allows for species identification and antifungal susceptibility testing to allow for targeted therapy.[24,25]

While culture is the most used and often the first step in diagnosis, it has several limitations. First, it is recommended that samples thought to contain fungus should be cultured for at least 7 days, delaying the time to diagnosis.[22] Culture is also a relatively insensitive method, with positivity rates ranging from 11.8% to 81.0% depending on the study.[20-22,26-30] Cultures also require specialized knowledge and experience to determine the identity of the colonies.[18,30] Growth of *Aspergillus sp.* in culture does not also always equate to a diagnosis of IPA, as the type of clinical sample used and the ubiquity of fungal spores lead to frequent contaminations during sample processing.[16,17,31,32] One of the main benefits of culture is the ability to perform antifungal susceptibility testing if positive for *Aspergillus*, allowing for targeted therapy.

1.2.3 Imaging and Histopathology

Imaging is another common method recognized by the EORTC/MSG that aids in the diagnosis of IPA. Early stages of IPA are often inconspicuous upon conventional thoracic radiography (x-ray), making it a suboptimal diagnostic tool.[33] The most common method of lung imaging for clinical purposes is not x-ray however, it is high-resolution computed tomography (HRCT).[25,34] A prevalent marker for IPA using HRCT is the “halo sign”. IPA is the most common

cause of halo sign in patients at high risk for fungal infections.[8,16-18] Halo sign is not, however, exclusive to IPA, as it can be linked to other infectious agents, bleeding, and leukemic infiltrates.[22,35] Using halo sign as a marker does not afford short time to diagnosis, as it does not appear until the third week of infection.[36] Other signs of IPA using HRCT include air crescent sign, multiple pulmonary nodules, bronchopneumonia, consolidation, cavitation, plural effusions, ground glass opacities, tree-in-bud opacities, and atelectasis. However, these signs are all nonspecific and do not only indicate IPA.[34] For example, tree-in-bud opacities can also be found in *Mycobacterium* infections and other non-infectious conditions.[16,18,22,37] Furthermore, another imaging modality that can be utilized for IPA is Magnetic resonance imaging (MRI). MRI of the lungs is challenging due to the lack of detectable protons in air-filled spaces, so it has received low amounts of attention as a diagnostic imaging tool for IPA.[37] Despite this, studies have been performed to evaluate MRI as a diagnostic tool. One study performed *in vivo* on mice showed that lung lesions due to IPA could be visualized and quantified using MRI.[38] This study, while promising, has not been replicated using human patients, and requires advanced MRI techniques that are not broadly available outside of research settings.

Histopathology of tissue specimens is another diagnostic technique used for IPA, often in tandem with imaging like HRCT.[39-41] The EORTC/MSG guidelines state that a histopathologic examination of sterile material can lead to a confirmed diagnosis of IPA.[25] Signs of IPA infection include areas of tissue necrosis where hyphae are aligned in a radial pattern, fusion of solidified lobules with a necrotic cavity in the center, infarction, and/or embolism.[40] The main drawback of histopathology is the specialized knowledge and experience needed to determine infection.

While culture, imaging, and histopathology are the most common modalities for detection and diagnosis of IPA, all have limitations, primarily that culture and imaging are

relatively insensitive, and that obtaining specimens for histopathology is invasive. More sensitive methods have been developed which decrease the time needed to obtain a diagnosis and are arguably less invasive.

1.2.4 PCR

The polymerase chain reaction (PCR) is a technique used to amplify small segments of DNA. PCR has been used to identify pathogenic fungi in a variety of samples since the late 1990s.[8,16,24] Kappe et. al. (1998) described one of the first techniques using PCR to identify A. fumigatus and A. flavus, among other fungal species, in human tissues. They used a targeted area of 18S rDNA, with primers designed based on sequence conservation among fungi with concurrent dissimilarity to other eukaryotic sequences. This region can be successfully amplified from many medically relevant fungal agents.[43] A study performed by Kawamura et. al. (1999) tested serum samples using an 18S-based nested PCR test. They showed that in comparison to two antibody/antigen assays, the nested PCR was the most sensitive of the three techniques, with a clinical sensitivity of 89% and selectivity of 100%.[44] Kami et. al. (2001) published the first report on the use of an 18S-based quantitative real-time PCR (qPCR) for the diagnosis of IPA.[45] In their work, DNA was extracted from both whole blood and plasma for their testing, as well as DNA from pathogenic fungal species like *A. fumigatus, A. niger, and A. terreus*. The samples were also run using ELISA and (1→3)-β-D-glucan to compare clinical sensitivity and specificity. The qPCR test had the highest clinical sensitivity of the three tests, at 79%, and the highest clinical specificity at 92%.[42] Lower clinical sensitivity reported in Kami et. al. was contributed to false positive results from control patients, and false positives in qPCR occurred more frequently than the other tests in the study.[45] Kami et. al. opined that the false-positives were likely not due to environmental contamination, but rather that "…*Aspergillus*-specific DNA might have existed

in these samples."[45] Since these first tests, numerous studies on qPCR for the diagnosis of IPA have been performed, and several reviews detailing the advancements in the technique have been written.[46-48] Due to these advancements and the extensive studies performed on qPCR for detection of IPA, the EORTC/MSG added qPCR testing as a diagnostic tool for IPA in 2020, along with publishing diagnostic criteria for plasma, serum, whole blood, and BAL fluid.[25] Table 1.1 describes the specificity and sensitivity of various PCR assays summarized in White et. al. (2015).[46]

Table 1.1: Sensitivity and Specificity of Aspergillus PCR assays [46]

Author	Sample type	Clinical Sensitivity	Clinical Specificity
Tuon[49]	BAL fluid	78.4%	93.7%
Sun[50]	BAL fluid	79.6%	94.1%
Avni[51]	BAL fluid	76.8%	94.5%
Mengoli[52]	Blood	88.0%	75.0%
Arvanitis[53]	Blood	84.0%	76.0%

Despite being added as a viable technique for diagnosis of IPA, there are still limitations to PCR and qPCR. There is a high diversity of PCR assays, leading to a lack of protocol standardization. This was the largest factor that limited the use of the technique in hospital routines.[54] The diversity in assays comes from the primers, the amount of sample that needs to be analyzed, and whether the assay performs basic PCR or qPCR. The method of DNA extraction is also a factor in the performance of the assays. Another limitation to qPCR is the signal produced by active infections. Signal produced in active infections also falls within the range for signals attributed to antifungal therapy in both experimental models and clinical contexts.[45] Antifungal

agents used for therapies in patients could account for some of the false-negative qPCR results reported.[30] To combat the assay diversity, false negatives, and quantitative issues with qPCR, more work needs to be done to improve the technique.

2.5 ELISA

Enzyme-linked immunosorbent assay (ELISA) is an assay technique designed to detect and quantify a soluble substance, such as peptides, proteins, antibodies, or antigens. Specifically, when the target of an ELISA is an antigen, the test is known as a biomarker assay. Galactomannan is a heat-stable heteropolysaccharide that is present in *Aspergillus sp*. cell walls.[30] Heteropolysaccharides are polysaccharides that contain two or more different monosaccharide units.[55] Detection for galactomannan molecules is achieved using a sandwich ELISA, shown in Figure 1.2, which is possible due to the multiple immunoreactive sites where antibodies can attach on a single molecule. The EORTC/MGS has determined that the PlateliaTM assay (Bio-Rad Laboratories, Marnes-la-coquette, France)[56], and other commercially available assays used to detect galactomannan (GM tests), are acceptable tools for diagnosis of IPA and have published diagnostic criteria for serum, plasma, BAL fluid, and cerebral spinal fluid.[25] GM tests are often used in conjunction with PCR to diagnose IPA. GM tests have a lower specificity than expected, ranging from 85-96%.[57-59] This is likely due to some form of cross reactivity in the ELISA, but it is unclear whether the lowered specificity comes from exogeneous galactomannan or other molecules that also react with the antibody used. The clinical sensitivity of galactomannan ELISA is variable, with a range of 29-100%.[8,30,44,57-59] The variability reported for fungal ELISA could be due to a variety of factors, including the patient group, antifungal therapy, and differences in sampling strategies. Studies show that the sensitivity for detection in profoundly immunocompromised patients is in excess of 90%, while in other settings (such as

patients undergoing antifungal therapy) sensitivity is lower. Finally, there has been no optimal sampling strategy defined for the detection of IPA which could affect the clinical sensitivity of the technique.

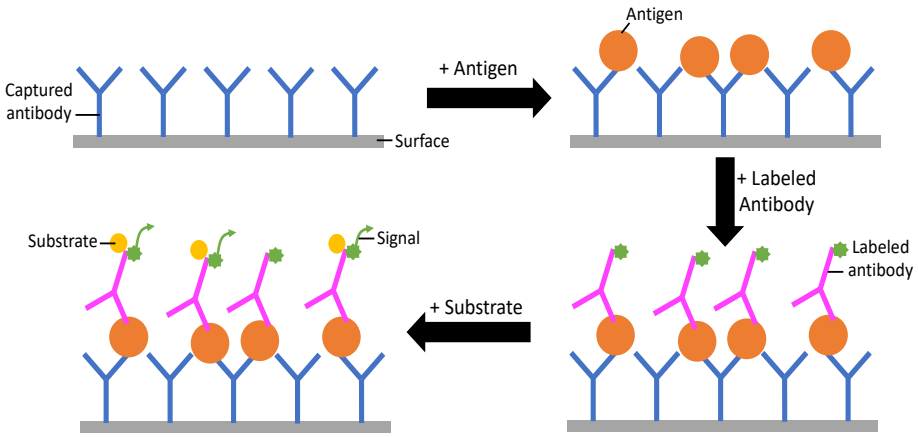

Figure 1.2: General scheme for sandwich ELISA signal detections – an antigen is added to an antibody captured on the surface of the ELISA. Then, a labeled antibody is added. When the molecule of interest (substrate) is added to the labeled antibody, a signal is produced.

2.6 Peptide Nucleic Acid-Fluorescence in situ hybridization (PNA-FISH)

Fluorescence in situ hybridization (FISH) is a molecular technique that uses single-cell identification to detect microorganisms rapidly and directly in environmental and medical samples.[60,61] FISH can be divided into four main steps, shown in Figure 1.3: fixation and permeabilization of the sample, hybridization of the target RNA with the fluorescent probe, a washing step where unhybridized probes are washed from the sample, and detection of the target sequence using epifluorescence microscopy.[60,62] Synthetic nucleic acid mimics (NAMs) have been developed for clinical samples using a peptide nucleic acid (PNA). In PNAs, the negatively charged sugar-phosphate backbone of DNA is replaced by a neutral polyamide backbone. PNA molecules are also neutral, leading to no electrostatic repulsion between the PNA and the negatively charged sugar phosphate backbone of the target molecule. This allows a stronger bond to the target sequence, and greater thermal stability of PNA/DNA duplexes when compared to

DNA/DNA or DNA/RNA duplexes.[60] PNA-FISH protocols are relatively short (60-90 minute time-to-result), no pre-treatment of the sample is required, and it is not necessary to extract DNA from the sample. This method also allows identification at the genus and species level.[63,64] The main limitation of PNA-FISH is the requirement of an organism concentration minimum between 10^2 and 10^5 colony-forming units/mL for detection.[63] These levels are much higher than expected at the early stages of IPA infection. Other microbiota in the sample may also exhibit autofluorescence, which decreases the signal-to-noise ratio and can mask some fluorescent signals.[18]

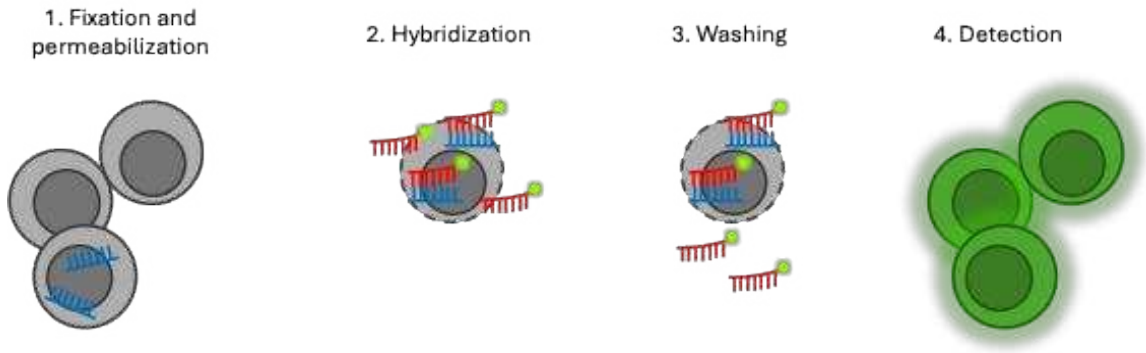

Figure 1.3: General schematic for PNA-FISH. First, the cell undergoes permeabilization and the RNA is fixated. Second, the target RNA is hybridized with the PNA probe. Third, excess probes are washed from the cells. Finally, the cells are detected using epifluorescence microscopy.

PNA-FISH was first developed to test for filamentous fungi, including *Aspergillus niger* in 2004.[65] In 2020, a kit was developed by Biomode 2, SA in Portugal and tested on a variety of clinical samples using PNA-FISH to detect *Aspergillus fumigatus*.[63] Reported total time-to-result were approximately 25.5 hours for clinical samples (including the 24-hour pre-enrichment step) with a specificity of 100%. With a clinical sensitivity of 79%, a lingering challenge with this technique is the persistence of false negative results.[63] PNA-FISH also relies on specialized microscopy, epifluorescence microscopy, that requires not only specialty equipment but also

expert visualization. PNA-FISH is currently not used in medical laboratories due to these issues, but with further testing shows promise as a detection method for IPA.

2.7 Lateral Flow Assays

Lateral flow assays (LFAs) are paper-based tests used widely in hospitals, physician's offices, and clinical laboratories. A variety of sample types can be tested using LFAs including urine, saliva, sweat, blood, and other fluids. LFAs are good candidates for new assays due to their low cost of production, ease-of-use, and rapid time to results, which can be as quick as 15 minutes.[31,66] *Aspergillus*-specific LFAs are a relatively new technology. One assay, developed by the University of Exeter, uses the monoclonal antibody JF5 to bind to a protein epitope present on an antigen secreted during the active growth of *A. fumigatus*.[31] Other LFAs, such as ELISA biomarker assays, target a specific antigen like galactomannan. As shown in Table 1.2, early trials and studies show a wide variety of sensitivity and selectivity.[67] The effectiveness of LFAs, to date, in clinical diagnosis is still limited, however, and more testing is needed on current assays.

Table 1.2: Selectivity and sensitivity of several LFAs published in literature

Company	Sample Type	Clinical Sensitivity	Clinical Specificity
OLM Diagnostics AspLFD	Serum[68]	68%	87%
	BAL fluid[31,68]	86-88%	93-95%
IMMY sona *Aspergillus* galactomannan LFD	Serum[69-71]	50-97%	83-92%
	BAL fluid[72]	77-92%	97-98%
Aspergillus ICT	Serum[73]	67.6%	81%

1.2.8 HPLC and Mass Spectrometry

HPLC coupled to a fluorescence detector (HPLC-DAD) has been used to detect aflatoxin B1 and ochratoxin A residues in *Aspergillus flavus* and *Aspergillus ochraceus* in processed beef meat samples.[74] While this study was performed in the food safety sphere and not in medical

diagnosis, it shows that HPLC-DAD can be used to target molecules produced by *Aspergillus* species for the purposes of detecting infections. The HPLC-DAD technique was only able to detect and quantify aflatoxin B1 in 15% of samples, and ochratoxin A in 10% of samples. This could be because only 50% of *A. flavus* strains produce aflatoxin B1, and the amount of ochratoxin A produced by these strains is variable.[74,75] In short, HPLC-DAD is limited by the analytes currently being targeted; only 50% of strains produce the target analytes. When coupled to alternate detectors, however, HPLC can be a powerful tool for detection of *Aspergillus* species.

Combination HPLC and mass spectrometry (LC-MS) allows for high analytical specificity and sensitivity. LC-MS, and its tandem mass spectrometry counterpart (LC-MSMS), is a rising technology in clinical laboratories for a variety of analyses.[75-83] A general schematic for LC-MS is shown in Figure 1.4. LC-MS provides shorter runtimes than immunoassays, eases workflow, and is significantly lower in cost than other instrumental techniques.[76-79] Allison et. al. (2021) described that mass spectrometry could be utilized as a screening method for fungal infections in clinical settings.[84] The method utilizes acid degradation of chitin, a fungal cell wall component, to its detectable low molecular weight products.[84] One of these products is glucosamine, a commonly studied amino monosaccharide.[85-87] Due to its low molecular weight and abundance in samples of *Aspergillus*, glucosamine has the potential to serve as a biomarker for *Aspergillus* infections.[84,88] Other methods using LC-MS for *Aspergillus* detection target other biomarkers. Compounds like Triacetylfusarine C, a fungal siderophore, and secondary metabolites like gliotoxin, aspergillic acid, spinulosin, among others, have been used as biomarkers for *Aspergillus*.[89-92] LC-MS is a rising technology in clinical laboratories; thus, these methods have great potential for new diagnostic standards in medical labs.[76]

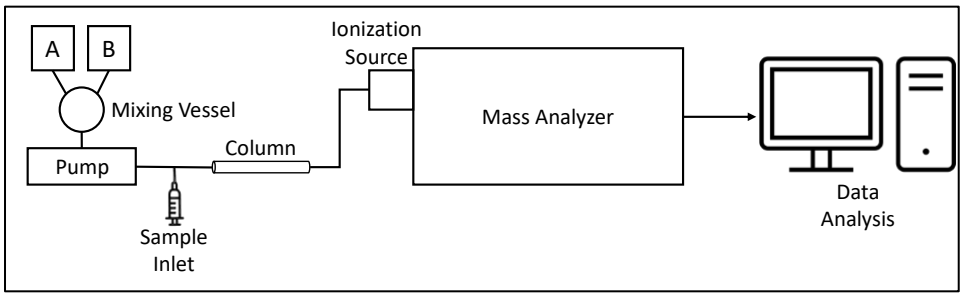

Figure 1.4: General schematic for LC-MS Analysis

One unique aspect of liquid chromatography is the variety of ionization sources that can be used. Soft ionization, a technique developed in the 1980's, allows for the direct analysis of large molecules, including proteins. Soft ionization does not fragment the large molecules into charged particles, but instead creates charged droplets.[93,94] One form of soft ionization is matrix assisted laser desorption ionization-time of flight mass spectrometry (MALDI-TOF MS).[95] MALDI-TOF MS is often used to identify microbes by comparing a characteristic spectrum of an unknown called a peptide mass fingerprint (PMF) to a database. MALDI-TOF MS is now being used to identify *Aspergillus* isolated in culture as well as directly in sample matrices.[16,96-98] With the use of PMF databases, MALDI-TOF MS is also being used to identify distinct species and strains of *Aspergillus*. Methods have been described that use MALDI-TOF MS to detect antifungal medication resistant strains of *Aspergillus fumigatus*.[98] MALDI-TOF MS was also used in another work to identify *Aspergillus* from blood culture. The identification rate was reported at 98.4% accurate.[16,96]

While mass spectrometric methods are promising for clinical applications, like early detection of *Aspergillus* infections, there are limitations that could affect their clinical viability. First, the majority of methods being developed for clinical applications use standard benchtop LC-MS systems, which are highly complex instruments. Benchtop LC-MS systems are large and require technical specialists to operate and maintain. LC-MS results can also vary depending on

the cleanliness of the instrument and its internal components, the sample vessel, and various matrix effects.[77,78,98] Matrix effects are defined as changes in signal due to components of a sample that are not the analyte and are very common in LC-MS methods.[99] Due to these matrix effects, a robustness in method development and validation prior to rollout of a clinical method is required, causing a high barrier to entry for new methods.[98-100] LC-MS is also not currently an automated platform, and when compared to other assays, has a high complexity for a relatively moderate to low throughput. Once LC-MS methods are eventually implemented for clinical use, they tend to boast low detection limits, especially when using LC-MSMS systems, high specificity and sensitivity, and low relative cost.[74-79,93-98,100]

1.3 Conclusions

Many species of *Aspergillus* are opportunistic pathogens of humans and animals. Infections like IPA have been described since ancient times, and in the past 20 years there has been a push for novel, more sensitive diagnostic methods. Currently, culture and imaging are the most common methods for detection of IPA. With these methods, there are many variables that impact the accuracy of diagnosis, including what specimens are cultured, the method of specimen collection, culture media, and stage of infection. Newer promising detection techniques have been developed. While PCR is the most studied alternate detection method, PNA-FISH, ELISA, Lateral Flow Assays, and LC-MS all have shown promise as more sensitive and standardizable techniques in the past 15 years. These techniques also show a decrease in diagnosis time, increasing the odds of survivability from infections like IPA.

LC-MS and its counterparts show particularly high promise as alternate detection methods. LC-MS methods are highly standardizable across labs, relatively low cost to operate,

and allow for high analytical specificity and sensitivity. Identifying biomarkers like glucosamine or Triacetylfusarine C at very low levels, could lead to earlier disease detection and lower mortality rates. Quantitative LC-MS applications using tandem mass spectrometry methods could lead to targeted dosing of antifungal agents, which would likely lead to decreased toxicity events among those undergoing treatment.

With all of the current detection methods in mind, continued investigation into diagnostic assay development for detecting *Aspergillus* is warranted for human patients. Continued investigation will lead to both a greater understanding of *Aspergillus* related diseases, and lower mortality rates from those diseases.

1.4 Dissertation Overview

The first portion of this dissertation aims to further investigate the use of liquid chromatography triple quadrupole mass spectrometry (LC-QQQ) as a detection method for glucosamine derived from fungal chitin, with the purpose that the developed method be applied to clinical samples for the diagnosis of IPA. In chapter 2, development of the LC-QQQ method used for the detection of glucosamine is described. The developed method was optimized for use in the studies described throughout the rest of the dissertation but was also compared to literature methods to demonstrate its comparative ease of use and strength of results. The limits of detection and quantification were discovered and described as well. The developed method was then applied to samples of pathogenic *Aspergillus* species, namely *A. parasiticus, A. nidulans, A. terreus, A. flavus, A niger, and A. fumigatus* to evaluate and compare their glucosamine concentrations after acid degradation. This study shows the validity of the developed method for

various pathogenic species of *Aspergillus* and allows for further exploration of the method as a diagnostic tool for IPA infection.

Chapter 3 describes the use of the method developed in Chapter 2 to detect glucosamine in simulated sputum and BAL fluid. Sputum and BAL fluid are two commonly used sample types for detection of IPA, along with other lung infections, so they are medically relevant to this study. The acid degradation protocol used for fungal samples was applied to the artificial media, and then samples were tested both containing glucosamine and without glucosamine. After initial testing, it was determined that a separation method was needed to extract the glucosamine from the biological media. Solid phase extraction was then applied to standards to evaluate the percent loss due to extraction so accurate quantification could continue. Unfortunately, the chosen solid phase extraction methods lead to a 100% loss of glucosamine from quality control samples. This study, however, warrants further investigation, as discussed in Chapter 5.

Lastly, Chapter 4 explores the development of a method for LC-QQQ to detect cannabinoids and their metabolites in human plasma samples. Cannabinoids are highly medically relevant, and understanding their metabolism and mechanism of action when consumed in varying forms (smoked cannabinoids vs. edibles) is crucial to further our understanding of how they should be regulated and what medical applications they can have. Two major cannabinoids, Δ^9-tetrahydrocannabinol and cannabidiol, along with their major metabolites, 11-hydroxy-Δ^9-tetrahydrocannabinol, 11-nor-9-carboxy-Δ^9-tetrahydrocannabinol, 7-hydroxycannabidiol, and 7-carboxycannabidiol, were selected for LC-QQQ method development and optimization. These compounds were quantified, and their limits of detection determined. Quality control samples were then prepared to quantify the percent loss from plasma samples after protein precipitation, of which two methods were evaluated. Results showed that the first protein precipitation method

employed was unsuccessful with a percent loss of over 50% and very high coefficients of variation. The second method was also unsuccessful, showing high coefficients of variation and high percent loss. This study also warrants further investigation, which is discussed in Chapter 5.

All supporting information is included in Appendices at the end of this dissertation. Appendix I shows the supporting information for Chapter 2, and Appendix II shows the supporting information for Chapter 4.

CHAPTER 1 – REFERENCES

(1) Fröhlich-Nowoisky, J.; Pickersgill, D. A.; Després, V. R.; Pöschl, U. High Diversity of Fungi in Air Particulate Matter. *Proc Natl Acad Sci USA* 2009, 106 (31), 12814–12819. https://doi.org/10.1073/pnas.0811003106.

(2) Veríssimo, C. Aspergillosis. In Environmental Mycology in Public Health: Fungi and Mycotoxins Risk Assessment and Management; Academic Press, 2015; pp 27–34.

(3) Bongomin, F.; Gago, S.; Oladele, R.; Denning, D. Global and Multi-National Prevalence of Fungal Diseases—Estimate Precision. *Journal of Fungi* 2017, 3 (4), 57. https://doi.org/10.3390/jof3040057.

(4) Samson, R. A.; Visagie, C. M.; Houbraken, J.; Hong, S.-B.; Hubka, V.; Klaassen, C. H. W.; Perrone, G.; Seifert, K. A.; Susca, A.; Tanney, J. B.; Varga, J.; Kocsubé, S.; Szigeti, G.; Yaguchi, T.; Frisvad, J. C. Phylogeny, Identification and Nomenclature of the Genus Aspergillus. *Stud Mycol* 2014, 78 (1), 141–173. https://doi.org/10.1016/j.simyco.2014.07.004.

(5) Samanta, I. Cutaneous, Subcutaneous and Systemic Mycology. In *Veterinary Mycology*; Springer India: New Delhi, 2015; pp 32–43. https://doi.org/10.1007/978-81-322-2280-4_4.

(6) Houbraken, J.; Kocsubé, S.; Visagie, C. M.; Yilmaz, N.; Wang, X.-C.; Meijer, M.; Kraak, B.; Hubka, V.; Bensch, K.; Samson, R. A.; Frisvad, J. C. Classification of Aspergillus, Penicillium, Talaromyces and Related Genera (Eurotiales): An Overview of Families, Genera, Subgenera, Sections, Series and Species. *Stud Mycol* 2020, 95, 5–169. https://doi.org/10.1016/j.simyco.2020.05.002.

(7) Kurup, V. P.; Kumar, A. Immunodiagnosis of Aspergillosis. *Clin Microbiol Rev* 1991, 4 (4), 439–456. https://doi.org/10.1128/CMR.4.4.439.

(8) Ledoux, M.-P.; Herbrecht, R. Invasive Pulmonary Aspergillosis. *Journal of Fungi* 2023, 9 (2), 131. https://doi.org/10.3390/jof9020131.

(9) Kidd, S.; Halliday, C.; Alexiou, H.; Ellis, D. Descriptions of Medical Fungi, Third edition.; Published by the Authors, 2016.

(10) About Aspergillosis. Centers for Disease Control and Prevention. https://www.cdc.gov/fungal/diseases/aspergillosis/definition.html (accessed 2024-03-20).

(11) Kontoyiannis, D. P.; Marr, K. A.; Park, B. J.; Alexander, B. D.; Anaissie, E. J.; Walsh, T. J.; Ito, J.; Andes, D. R.; Baddley, J. W.; Brown, J. M.; Brumble, L. M.; Freifeld, A. G.; Hadley, S.; Herwaldt, L. A.; Kauffman, C. A.; Knapp, K.; Lyon, G. M.; Morrison, V. A.; Papanicolaou, G.; Patterson, T. F.; Perl, T. M.; Schuster, M. G.; Walker, R.; Wannemuehler, K. A.; Wingard, J. R.; Chiller, T. M.; Pappas, P. G. Prospective Surveillance for Invasive Fungal Infections in Hematopoietic Stem Cell Transplant Recipients, 2001-2006: Overview of the Transplant-Associated Infection Surveillance Network (TRANSNET) Database. *Clin Infect Dis* 2010, 50 (8), 1091–1100. https://doi.org/10.1086/651263.

(12) Denning, D. W.; Page, I. D.; Chakaya, J.; Jabeen, K.; Jude, C. M.; Cornet, M.; Alastruey-Izquierdo, A.; Bongomin, F.; Bowyer, P.; Chakrabarti, A.; Gago, S.; Guto, J.; Hochhegger, B.; Hoenigl, M.; Irfan, M.; Irurhe, N.; Izumikawa, K.; Kirenga, B.; Manduku, V.; Moazam, S.; Oladele, R. O.; Richardson, M. D.; Tudela, J. L. R.; Rozaliyani, A.; Salzer, H. J. F.; Sawyer, R.; Simukulwa, N. F.; Skrahina, A.; Sriruttan, C.; Setianingrum, F.; Wilopo, B. A. P.; Cole, D. C.; Getahun, H. Case Definition of Chronic Pulmonary

Aspergillosis in Resource-Constrained Settings. *Emerg Infect Dis* 2018, 24 (8). https://doi.org/10.3201/eid2408.171312.

(13) Alastruey-Izquierdo, A.; Cadranel, J.; Flick, H.; Godet, C.; Hennequin, C.; Hoenigl, M.; Kosmidis, C.; Lange, C.; Munteanu, O.; Page, I.; Salzer, H. J. F.; on behalf of CPAnet. Treatment of Chronic Pulmonary Aspergillosis: Current Standards and Future Perspectives. *Respiration* 2018, 96 (2), 159–170. https://doi.org/10.1159/000489474.

(14) Rick, E. M.; Woolnough, K.; Pashley, C. H.; Wardlaw, A. J. Allergic Fungal Airway Disease. *J Investig Allergol Clin Immunol* 2016, 26 (6), 344–354. https://doi.org/10.18176/jiaci.0122.

(15) Li, Z.; Denning, D. W. The Impact of Corticosteroids on the Outcome of Fungal Disease: A Systematic Review and Meta-Analysis. *Curr Fungal Infect Rep* 2023, 17 (1), 54–70. https://doi.org/10.1007/s12281-023-00456-2.

(16) Stemler, J.; Többen, C.; Lass-Flörl, C.; Steinmann, J.; Ackermann, K.; Rath, P.-M.; Simon, M.; Cornely, O. A.; Koehler, P. Diagnosis and Treatment of Invasive Aspergillosis Caused by Non-Fumigatus Aspergillus Spp. *J Fungi (Basel)* 2023, 9 (4). https://doi.org/10.3390/jof9040500.

(17) Barac, A.; Vujovic, A.; Drazic, A.; Stevanovic, G.; Paglietti, B.; Lukic, K.; Stojanovic, M.; Stjepanovic, M. Diagnosis of Chronic Pulmonary Aspergillosis: Clinical, Radiological or Laboratory? *Journal of Fungi* 2023, 9 (11), 1084. https://doi.org/10.3390/jof9111084.

(18) Moura, S.; Cerqueira, L.; Almeida, A. Invasive Pulmonary Aspergillosis: Current Diagnostic Methodologies and a New Molecular Approach. *European Journal of Clinical Microbiology & Infectious Diseases* 2018, 37 (8), 1393–1403. https://doi.org/10.1007/s10096-018-3251-5.

(19) von Eiff, M.; Roos, N.; Schulten, R.; Hesse, M.; Zühlsdorf, M.; van de Loo, J. Pulmonary Aspergillosis: Early Diagnosis Improves Survival. *Respiration* 1995, 62 (6), 341–347. https://doi.org/10.1159/000196477.

(20) Takazono, T.; Izumikawa, K. Recent Advances in Diagnosing Chronic Pulmonary Aspergillosis. *Front Microbiol* 2018, 9, 1810. https://doi.org/10.3389/fmicb.2018.01810.

(21) Tarrand, J. J.; Lichterfeld, M.; Warraich, I.; Luna, M.; Han, X. Y.; May, G. S.; Kontoyiannis, D. P. Diagnosis of Invasive Septate Mold Infections. A Correlation of Microbiological Culture and Histologic or Cytologic Examination. *Am J Clin Pathol* 2003, 119 (6), 854–858. https://doi.org/10.1309/EXBV-YAUP-ENBM-285Y.

(22) Ruhnke, M.; Böhme, A.; Buchheidt, D.; Cornely, O.; Donhuijsen, K.; Einsele, H.; Enzensberger, R.; Hebart, H.; Heussel, C. P.; Horger, M.; Hof, H.; Karthaus, M.; Krüger, W.; Maschmeyer, G.; Penack, O.; Ritter, J.; Schwartz, S.; Infectious Diseases Working Party in Haematology and Oncology of the German Society for Haematology and Oncology. Diagnosis of Invasive Fungal Infections in Hematology and Oncology--Guidelines from the Infectious Diseases Working Party in Haematology and Oncology of the German Society for Haematology and Oncology (AGIHO). *Ann Oncol* 2012, 23 (4), 823–833. https://doi.org/10.1093/annonc/mdr407.

(23) Nuh, A.; Ramadan, N.; Shah, A.; Armstrong-James, D. Sputum Galactomannan Has Utility in the Diagnosis of Chronic Pulmonary Aspergillosis. *Journal of Fungi* 2022, 8 (2), 188. https://doi.org/10.3390/jof8020188.

(24) Denning, D. W. Global Incidence and Mortality of Severe Fungal Disease. *Lancet Infect Dis* 2024. https://doi.org/10.1016/S1473-3099(23)00692-8.

(25) Donnelly, J. P.; Chen, S. C.; Kauffman, C. A.; Steinbach, W. J.; Baddley, J. W.; Verweij, P. E.; Clancy, C. J.; Wingard, J. R.; Lockhart, S. R.; Groll, A. H.; Sorrell, T. C.; Bassetti, M.; Akan, H.; Alexander, B. D.; Andes, D.; Azoulay, E.; Bialek, R.; Bradsher, R. W.; Bretagne, S.; Calandra, T.; Caliendo, A. M.; Castagnola, E.; Cruciani, M.; Cuenca-Estrella, M.; Decker, C. F.; Desai, S. R.; Fisher, B.; Harrison, T.; Heussel, C. P.; Jensen, H. E.; Kibbler, C. C.; Kontoyiannis, D. P.; Kullberg, B.-J.; Lagrou, K.; Lamoth, F.; Lehrnbecher, T.; Loeffler, J.; Lortholary, O.; Maertens, J.; Marchetti, O.; Marr, K. A.; Masur, H.; Meis, J. F.; Morrisey, C. O.; Nucci, M.; Ostrosky-Zeichner, L.; Pagano, L.; Patterson, T. F.; Perfect, J. R.; Racil, Z.; Roilides, E.; Ruhnke, M.; Prokop, C. S.; Shoham, S.; Slavin, M. A.; Stevens, D. A.; Thompson, G. R.; Vazquez, J. A.; Viscoli, C.; Walsh, T. J.; Warris, A.; Wheat, L. J.; White, P. L.; Zaoutis, T. E.; Pappas, P. G. Revision and Update of the Consensus Definitions of Invasive Fungal Disease From the European Organization for Research and Treatment of Cancer and the Mycoses Study Group Education and Research Consortium. *Clinical Infectious Diseases* 2020, 71 (6), 1367–1376. https://doi.org/10.1093/cid/ciz1008.

(26) Denning, D. W.; Kibbler, C. C.; Barnes, R. A.; on behalf of the British Society for Medical Mycology. British Society for Medical Mycology Proposed Standards of Care for Patients with Invasive Fungal Infections. *Lancet Infect Dis* 2003, 3 (4), 230–240. https://doi.org/10.1016/S1473-3099(03)00580-2.

(27) Kitasato, Y.; Tao, Y.; Hoshino, T.; Tachibana, K.; Inoshima, N.; Yoshida, M.; Takata, S.; Okabayashi, K.; Kawasaki, M.; Iwanaga, T.; Aizawa, H. Comparison of Aspergillus Galactomannan Antigen Testing with a New Cut-off Index and Aspergillus Precipitating

Antibody Testing for the Diagnosis of Chronic Pulmonary Aspergillosis. *Respirology* 2009, 14 (5), 701–708. https://doi.org/10.1111/j.1440-1843.2009.01548.x.

(28) Kohno, S.; Izumikawa, K.; Ogawa, K.; Kurashima, A.; Okimoto, N.; Amitani, R.; Kakeya, H.; Niki, Y.; Miyazaki, Y.; Japan Chronic Pulmonary Aspergillosis Study Group (JCPASG). Intravenous Micafungin versus Voriconazole for Chronic Pulmonary Aspergillosis: A Multicenter Trial in Japan. *J Infect* 2010, 61 (5), 410–418. https://doi.org/10.1016/j.jinf.2010.08.005.

(29) Nam, H.-S.; Jeon, K.; Um, S.-W.; Suh, G. Y.; Chung, M. P.; Kim, H.; Kwon, O. J.; Koh, W.-J. Clinical Characteristics and Treatment Outcomes of Chronic Necrotizing Pulmonary Aspergillosis: A Review of 43 Cases. *International Journal of Infectious Diseases* 2010, 14 (6), e479–e482. https://doi.org/10.1016/j.ijid.2009.07.011.

(30) Shin, B.; Koh, W.-J.; Jeong, B.-H.; Yoo, H.; Park, H. Y.; Suh, G. Y.; Kwon, O. J.; Jeon, K. Serum Galactomannan Antigen Test for the Diagnosis of Chronic Pulmonary Aspergillosis. *J Infect* 2014, 68 (5), 494–499. https://doi.org/10.1016/j.jinf.2014.01.005.

(31) Hope, W.; Walsh, T.; Denning, D. Laboratory Diagnosis of Invasive Aspergillosis. *Lancet Infect Dis* 2005, 5 (10), 609–622. https://doi.org/10.1016/S1473-3099(05)70238-3.

(32) Hoenigl, M.; Prattes, J.; Spiess, B.; Wagner, J.; Prueller, F.; Raggam, R. B.; Posch, V.; Duettmann, W.; Hoenigl, K.; Wölfler, A.; Koidl, C.; Buzina, W.; Reinwald, M.; Thornton, C. R.; Krause, R.; Buchheidt, D. Performance of Galactomannan, Beta-d-Glucan, Aspergillus Lateral-Flow Device, Conventional Culture, and PCR Tests with Bronchoalveolar Lavage Fluid for Diagnosis of Invasive Pulmonary Aspergillosis. *J Clin Microbiol* 2014, 52 (6), 2039–2045. https://doi.org/10.1128/JCM.00467-14.

(33) Larkin, P. M. K.; Multani, A.; Beaird, O. E.; Dayo, A. J.; Fishbein, G. A.; Yang, S. A Collaborative Tale of Diagnosing and Treating Chronic Pulmonary Aspergillosis, from the Perspectives of Clinical Microbiologists, Surgical Pathologists, and Infectious Disease Clinicians. *J Fungi (Basel)* 2020, 6 (3). https://doi.org/10.3390/jof6030106.

(34) Oude Nijhuis, C. S. M.; Gietema, J. A.; Vellenga, E.; Daenen, S. M. G. J.; De Bont, E. S. J. M.; Kamps, W. A.; Groen, H. J. M.; van der Jagt, E. J.; van der Graaf, W. T. A. Routine Radiography Does Not Have a Role in the Diagnostic Evaluation of Ambulatory Adult Febrile Neutropenic Cancer Patients. *Eur J Cancer* 2003, 39 (17), 2495–2498. https://doi.org/10.1016/j.ejca.2003.06.002.

(35) Alexander, B. D.; Lamoth, F.; Heussel, C. P.; Prokop, C. S.; Desai, S. R.; Morrissey, C. O.; Baddley, J. W. Guidance on Imaging for Invasive Pulmonary Aspergillosis and Mucormycosis: From the Imaging Working Group for the Revision and Update of the Consensus Definitions of Fungal Disease from the EORTC/MSGERC. *Clinical Infectious Diseases* 2021, 72 (Supplement_2), S79–S88. https://doi.org/10.1093/cid/ciaa1855.

(36) Xu, S.-C.; Qiu, L.-H.; Liu, W.-Y.; Feng, Y.-L. Initial Computed Tomography Findings of Invasive Pulmonary Aspergillosis in Non-Hematological Patients. *Chin Med J* (Engl) 2012, 125 (17), 2979–2985.

(37) Saghrouni, F.; Ben Youssef, Y.; Gheith, S.; Bouabid, Z.; Ben Abdeljelil, J.; Khammari, I.; Fathallah, A.; Khlif, A.; Ben Saïd, M. Twenty-Nine Cases of Invasive Aspergillosis in Neutropenic Patients. *Med Mal Infect* 2011, 41 (12), 657–662. https://doi.org/10.1016/j.medmal.2011.09.011.

(38) Thornton, C. R. Molecular Imaging of Invasive Pulmonary Aspergillosis Using ImmunoPET/MRI: The Future Looks Bright. *Front Microbiol* 2018, 9. https://doi.org/10.3389/fmicb.2018.00691.

(39) Poelmans, J.; Hillen, A.; Vanherp, L.; Govaerts, K.; Maertens, J.; Dresselaers, T.; Himmelreich, U.; Lagrou, K.; Vande Velde, G. Longitudinal, in Vivo Assessment of Invasive Pulmonary Aspergillosis in Mice by Computed Tomography and Magnetic Resonance Imaging. *Lab Invest* 2016, 96 (6), 692–704. https://doi.org/10.1038/labinvest.2016.45.

(40) Vuong, M. F.; Hollingshead, C. M.; Waymack, J. R. Aspergillosis. *StatPearls* [Internet]. https://www.ncbi.nlm.nih.gov/books/NBK482241/ (accessed 2024-09-25).

(41) Tochigi, N.; Okubo, Y.; Ando, T.; Wakayama, M.; Shinozaki, M.; Gocho, K.; Hata, Y.; Ishiwatari, T.; Nemoto, T.; Shibuya, K. Histopathological Implications of Aspergillus Infection in Lung. *Mediators Inflamm* 2013, 2013, 1–8. https://doi.org/10.1155/2013/809798.

(42) Kanaujia, R.; Singh, S.; Rudramurthy, S. M. Aspergillosis: An Update on Clinical Spectrum, Diagnostic Schemes, and Management. *Curr Fungal Infect Rep* 2023, 17 (2), 144–155. https://doi.org/10.1007/s12281-023-00461-5.

(43) Abdin, M. Z.; Ahmad, M. M.; Javed, S. Advances in Molecular Detection of Aspergillus: An Update. *Arch Microbiol* 2010, 192 (6), 409–425. https://doi.org/10.1007/s00203-010-0563-y.

(44) Kappe, R.; Okeke, C. N.; Fauser, C.; Maiwald, M.; Sonntag, H. G. Molecular Probes for the Detection of Pathogenic Fungi in the Presence of Human Tissue. *J Med Microbiol* 1998, 47 (9), 811–820. https://doi.org/10.1099/00222615-47-9-811.

(45) Kawamura, S.; Maesaki, S.; Noda, T.; Hirakata, Y.; Tomono, K.; Tashiro, T.; Kohno, S. Comparison between PCR and Detection of Antigen in Sera for Diagnosis of Pulmonary Aspergillosis. *J Clin Microbiol* 1999, 37 (1), 218–220. https://doi.org/10.1128/JCM.37.1.218-220.1999.

(46) Kami, M.; Fukui, T.; Ogawa, S.; Kazuyama, Y.; Machida, U.; Tanaka, Y.; Kanda, Y.; Kashima, T.; Yamazaki, Y.; Hamaki, T.; Mori, S.; Akiyama, H.; Mutou, Y.; Sakamaki, H.; Osumi, K.; Kimura, S.; Hirai, H. Use of Real-Time PCR on Blood Samples for Diagnosis of Invasive Aspergillosis. *Clinical Infectious Diseases* 2001, 33 (9), 1504–1512. https://doi.org/10.1086/323337.

(47) White, P. L.; Wingard, J. R.; Bretagne, S.; Löffler, J.; Patterson, T. F.; Slavin, M. A.; Barnes, R. A.; Pappas, P. G.; Donnelly, J. P. Aspergillus Polymerase Chain Reaction: Systematic Review of Evidence for Clinical Use in Comparison With Antigen Testing. *Clinical Infectious Diseases* 2015, 61 (8), 1293–1303. https://doi.org/10.1093/cid/civ507.

(48) White, P. L.; Posso, R. B.; Barnes, R. A. Analytical and Clinical Evaluation of the PathoNostics AsperGenius Assay for Detection of Invasive Aspergillosis and Resistance to Azole Antifungal Drugs Directly from Plasma Samples. *J Clin Microbiol* 2017, 55 (8), 2356–2366. https://doi.org/10.1128/JCM.00411-17.

(49) Heng, S. C.; Morrissey, O.; Chen, S. C.-A.; Thursky, K.; Manser, R. L.; Nation, R. L.; Kong, D. C.-M.; Slavin, M. Utility of Bronchoalveolar Lavage Fluid Galactomannan Alone or in Combination with PCR for the Diagnosis of Invasive Aspergillosis in Adult Hematology Patients: A Systematic Review and Meta-Analysis. *Crit Rev Microbiol* 2015, 41 (1), 124–134. https://doi.org/10.3109/1040841X.2013.804033.

(50) Tuon, F. F. A Systematic Literature Review on the Diagnosis of Invasive Aspergillosis Using Polymerase Chain Reaction (PCR) from Bronchoalveolar Lavage Clinical Samples. *Rev Iberoam Micol* 2007, 24 (2), 89–94.

(51) Sun, W.; Wang, K.; Gao, W.; Su, X.; Qian, Q.; Lu, X.; Song, Y.; Guo, Y.; Shi, Y. Evaluation of PCR on Bronchoalveolar Lavage Fluid for Diagnosis of Invasive Aspergillosis: A Bivariate Metaanalysis and Systematic Review. *PLoS One* 2011, 6 (12), e28467. https://doi.org/10.1371/journal.pone.0028467.

(52) Avni, T.; Levy, I.; Sprecher, H.; Yahav, D.; Leibovici, L.; Paul, M. Diagnostic Accuracy of PCR Alone Compared to Galactomannan in Bronchoalveolar Lavage Fluid for Diagnosis of Invasive Pulmonary Aspergillosis: A Systematic Review. *J Clin Microbiol* 2012, 50 (11), 3652–3658. https://doi.org/10.1128/JCM.00942-12.

(53) Mengoli, C.; Cruciani, M.; Barnes, R. A.; Loeffler, J.; Donnelly, J. P. Use of PCR for Diagnosis of Invasive Aspergillosis: Systematic Review and Meta-Analysis. *Lancet Infect Dis* 2009, 9 (2), 89–96. https://doi.org/10.1016/S1473-3099(09)70019-2.

(54) Arvanitis, M.; Ziakas, P. D.; Zacharioudakis, I. M.; Zervou, F. N.; Caliendo, A. M.; Mylonakis, E. PCR in Diagnosis of Invasive Aspergillosis: A Meta-Analysis of Diagnostic Performance. *J Clin Microbiol* 2014, 52 (10), 3731–3742. https://doi.org/10.1128/JCM.01365-14.

(55) Heteropolysaccharides. Encyclopaedia Brtannica. https://www.britannica.com/science/carbohydrate/Heteropolysaccharides (accessed 2024-03-20).

(56) Platelia Aspergillus AG 1 plate. Bio-Rad. https://commerce.bio-rad.com/webroot/web/pdf/inserts/CDG/en/62794_881115_EN.pdf (accessed 2024-03-20).

(57) Duarte, R. F.; Sanchez-Ortega, I.; Cuesta, I.; Arnan, M.; Patino, B.; Fernandez de Sevilla, A.; Gudiol, C.; Ayats, J.; Cuenca-Estrella, M. Serum Galactomannan-Based Early Detection of Invasive Aspergillosis in Hematology Patients Receiving Effective Antimold Prophylaxis. *Clinical Infectious Diseases* 2014, 59 (12), 1696–1702. https://doi.org/10.1093/cid/ciu673.

(58) D'Haese, J.; Theunissen, K.; Vermeulen, E.; Schoemans, H.; De Vlieger, G.; Lammertijn, L.; Meersseman, P.; Meersseman, W.; Lagrou, K.; Maertens, J. Detection of Galactomannan in Bronchoalveolar Lavage Fluid Samples of Patients at Risk for Invasive Pulmonary Aspergillosis: Analytical and Clinical Validity. *J Clin Microbiol* 2012, 50 (4), 1258–1263. https://doi.org/10.1128/JCM.06423-11.

(59) Chong, G. M.; Maertens, J. A.; Lagrou, K.; Driessen, G. J.; Cornelissen, J. J.; Rijnders, B. J. A. Diagnostic Performance of Galactomannan Antigen Testing in Cerebrospinal Fluid. *J Clin Microbiol* 2016, 54 (2), 428–431. https://doi.org/10.1128/JCM.02913-15.

(60) Cerqueira, L.; Azevedo, N. F.; Almeida, C.; Jardim, T.; Keevil, C. W.; Vieira, M. J. DNA Mimics for the Rapid Identification of Microorganisms by Fluorescence in Situ Hybridization (FISH). *Int J Mol Sci* 2008, 9 (10), 1944–1960. https://doi.org/10.3390/ijms9101944.

(61) Moter, A.; Göbel, U. B. Fluorescence in Situ Hybridization (FISH) for Direct Visualization of Microorganisms. *J Microbiol Methods* 2000, 41 (2), 85–112. https://doi.org/10.1016/S0167-7012(00)00152-4.

(62) Amann, R.; Fuchs, B. M.; Behrens, S. The Identification of Microorganisms by Fluorescence in Situ Hybridisation. *Curr Opin Biotechnol* 2001, 12 (3), 231–236. https://doi.org/10.1016/S0958-1669(00)00204-4.

(63) Cerqueira, L.; Moura, S.; Almeida, C.; Vieira, M. J.; Azevedo, N. F. Establishment of a New PNA-FISH Method for Aspergillus Fumigatus Identification: First Insights for Future Use in Pulmonary Samples. *Microorganisms* 2020, 8 (12), 1950. https://doi.org/10.3390/microorganisms8121950.

(64) Lamoth, F. Aspergillus Fumigatus-Related Species in Clinical Practice. *Front Microbiol* 2016, 7. https://doi.org/10.3389/fmicb.2016.00683.

(65) Teertstra, W. R.; Lugones, L. G.; Wösten, H. A. B. In Situ Hybridisation in Filamentous Fungi Using Peptide Nucleic Acid Probes. *Fungal Genet Biol* 2004, 41 (12), 1099–1103. https://doi.org/10.1016/j.fgb.2004.08.010.

(66) Koczula, K. M.; Gallotta, A. Lateral Flow Assays. *Essays Biochem* 2016, 60 (1), 111–120. https://doi.org/10.1042/EBC20150012.

(67) Jenks, J. D.; Miceli, M. H.; Prattes, J.; Mercier, T.; Hoenigl, M. The Aspergillus Lateral Flow Assay for the Diagnosis of Invasive Aspergillosis: An Update. *Curr Fungal Infect Rep* 2020, 14 (4), 378–383. https://doi.org/10.1007/s12281-020-00409-z.

(68) Pan, Z.; Fu, M.; Zhang, J.; Zhou, H.; Fu, Y.; Zhou, J. Diagnostic Accuracy of a Novel Lateral-Flow Device in Invasive Aspergillosis: A Meta-Analysis. *J Med Microbiol* 2015, 64 (7), 702–707. https://doi.org/10.1099/jmm.0.000092.

(69) Lass-Flörl, C.; Lo Cascio, G.; Nucci, M.; Camargo dos Santos, M.; Colombo, A. L.; Vossen, M.; Willinger, B. Respiratory Specimens and the Diagnostic Accuracy of Aspergillus Lateral Flow Assays (LFA-IMMYTM): Real-Life Data from a Multicentre Study. *Clinical Microbiology and Infection* 2019, 25 (12), 1563.e1-1563.e3. https://doi.org/10.1016/j.cmi.2019.08.009.

(70) Mercier, T.; Dunbar, A.; de Kort, E.; Schauwvlieghe, A.; Reynders, M.; Guldentops, E.; Blijlevens, N. M. A.; Vonk, A. G.; Rijnders, B.; Verweij, P. E.; Lagrou, K.; Maertens, J. Lateral Flow Assays for Diagnosing Invasive Pulmonary Aspergillosis in Adult Hematology Patients: A Comparative Multicenter Study. *Med Mycol* 2020, 58 (4), 444–452. https://doi.org/10.1093/mmy/myz079.

(71) Jenks, J. D.; Prattes, J.; Frank, J.; Spiess, B.; Mehta, S. R.; Boch, T.; Buchheidt, D.; Hoenigl, M. Performance of the Bronchoalveolar Lavage Fluid Aspergillus Galactomannan Lateral Flow Assay With Cube Reader for Diagnosis of Invasive Pulmonary Aspergillosis: A Multicenter Cohort Study. *Clinical Infectious Diseases* 2021, 73 (7), e1737–e1744. https://doi.org/10.1093/cid/ciaa1281.

(72) White, P. L.; Price, J. S.; Posso, R.; Cutlan-Vaughan, M.; Vale, L.; Backx, M. Evaluation of the Performance of the IMMY Sona Aspergillus Galactomannan Lateral Flow Assay When Testing Serum To Aid in Diagnosis of Invasive Aspergillosis. *J Clin Microbiol* 2020, 58 (6). https://doi.org/10.1128/JCM.00053-20.

(73) Singh, D. K.; Ray, A. R. Biomedical Applications of Chitin, Chitosan, and Their Derivatives. *Journal of Macromolecular Science, Part C: Polymer Reviews* 2000, 40 (1), 69–83. https://doi.org/10.1081/MC-100100579.

(74) Algammal, A. M.; Elsayed, M. E.; Hashem, H. R.; Ramadan, H.; Sheraba, N. S.; El-Diasty, E. M.; Abbas, S. M.; Hetta, H. F. Molecular and HPLC-Based Approaches for Detection of Aflatoxin B1 and Ochratoxin A Released from Toxigenic Aspergillus Species in Processed Meat. *BMC Microbiol* 2021, 21 (1), 82. https://doi.org/10.1186/s12866-021-02144-y.

(75) Makhlouf, J.; Carvajal-Campos, A.; Querin, A.; Tadrist, S.; Puel, O.; Lorber, S.; Oswald, I. P.; Hamze, M.; Bailly, J.-D.; Bailly, S. Morphologic, Molecular and Metabolic Characterization of Aspergillus Section Flavi in Spices Marketed in Lebanon. *Sci Rep* 2019, 9 (1), 5263. https://doi.org/10.1038/s41598-019-41704-1.

(76) Grebe, S. K.; Singh, R. J. LC-MS/MS in the Clinical Laboratory - Where to From Here? *Clin Biochem Rev* 2011, 32 (1), 5–31.

(77) Banerjee, S. Empowering Clinical Diagnostics with Mass Spectrometry. *ACS Omega* 2020, 5 (5), 2041–2048. https://doi.org/10.1021/acsomega.9b03764.

(78) Dong, X.; Mondello, S.; Kobeissy, F.; Ferri, R.; Mechref, Y. Serum Glycomics Profiling of Patients with Primary Restless Legs Syndrome Using LC-MS/MS. *J Proteome Res* 2020, 19 (8), 2933–2941. https://doi.org/10.1021/acs.jproteome.9b00549.

(79) Saadi, J.; Oueslati, S.; Bellanger, L.; Gallais, F.; Dortet, L.; Roque-Afonso, A.-M.; Junot, C.; Naas, T.; Fenaille, F.; Becher, F. Quantitative Assessment of SARS-CoV-2 Virus in Nasopharyngeal Swabs Stored in Transport Medium by a Straightforward LC-MS/MS Assay Targeting Nucleocapsid, Membrane, and Spike Proteins. *J Proteome Res* 2021, 20 (2), 1434–1443. https://doi.org/10.1021/acs.jproteome.0c00887.

(80) Whiley, L.; Nye, L. C.; Grant, I.; Andreas, N.; Chappell, K. E.; Sarafian, M. H.; Misra, R.; Plumb, R. S.; Lewis, M. R.; Nicholson, J. K.; Holmes, E.; Swann, J. R.; Wilson, I. D. Ultrahigh-Performance Liquid Chromatography Tandem Mass Spectrometry with Electrospray Ionization Quantification of Tryptophan Metabolites and Markers of Gut Health in Serum and Plasma-Application to Clinical and Epidemiology Cohorts. *Anal Chem* 2019, 91 (8), 5207–5216. https://doi.org/10.1021/acs.analchem.8b05884.

(81) Spiller, S.; Frolov, A.; Hoffmann, R. Quantification of Specific Glycation Sites in Human Serum Albumin as Prospective Type 2 Diabetes Mellitus Biomarkers. *Protein Pept Lett* 2017, 24 (10), 887–896. https://doi.org/10.2174/0929866524666170202124120.

(82) Benito, S.; Sánchez-Ortega, A.; Unceta, N.; Goicolea, M. A.; Barrio, R. J. LC-QQQ-MS Routine Analysis Method for New Biomarker Quantification in Plasma Aimed at Early Chronic Kidney Disease Diagnosis. *J Pharm Biomed Anal* 2019, 169, 82–89. https://doi.org/10.1016/j.jpba.2019.02.042.

(83) Chitnis, T.; Glanz, B. I.; Gonzalez, C.; Healy, B. C.; Saraceno, T. J.; Sattarnezhad, N.; Diaz-Cruz, C.; Polgar-Turcsanyi, M.; Tummala, S.; Bakshi, R.; Bajaj, V. S.; Ben-Shimol, D.; Bikhchandani, N.; Blocker, A. W.; Burkart, J.; Cendrillon, R.; Cusack, M. P.; Demiralp, E.; Jooste, S. K.; Kharbouch, A.; Lee, A. A.; Lehár, J.; Liu, M.; Mahadevan, S.; Murphy, M.; Norton, L. C.; Parlikar, T. A.; Pathak, A.; Shoeb, A.; Soderberg, E.; Stephens, P.; Stoertz, A. H.; Thng, F.; Tumkur, K.; Wang, H.; Rhodes, J.; Rudick, R. A.; Ransohoff, R. M.; Phillips, G. A.; Bruzik, E.; Marks, W. J.; Weiner, H. L.; Snyder, T. M. Quantifying Neurologic Disease Using Biosensor Measurements In-Clinic and in Free-Living Settings in Multiple Sclerosis. *NPJ Digit Med* 2019, 2 (1), 123. https://doi.org/10.1038/s41746-019-0197-7.

(84) Allison, C. L.; Moskaluk, A.; VandeWoude, S.; Reynolds, M. M. Detection of Glucosamine as a Marker for Aspergillus Niger: A Potential Screening Method for Fungal Infections. *Anal Bioanal Chem* 2021, 413 (11), 2933–2941. https://doi.org/10.1007/s00216-021-03225-7.

(85) Beaudry, F.; Vachon, P. Determination of Glucosamine in Horse Plasma by Liquid Chromatography Tandem Mass Spectrometry. *Biomed Chromatogr* 2008, 22 (1), 1–4. https://doi.org/10.1002/bmc.906.

(86) Song, M.; Hang, T.-J.; Wang, C.; Yang, L.; Wen, A.-D. Precolumn Derivatization LC-MS/MS Method for the Determination and Pharmacokinetic Study of Glucosamine in Human Plasma and Urine. *J Pharm Anal* 2012, 2 (1), 19–28. https://doi.org/10.1016/j.jpha.2011.08.003.

(87) Persiani, S.; Rotini, R.; Trisolino, G.; Rovati, L. C.; Locatelli, M.; Paganini, D.; Antonioli, D.; Roda, A. Synovial and Plasma Glucosamine Concentrations in Osteoarthritic Patients Following Oral Crystalline Glucosamine Sulphate at Therapeutic Dose. *Osteoarthritis Cartilage* 2007, 15 (7), 764–772. https://doi.org/10.1016/j.joca.2007.01.019.

(88) Mohammadi, M.; Zamani, A.; Karimi, K. Determination of Glucosamine in Fungal Cell Walls by High-Performance Liquid Chromatography (HPLC). *J Agric Food Chem* 2012, 60 (42), 10511–10515. https://doi.org/10.1021/jf303488w.

(89) Hoenigl, M.; Orasch, T.; Faserl, K.; Prattes, J.; Loeffler, J.; Springer, J.; Gsaller, F.; Reischies, F.; Duettmann, W.; Raggam, R. B.; Lindner, H.; Haas, H. Triacetylfusarinine C: A Urine Biomarker for Diagnosis of Invasive Aspergillosis. *Journal of Infection* 2019, 78 (2), 150–157. https://doi.org/10.1016/j.jinf.2018.09.006.

(90) Lewis, R. E.; Wiederhold, N. P.; Chi, J.; Han, X. Y.; Komanduri, K. V.; Kontoyiannis, D. P.; Prince, R. A. Detection of Gliotoxin in Experimental and Human Aspergillosis. *Infect Immun* 2005, 73 (1), 635–637. https://doi.org/10.1128/IAI.73.1.635-637.2005.

(91) Carroll, C. S.; Amankwa, L. N.; Pinto, L. J.; Fuller, J. D.; Moore, M. M. Correction: Detection of a Serum Siderophore by LC-MS/ MS as a Potential Biomarker of Invasive

Aspergillosis. *PLoS One* 2016, 11 (5), e0155451. https://doi.org/10.1371/journal.pone.0155451.

(92) Saldan, N. C.; Almeida, R. T. R.; Avíncola, A.; Porto, C.; Galuch, M. B.; Magon, T. F. S.; Pilau, E. J.; Svidzinski, T. I. E.; Oliveira, C. C. Development of an Analytical Method for Identification of Aspergillus Flavus Based on Chemical Markers Using HPLC-MS. *Food Chem* 2018, 241, 113–121. https://doi.org/10.1016/j.foodchem.2017.08.065.

(93) Pontis, H. G. General Introduction to Mass Spectrometry and Nuclear Magnetic Resonance. In Methods for Analysis of Carbohydrate Metabolism in Photosynthetic Organisms; *Academic Press* 2017; pp 71–76.

(94) Singhal, N.; Kumar, M.; Kanaujia, P. K.; Virdi, J. S. MALDI-TOF Mass Spectrometry: An Emerging Technology for Microbial Identification and Diagnosis. *Front Microbiol* 2015, 6, 791. https://doi.org/10.3389/fmicb.2015.00791.

(95) Vidal-Acuña, M. R.; Ruiz-Pérez de Pipaón, M.; Torres-Sánchez, M. J.; Aznar, J. Identification of Clinical Isolates of Aspergillus, Including Cryptic Species, by Matrix Assisted Laser Desorption Ionization Time-of-Flight Mass Spectrometry (MALDI-TOF MS). *Med Mycol* 2018, 56 (7), 838–846. https://doi.org/10.1093/mmy/myx115.

(96) Bille, E.; Dauphin, B.; Leto, J.; Bougnoux, M.-E.; Beretti, J.-L.; Lotz, A.; Suarez, S.; Meyer, J.; Join-Lambert, O.; Descamps, P.; Grall, N.; Mory, F.; Dubreuil, L.; Berche, P.; Nassif, X.; Ferroni, A. MALDI-TOF MS Andromas Strategy for the Routine Identification of Bacteria, Mycobacteria, Yeasts, Aspergillus Spp. and Positive Blood Cultures. *Clin Microbiol Infect* 2012, 18 (11), 1117–1125. https://doi.org/10.1111/j.1469-0691.2011.03688.x.

(97) Zvezdanova, M. E.; Arroyo, M. J.; Méndez, G.; Candela, A.; Mancera, L.; Rodríguez, J. G.; Serra, J. L.; Jiménez, R.; Lozano, I.; Castro, C.; López, C.; Muñoz, P.; Guinea, J.; Escribano, P.; Rodríguez-Sánchez, B.; ASPEIN group. Detection of Azole Resistance in Aspergillus Fumigatus Complex Isolates Using MALDI-TOF Mass Spectrometry. *Clin Microbiol Infect* 2022, 28 (2), 260–266. https://doi.org/10.1016/j.cmi.2021.06.005.

(98) Stone, J. A.; van der Gugten, J. G. Quantitative Tandem Mass Spectrometry in the Clinical Laboratory: Regulation and Opportunity for Validation of Laboratory Developed Tests. *Journal of mass spectrometry and advances in the clinical lab* 2023, 28, 82–90. https://doi.org/10.1016/j.jmsacl.2023.03.001.

(99) Harris, D. C. Quality Assurance and Calibration Methods. In *Quantitative Chemical Analysis*; W. H. Freema and Company: New York, 2007; pp 78–92.

(100) Stone, J. The Way Forward for Clinical Mass Spectrometry in Hospital Laboratories. *Clinical Laboratory News*. November 1, 2019.

(101) Wasim, K.; Haq, I.; Ashraf, M. Antimicrobial studies of the Leaf of Cannabis Sativa L. *Pak J Pharm Sci* 1995, *8* (1), 29-38.

(102) Appendino, G.; Gibbons, S.; Giana, A.; Pagani, A.; Grassi, G.; Stavri, M.; Smith, E.; Rahman, M. M. Antibacterial Cannabinoids from Cannabis Sativa: A Structure-Activity Study. *J Nat Prod* 2008, *71* (8), 1427-1430. https://doi.org/10.1021/np8002673

(103) Feldman, M.; Sionov, R. V.; Mechoulam, R.; Steinberg, D. Anti-Biofilm Activity of Cannabidiol against Candida Albicans. *Microorganisms* 2021, *9* (2), 441. https://doi.org/10.3390/microorganisms9020441.

(104) Blaskovch, M. A. T.; Kavanagh, A. M.; Elliott, A. G.; Zhang, B.; Ramu, S.; Amado, M.; Lowe, G. J.; Hinton, A. O.; Pham, D. M. T.; Zuegg, J.; Beare, N.; Quach, D.; Sharp, M.

D.; Pogliano, J.; Rogers, A. P.; Lyras, D.; Tan, L.; West, N. P.; Crawford, D. W.; Peterson, M. L.; Callahan, M.; Thurn, M. The Antimicrobial Potential of Cannabidiol. *Commun Biol* 2021, *4* (1), 7. https://doi.org/10.1038/s42003-020-01530-y.

CHAPTER 2[3]

Development of an LC-MS/QQQ method to detect glucosamine derived from *Aspergillus* Species

2.1 Overview

In this chapter, I discuss the development of a method that uses glucosamine as a biomarker to detect *Aspergillus species*. The results discussed in this chapter provide insights into the quantitative degradation of glucosamine from opportunistic pathogens for Aspergillosis. It also discusses the rationale behind the mobile phase chosen for this analysis, and the resulting method developed. The method was then applied to six pathogenic species of *Aspergillus*, and the quantitative results of the degradation and detection is discussed.

The liquid chromatography mass spectrometry method used in this chapter was developed and constructed by Madeline Schwarz. Fungal samples used in this chapter were cultured and harvested by Madeline Schwarz. The fungal degradation method used was developed by Chris Allison[1] and performed by Madeline Schwarz. Analysis of degraded products was performed by Madeline Schwarz. Melissa M. Reynolds was the advisor on this project.

2.2 Introduction

Daily, humans are exposed to fungal spores[1] but only approximately one percent of fungal species cause fungal infections.[2] These infections can occur superficially (e.g. athlete's foot) or invasively.[2] Despite low occurrence rates of invasive fungal infections, a study

[3] Chapter 2 is adapted from a manuscript submitted to *The Microchemical Journal with* coauthor Melissa M. Reynolds.

performed in 2017 estimated that fungal infections kill more than 1.5 million people per year globally.[3] This is similar to the mortality rate of tuberculosis and three times greater than malaria.[3] Given the omnipresence of airborne fungal spores and the high mortality rates of invasive fungal infections, pulmonary fungal infections are of significant concern. Pulmonary infections are an even larger concern in immunocompromised individuals.[4]

Aspergillus is a diverse genus of fungi associated with food spoilage, mycotoxin production, and occasional human and animal disease.[5] *Aspergillus* species are characterized as filamentous fungi, meaning a fungus that forms a threadlike, multicellular structure with branching.[5] One of the most ubiquitous species of the *Aspergillus* genus is *Aspergillus niger*, commonly found in households on certain fruits and vegetables. *A. niger* is also an occasional opportunistic human pathogen. Immunocompromised individuals are most susceptible to invasive pulmonary form of aspergillosis, which can lead to chronic obstructive pulmonary disease if not treated aggressively.[6]

Early and accurate diagnosis of fungal infections, such as aspergillosis, is crucial because mortality from aspergillosis is more than 70% if diagnosis is delayed.[7] Despite the severity of pulmonary fungal infections, current screening methods used for diagnosis are slow and inaccurate, leading to delayed treatment and/or misdiagnoses.[8] Laboratory testing is primarily used to diagnose fungal infections and identify the fungus responsible for the infection. Depending on the location of the infection, samples analyzed include blood, cerebrospinal fluid, bronchioalveolar lavage and sputum.[9] The main methods of identification of fungi are culture, imaging, histopathology, and quantitative polymerase chain reaction (qPCR).[8-13] Early stages of pulmonary aspergillosis are often not detected by conventional pulmonary radiographs, one of the most common imaging procedures. Lung biopsies are not often performed as these are

invasive procedures, and fungal elements are not always easily interpreted when analyzed via microscopy.[12] Polymerase chain reaction is a newer method for *Aspergillus* detection in blood. This method, while promising, is heavily dependent on the test setting. For example, *Aspergillus* PCR works well in patients with low white blood cell counts (neutropenia) who have not been treated with antifungal agents.[13,14] PCR may result in false negative findings due to interferences from antifungal medications.[13,15] Further, fungal PCR tests have not been thoroughly standardized.[13,16] The most common method for detection of fungal cells is fungal cultures, but cultures require at least 7 days.[12] Blood cultures are also unreliable for immunocompromised patients, due to a mold-active prophylaxis often prescribed giving rise to false positives.[13] Therefore, the use of fungal culturing for diagnosis is not conducive to the speed needed to aggressively treat these infections.

A combination of high-pressure liquid chromatography and triple quadrupole mass spectrometry (LC-QQQ) can overcome these challenges by allowing for high analytical specificity, the ability to measure specific biomarkers, and high analytical sensitivity, the smallest amount of substance in a sample that can be measured. The use of LC-QQQ also leads to relatively short run-times when compared to other instrumental counterparts. LC-QQQ is currently being used in clinical settings due to a variety of factors.[17,18] When compared to HPLC-DAD or GCMS, LC-QQQ provides an ease in workflow and higher throughput. Overall, LC-QQQ is significantly lower in cost to other instrumental techniques.[17-20] Also, different immunoassays for the same analyte often end up in poor agreement with each other.[13,15-17] If no commercial immunoassay is available for an analyte of interest, designing and validating a new immunoassay can be a significant undertaking. In comparison, LC-QQQ assays are relatively much easier to develop, reagent costs are negligible, and results are these assays tend to have

higher inter-laboratory fidelity.[17] LC-QQQ also offers quantitative capabilities, and quantitation is frequently used in clinical settings to determine the extent of an infection or disease to determine appropriate treatment.[21-24]

One molecule prevalent in all fungi that could serve as a potential biomarker is D-glucosamine (GlcN, Figure 2.1). GlcN is a low molecular weight molecule derived from chitin that is easily characterized by mass spectrometric analysis.[25] Chitin is found in the cell walls of all pathogenic fungi.[26,27] Chitin is a branched polymer composed of repeating N-acetylglucosamine monomers. Chitin is often chemically modified via alkaline deacetylation to produce chitosan.[28] Chitosan then decomposes into low molecular weight chitosan oligosaccharides. Due to their lower molecular weight chitosan oligosaccharides, like GlcN, can be easily characterized by mass spectrometric analysis.[25] Due to the prevalence of chitin in the cell walls of fungi, GlcN can be extracted from fungal cells and used as a fungal biomarker. Allison et. al. (2021) demonstrated that GlcN could be qualitatively detected from fungal-derived chitin using LC-MS in under 24 hours, compared to the current "gold standard" of 7+ days.[29]

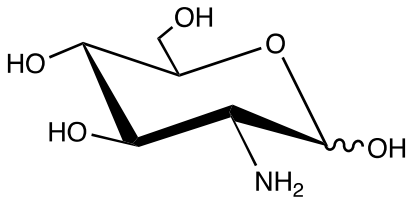

Figure 2.1: Structure of glucosamine, the target biomarker for this study

LC-QQQ analysis is a common method for detection of glucosamine[30-35] but has not been applied to fungal detection systems. LC-QQQ is used to quantify the GlcN in plasma, synovial fluid, and urine after ingestion of supplements.[30-35] This work reports a new LC-QQQ method to quantify the GlcN produced from the acid degradation of *A. niger* cells. This method provides an

extremely sensitive and selective potential diagnostic tool which promises to aid in the detection of glucosamine from pulmonary fungal infections.

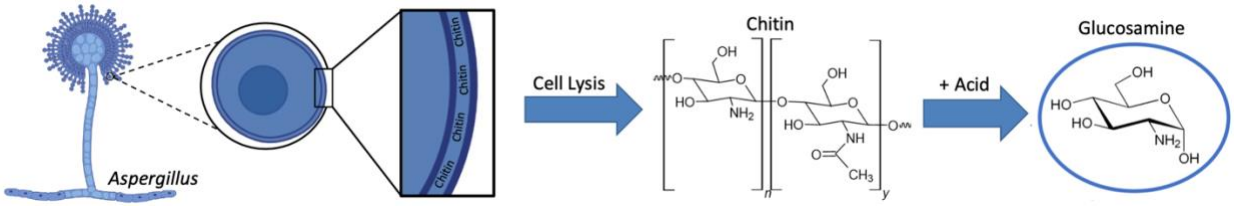

Figure 2.2: Extraction of glucosamine (circle in blue) from cell walls of *Aspergillus* fungal cells. Generic structure of chitin shows GlcN (n) and GlcNAc (y) subunits.

2.3 Experimental

2.3.1 Materials

D-Glucosamine HCl was obtained from MP Biomedicals (Santa Ana, CA). ACS-grade acetone, Optima LC-MS grade formic acid, Optima LC-MS acetonitrile, Optima LC-MS water, and ammonium acetate (>98.0%) were obtained from Fisher Chemical (Waltham, MA). Hydrochloric acid was obtained from Ward's Science (Rochester, NY). 0.2-µm Captiva Econofilters were obtained from Agilent (Palo Alto, CA). *A. niger* fungi were obtained from domestic cat hair samples and cultured on an agar medium for 14 days. *A. fumigatus, A. flavus, A. nidulans, A. terreus, and A. parasiticus* were obtained from ATCC (Manassas, VA) and cultured on an agar medium for 14 days. All fungal samples used for quantification were taken from the same culture plate at the same incubation time.

2.3.2 Sample preparation

A. fumigatus, A. flavus, A. nidulans, A. niger, A. terreus, and A. parasiticus were grown and maintained on potato dextrose agar at 25 °C until harvesting. Fungal cells were transferred into 15-mL centrifuge tubes containing 5 mL chilled acetone (-20 °C) in a biosafety hood. To promote cell lysis, samples were incubated at -20 °C for 60 minutes. Samples were then

centrifuged for 10 min at 1300 kxg. The supernatant was decanted, and the sample was dried under vacuum to determine the weight of the lysed fungal cells. These dried samples were then transferred to a 50 mL round bottom flask and degraded in 5 mL of 10 M HCl in a hot oil bath (90 °C) for approximately 3 hours, or until all HCl was evaporated.[29] The degraded samples were reconstituted in 5 mL of Millli-Q grade water (18.2 MΩ·cm) and stirred at 90°C for 30 minutes. The reconstituted samples were then passed through 0.2-µm filters, and analyzed via the LC-QQQ method developed.

2.3.3 LC-QQQ Methods

LC-QQQ analyses were carried out on an Agilent 6470 triple quadrupole mass spectrometer coupled to a 1290 high speed liquid chromatograph. Separations were performed using a Thermo Fisher Acclaim HILIC-10 column with dimensions of 4.6x150 mm and 5-µm particle size. Mobile phase A was composed of LC-MS grade water with 10 mM ammonium acetate and 0.1% (v/v) formic acid. Mobile phase B was acetonitrile (ACN) with 0.1% (v/v) formic acid. The flow rate was 0.500 mL/min, and a 20-minute runtime was used. The elution was isocratic at 80:20 for the duration of the separation. Electrospray ionization source was used in positive ionization mode. Ion source conditions were as follows: capillary voltage 1500 V; drying gas flow rate 6 L/min; desolvation line temperature 350 °C; nebulizer gas flow rate 55 L/min; nozzle voltage 2000 V; shielding gas flow 11 L/min; shielding gas temperature 400 °C.

2.3.4 Calculations

The line of best fit for the calibration curve described in this work was calculated using the method of least squares regression model. All values are reported as an average ± standard deviation unless otherwise indicated. The limit of detection and quantification were calculated

using the method of least squared, and the uncertainty that is described was calculated using statistical error propagation. All samples were run with an n=5 unless otherwise indicated.

2.4 Results and Discussion

2.4.1 Mass Spectrometry Method Development

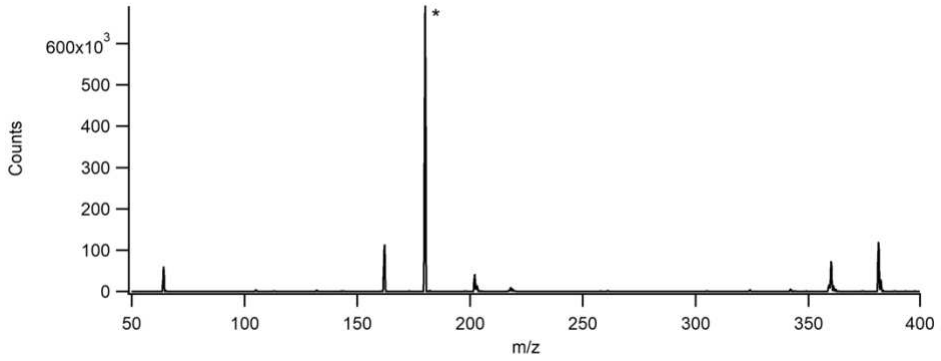

Figure 2.3: Total Mass Spectra of GlcN standard. Parent ion (180.1) is marked by *.

Multiple reaction monitoring (MRM), a method of molecule separation in the three quadrupoles of the mass spectrometer, allows for the targeted analysis of only GlcN and its fragments without the need for derivatization. MRM is a common method for isolating monosaccharides like GlcN.[31, 36-37] For each compound in an MRM method, the following steps must be followed. First, a scan of all ions generated from the separation (MS2 scan) must be analyzed, and the parent ion for the compound of interest must be selected. In an MS2 scan the third quadrupole operates in scan mode, and the other two quadrupoles allow all ions to pass. To confirm the method would be designed to detect GlcN, an MS2 scan was performed on GlcN standards and is shown in Figure 2.3. Table 2.1 describes all known ions in the MS2 scan. The MS2 scan shows that GlcN has a parent ion (indicated in Figure 2.3 with a star) of 180.1. The peak at 202.1indicates a sodium adduct on the GlcN molecule. The peaks at 359.2 and 381.2 indicate dimerized glucosamine, the latter with a sodium adduct, and the peaks at 84.1 and 162.1

indicate fragmented glucosamine ions. The peaks described are consistent with other ESI-MS studies presented in literature.[18, 36-37]

Table 2.1: Known ions in the MS2 scan

Mass to Charge Ratio (m/z)	Molecular Identifier
84.1	$[M - OCHCH_2OH + H]^+$
162.1	$[M - OH + H]^+$
180.1	$[M + H]^+$
202.1	$[M + Na]^+$
359.2	$[2M + H]^+$
381.2	$[2M + Na]^+$

Next, the fragmentor voltage (voltage applied at the end of the capillary before the ions pass from the ESI source into the first quadrupole) is roughly optimized. This rough optimization is then used in a third step to fine tune the fragmentor voltage for the compound of interest. Using the optimal fragmentor voltage, the analyte is injected using "Product Ion Scan" mode. This mode determines the most abundant product ions at varying collision energies, which are selected for future use. MRM mode is then used at varying collision energies to determine the optimal collision energy for each product ion. These settings are then used to perform a narrow mass scan to accurately determine the m/z value for each product ion. These results are then compiled to form the usable MRM method.[38] This process was performed using a GlcN standard (10 ppm). The mass spectra generated from this process used for analysis is shown in Figure 2.4. The parameters chosen to generate this analysis are summarized in Appendix 1, and the raw data

is also found in Appendix 1. The most abundant product ion (162.1) was chosen to be the quantifier, which is the ion all quantification is based on.

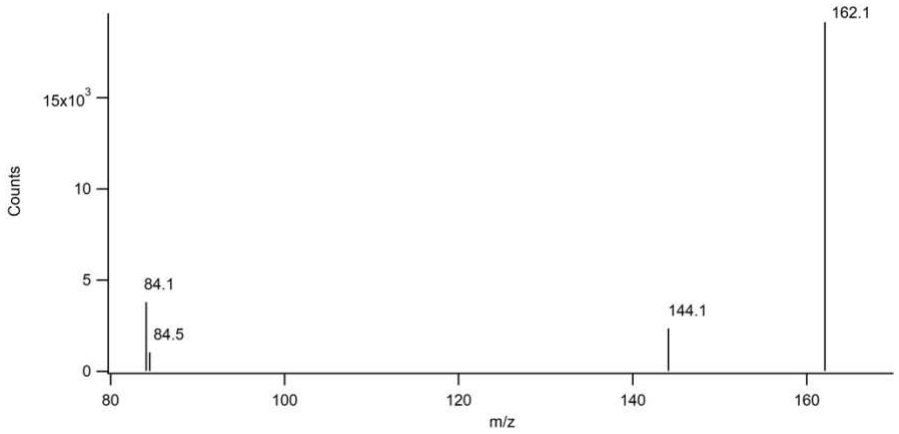

Figure 2.4: Overlay of all MRM transitions used for GlcN analysis in this study.

2.4.2 Liquid Chromatography Method Development

The mobile phase components are extremely important to the overall signal produced since the composition of both the stationary and mobile phases determines the rate at which the analytes pass through the column. The amount of time it will take for a compound to travel the length of the column is determined by the amount of time a compound spends adsorbed to the stationary phase and the amount of time the same compound spends in solution in the mobile phase.[39] For this analysis, a binary solvent system was chosen. GlcN is soluble in water, so water was chosen as the aqueous phase. Changing the pH of the aqueous solvent, percent organic composition, and/or identity of the organic solvent drastically changes the overall chromatography. Changes in pH can affect the protonation state of analytes, changing the percent organic composition affects the overall polarity of the mobile phase, which changes the retention time of the compounds, and changing the identity of the organic phase changes the viscosity, pressure, and polarity relative to percent organic composition for the liquid phase.[40] To ensure protonation of the GlcN molecules, 0.1% Formic Acid (v/v) was added to both the aqueous phase

and the organic phase. 10 mM ammonium acetate was added to the aqueous phase to improve the signal stability and reproducibility.[41,42] Acetonitrile (ACN) was chosen as the organic phase because it is a polar aprotic solvent. ACN is much less capable of hydrogen bonding with itself, but still has a high dielectric constant. This allows compounds like GlcN to retain on the column and clearly elute at a later time. Polar protic solvents, like methanol (MeOH) have a high elution strength, so they will push compounds like GlcN off the column too quickly.[43]

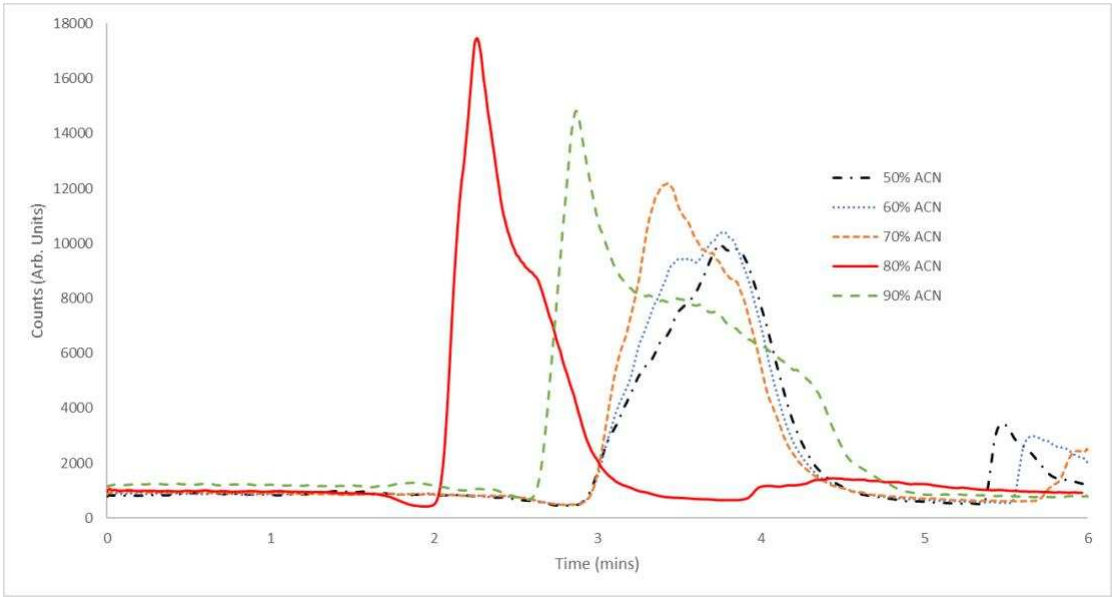

Figure 2.5: Total Ion Chromatograms for GlcN with various mixtures of organic and aqueous solvents as the mobile phase. Legend details percent of organic solvent (ACN) in mobile phase.

To determine the ratio of organic to aqueous phase optimal for the analysis of GlcN, runs at varying ACN:H_2O ratios were carried out and the data compared. The total ion chromatograms for each ratio are shown in Figure 2.5. The ratio of 80:20 ACN:H_2O was chosen due to the overall peak shape and height. The peak (depicted in red in Figure 2.5) is fairly gaussian in distribution, with a tail off the back end that is not nearly as pronounced as that of other peaks (90:10 ACN:H_2O). It also is the highest intensity peak, which will allow for the most accurate data collection, as it has the highest signal to noise. This isocratic mobile phase, 80% ACN with

0.1% formic acid and 20% H_2O with 0.1% formic acid and 10 mM ammonium acetate, was used for all analysis in this chapter.

The mobile phase was also compared to the mobile phases for other works that describe a detection of glucosamine.[29, 33-35] The results of this comparison can be found in Table 2.2 and Appendix 1. This comparison showed the mobile phase used for this work lead to the highest integrated peak area for glucosamine. The method used by Zhong et. al.[33] was more gaussian, had a higher maximum peak height, and had a lower retention time than the other tested methods. However, due to the trend toward simpler mobile phases in pharmaceutical and medical applications, acidic additives over 1% are discouraged due to their extremely low pH.[44] Due to these factors, the mobile phase developed for this work was chosen for analysis of glucosamine.

Table 2.2: Comparison of Recent Reported UHPLC Methods for Glucosamine Detection

Work	Mobile Phase	Integrated Peak Area
This work	80:20 ACN with 0.1% formic acid:H_2O with 0.1% formic acid and 10 mM ammonium acetate	3748094.61
Zhong et. al. (2007)[33]	50:50:2.5 v/v/v ACN:H_2O:Acetic Acid	4788209.73
Pastorini et. al. (2011)[35]	80:20 ACN:10 mM ammonium acetate	5114357.99
Allison et. al. (2021)[29]	80:20 ACN with 10mM ammonium acetate and 0.05% formic acid:H_2O with 10 mM ammonium acetate and 0.05% formic acid	3958200.10

2.4.3 Method Validation

Using the developed mass spectra method and the developed mobile phase, a calibration curve was generated using GlcN standards and the peak area of the most abundant fragment, m/z 161.2. This calibration curve is shown in Figure 2.6.

As shown in Figure 2.6, GlcN detection method displays high internal repeatability, with an R^2 of 0.9996, and less than 8% variance for each point, with most points having variances less than 5%. The limits of detection and quantification were determined using linear least-squares analysis and were calculated to be 0.020 ± 0.001 ng/mL and 0.061 ± 0.004 ng/mL, respectively. These values are comparable to other reported LC-QQQ methods (Table 2.3) with the aim of detecting GlcN in complex matrices using UHPLC-ESI-MS-MS.[31,35,45] This assay is the first to use this detection method for the purpose of detecting GlcN in fungal matrices

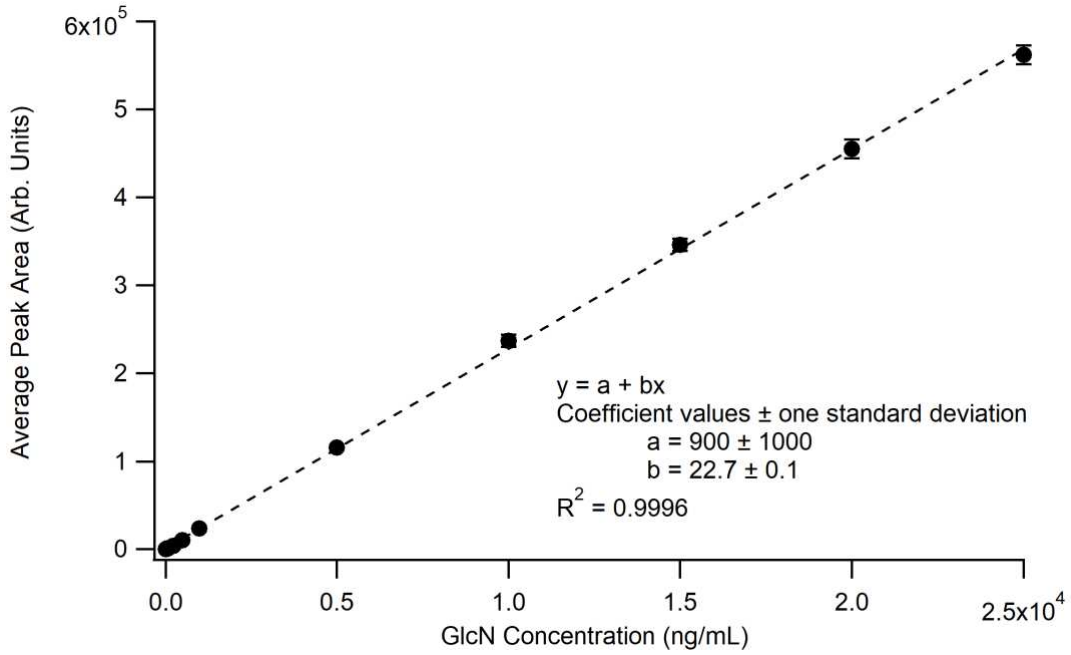

Figure 2.6: Calibration curve obtained and used for calculations in this work. Each data point represents an n=5.

Table 2.3: Comparison of recent reports using UHPLC-ESI-MS-MS for analysis of GlcN.
*Work included a pre-column derivatization step.

Work	Limit of Detection
This study	0.12 µg/mL
Song et. al. (2012)[31]	1.80 µg/mL in urine and 0.012 µg/mL in plasma*
Quigley et. al. (2017)[45]	0.25 µg/mL
Pastorini et. al. (2009)[35]	0.01 µg/mL – samples were prepared in ammonium acetate buffer rather than water

2.4.4 Quantification of GlcN in Aspergillus Cells

To demonstrate the validity of detection of GlcN from a complex matrix, samples of *A. niger* were obtained from cultures on an agar medium. Samples were lysed, vortexed, dried and weighed, and degraded in 10 M HCl. The degraded samples were then reconstituted in water, filtered, and analyzed using the method developed. The results of this analysis are shown in Figure 2.7.

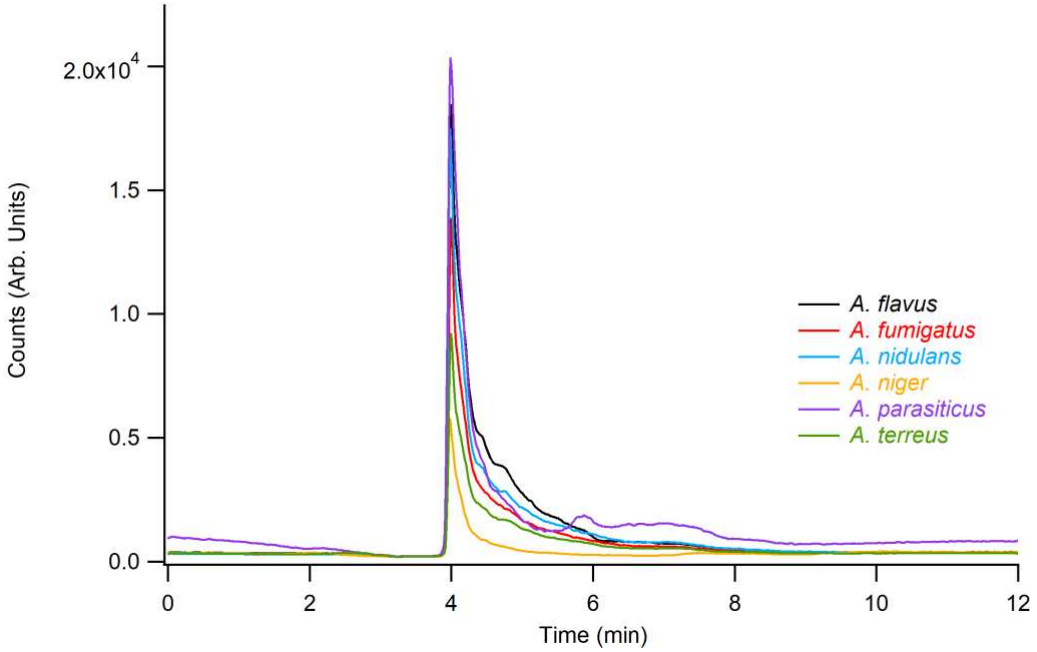

Figure 2.7: Comparison of Total Ion Chromatograms generated from representative samples of HCl degraded *Aspergillus* species

The amount of glucosamine in each species was compared to the starting mass of fungus used in each sample, and the percent by weight for each species was calculated. These results can be found in Table 2.4. Each species shows a statistically significantly different percent glucosamine by mass, which shows that this method has a potential for the method to also be species specific, rather than just a general quantification method. However, more studies to validate the difference in glucosamine percent by species are needed to validate this claim.

Table 2.4: Comparison of glucosamine detected from several pathogenic species of *Aspergillus*.

Aspergillus species	Percent glucosamine by weight
A. flavus	1.35 ± 0.02%
A. fumigatus	3.04 ± 0.02%
A. nidulans	4.09 ± 0.03%
A. niger	1.05 ± 0.08%
A. parasiticus	1.43 ± 0.02%
A. terreus	0.76 ± 0.03%

Excitingly, the results described show the validity of the method and demonstrate that the amount of GlcN is both qualitatively and quantitatively available for analysis in *Aspergillus*. This method can serve as a low-level detection method for fungus in biological samples due to its specificity. Quantification can be used to determine the amount of fungus in a sample as well as comparisons of GlcN in fungal samples at different stages of growth.

2.5 Conclusions

This chapter details a qualitative and quantitative method to detect GlcN from samples containing *Aspergillus* species. The method reported here is more sensitive compared to other GlcN detection assays, has high levels of repeatability, and does not require a derivatization step which enhances assay specificity. This is the first study to use tandem mass spectrometry to quantify the amount of GlcN in *Aspergillus* species, with the potential to compare stages of

growth. Developing methods for detecting *Aspergillus sp*. in biological matrices and clinical samples is a logical next step to achieve this goal of a new diagnostic standard. With these future tests in mind, this method represents a potential new diagnostic standard for detection of *Aspergillus sp.* in human patients with suspected pulmonary fungal infections.

CHAPTER 2 – REFERENCES

(1) Allison, C.; Moskaluk, A.; VandeWoude, S.; Reynolds, M. Detection Of Glucosamine As A Marker For Aspergillus Niger: A Potential Screening Method For Fungal Infections. *Anal Bioanal Chem* 2021, 413 (11), 2933-2941. https://doi.org/10.1007/s00216-021-03225-7.

(2) *About Fungal Diseases*. CDC. https://www.cdc.gov/fungal/about/?CDC_AAref_Val= (accessed April 5, 2021).

(3) Veríssimo, C. Fungal Infections. In *Environmental Mycology in Public Health*; Viegas, C.; Pinheiro, A. C., Sabino, R., Viegas, S., Brandão, J., Veríssimo, C., Eds.; Elsevier, 2016; pp 27-34.

(4) Bongomin, F.; Gago, S.; Oladele, R.; Denning, D. Global and Multi-National Prevalence Of Fungal Diseases – Estimate Precision. *Journal of Fungi* 2017, *3* (4), 57. https://doi.org/103390/jof3040057.

(5) Li, Z.; Lu, G.; Meng, G. Pathogenic Fungal Infection in the Lung. *Front Immunol* 2019, *10*. https://doi.org/10.3389/fimmu.2019.01524.

(6) Samson, R. A.; Visagie, C. M.; Houbraken, J.; Hong, S. -B.; Hubka, V.; Klaassen, C. H. W.; Perrone, G.; Seifert, K. A.; Susca, A.; Tanney, J. B.; Varga, J.; Kocsubé, S.; Szigeti, G.; Yaguchi, T.; Frisvad, J. C. Phylogeny, Identification and Nomenclature of the Genus *Aspergillus*. *Stud Mycol* 2014, *78* (1), 141-173. https://doi.org/10.1016/j.simyco.2014.07.004.

(7) Person, A. K.; Chudgar, S. M.; Norton, B. B.; Tong, B. C.; Stout, J. E. Aspergillus Niger: An Unusual Cause of Invasive Pulmonary Aspergillosis. *J Med Microbiol* 2010, *59* (7), 834-838. https://doi.org/10.1099/jmm.0.018309-0.

(8) von Eiff, M.; Roos, N.; Schulten, R.; Hesse, M.; Zühlsdorf, M.; van de Loo, J. Pulmonary Aspergillosis: Early Diagnosis Improves Survival. *Respiration* 1995, *62* (6), 341-347. https://doi.org/10.1159/000196477.

(9) *Fungal Disease Frequency - Gaffi*. https://www.gaffi.org/why/fungal-disease-frequency/ (accessed Apr 5, 2021).

(10) Donnelly, J. P; Chen, S. C.; Kauffman, C. A.; Steinbach, W. J.; Baddley, J. W.; Werweij, P. E.; Clancy, C. J.; Wingard, J. R.; Lockhard, S. R.; Groll, A. H.; Sorrell, T. C.; Bassetti, M.; Akan, H.; Alexander, B. D.; Andes, D.; Azoulay, E.; Bialek, R.; Bradsher, R. W.; Bretagne, S.; Calandra, T.; Caliendo, A. M.; Castagnola, E.; Cruciani, M.; Cuenca-Estrella, M.; Decker, C. F.; Desai, S. R.; Fisher, B.; Harrison, T.; Heussel, C. P.; Jensen, H. E.; Kibbler, C. C.; Kontoyiannis, D. P.; Kullberg, B.-J.; Lagrou, K.; Lamoth F.; Lehyrnbecher. T.; Loeffler, J.; Lortholary, O.; Maertens, J.; Marchetti, O.; Marr, K. A.; Masur, H.; Meis, J. F.; Morrisey, C. O.; Nucci, M.; Ostrosky-Zeichner, L.; Pagano, L.; Patterson, T. F.; Perfect, J. R.; Racil, Z.; Roilides, E.; Ruhnke, M.; Prokop, C. S.; Shoham, S.; Slavin, M. A.; Stevens, D. A.; Thompson, G. R.; Vazquez, J. A.; Viscoli, C.; Walsh, T. J.; Warris, A.; Wheat, L. J.; White, P. L.; Zaoutis, T. E.; Pappas, P. G. Revision and Update of the Consensus Definitions of Invasive Fungal Disease From the European Organization for Research and Treatment of Cancer and the Mycoses Study Group Education and Research Consortium. *Clinical Infectious Diseases* 2020, *71* (6), 1367–1376. https://doi.org/10.1093/cid/ciz1008.

(11) Bosshard, P. P. Incubation of Fungal Cultures: How Long Is Long Enough? *Mycoses* 2011, *54* (5), e539-e545. https://doi.org/10.1111/j.1439-0507.2010.01977.x.

(12) Barton, R C. Laboratory Diagnosis of Invasive Aspergillosis: From Diagnosis to Prediction Of Outcome. *Scientifica (Cairo)* 2013, *2013*, 1-29. https://doi.org/10.1155/2016/459405.

(13) Ruhnke, M.; Böhme, A.; Buchheidt, D.; Cornely, O.; Donhuijsen, K.; Einsele, H.; Enzensberger, R.; Hebart, H.; Heussel, C. P.; Horger, M.; Hof, H.; Karthaus, M.; Krüger, W.; Maschmeyer, G.; Penack, O.; Ritter, J.; Schwartz, S. Diagnosis Of Invasive Fungal Infections In Hematology And Oncology—Guidelines From The Infectious Diseases Working Party In Haematology And Oncology Of The German Society For Haematology And Oncology (AGIHO). *Annals of Oncology* 2012, *23* (4), 823-833. https://doi.org/10.1093/annonc/mdr407.

(14) Egger, M.; Jenks, J. D.; Hoenigl, M.; Prattes, J. Blood Aspergillus PCR: The Good, The Bad, and the Ugly. *Journal of Fungi* 2020, *6* (1), 18. https://doi.org/10.3390/jof/6010018.

(15) Cruciani, M.; Mengoli, C.; Barnes, R.; Donnelly, J. P.; Loeffler, J.; Jones, B. L.; Klingspor, L.; Maertens, J.; Morton, C. O.; White, L. P. Polymerase Chain Reaction Blood Tests for the Diagnosis of Invasive Aspergillosis in Immunocompromised People. *Cochrane Database of Systematic Reviews* 2019, *2019* (9). https://doi.org/10.1002/14651858.CD00951.pub4.

(16) Cornely, O. A., Hoenigl, M., Lass-Flörl, C., Chen, S.C.; Kontoyiannis, D.P.; Morrissey, C.O.; et. al. Defining Breakthrough Invasive Fungal Infection-Position Paper of the Mycoses Study Group Education and Research Consortium and the European

Confederation of Medical Mycology, *Mycoses.* 2019, *62* (9), 716-729. https://doi.org/10.1111/myc.12960.

(17) Rath, P.M.; Steinmann, J.; Overview of Commercially Available PCR Assays for the Detection of Aspergillus Spp. DNA in Patient Samples., *Frontiers in Microbiology*. Frontiers Media S.A. April 24, 2018. https://doi.org/10.3389/fmicb.2018.00740.

(18) Grebe, S.; Singh, R. LC-MS/MS In The Clinical Laboratory - Where To From Here?. The Clinical Biochemist Reviews 2011, 32 (2), 5-31.

(19) Banerjee, S. Empowering Clinical Diagnostics with Mass Spectrometry. *ACS Omega* 2020, *5* (5), 2041-2048. https://doi.org/10.1021/acsomega.9b03764.

(20) Dong, X.; Mondello, S.; Kobeissy, F.; Ferri, R.; Mechref, Y. Serum Glycomics Profiling of Patients With Primary Restless Legs Syndrome Using LC–MS/MS. *J Proteome Res* 2020, *19* (8), 2933-2941. https://doi.org/10.1021/acs.jproteome.9b00549.

(21) Saadi, J.; Oueslati, S.; Bellanger, L.; Gallais, F.; Dortet, L.; Roque-Afonso, A.-M.; Junot, C.; Naas, T.; Fenaille, F.; Becher, F. Quantitative Assessment Of SARS-Cov-2 Virus in Nasopharyngeal Swabs Stored in Transport Medium by a Straightforward LC-MS/MS Assay Targeting Nucleocapsid, Membrane, And Spike Proteins. *J Proteome Res* 2021, *20* (2), 1434-1443. https://doi.org/10.1021/acs.jproteome.0c00887.

(22) Chitnis, T.; Glanz, B. I.; Gonzalez, C.; Healy, B. C.; Saraceno, T. J.; Sattarnezhad, N.; Diaz-Cruz, C.; Polgar-Turcsanyi, M.; Tummala, S.; Bakshi, R.; Bajaj, V. S.; Ben-Shimol, D.; Bikhchandani, N.; Blocker, A. W.; Burkart, J.; Cendrillon, R.; Cusack, M. P.; Demiralp, E.; Jooste, S. K.; Kharbouch, A.; Lee, A. A.; Lehár, J.; Liu, M.; Mahadevan, S.; Murphy, M.; Norton, L. C.; Parlikar, T. A.; Pathak, A.; Shoeb, A.; Soderberg, E.; Stephens, P.; Stoertz, A. H.; Thng, F.; Tumkur, K.; Wang, H.; Rhodes, J.; Rudick, R. A.; Ransohoff,

R. M.; Phillips, G. A.; Bruzik, E.; Marks, W. J.; Weiner, H. L.; Snyder, T. M. Quantifying Neurologic Disease Using Biosensor Measurements In-Clinic and in Free-Living Settings in Multiple Sclerosis. *NPJ Digit Med* 2019, *2* (1), 123. https://doi.org/10.1038/s41746-019-0197-7.

(23) Whiley, L.; Nye, L. C.; Grant, I.; Andreas, N.; Chappell, K. E.; Sarafian, M. H.; Misra, R.; Plumb, R. S.; Lewis, M. R.; Nicholson, J. K.; Holmes, E.; Swann, J. R.; Wilson, I. D. Ultrahigh-Performance Liquid Chromatography Tandem Mass Spectrometry with Electrospray Ionization Quantification of Tryptophan Metabolites and Markers of Gut Health in Serum and Plasma—Application to Clinical and Epidemiology Cohorts. *Anal Chem* 2019, *91* (8), 5207–5216. https://doi.org/10.1021/acs.analchem.8b05884.

(24) Spiller, S.; Frolov, A.; Hoffmann, R. Quantification of Specific Glycation Sites in Human Serum Albumin as Prospective Type 2 Diabetes Mellitus Biomarkers. *Protein & Peptide Letters* 2018, *24* (10), 887-896. https://doi.org/10.2174/0929866524666170202124120.

(25) Benito, S.; Sánchez-Ortega, A.; Unceta, N.; Goicolea, M. A.; Barrio, R. J. LC-QQQ-MS Routine Analysis Method for New Biomarker Quantification in Plasma Aimed at Early Chronic Kidney Disease Diagnosis. *J Pharm Biomed Anal* 2019, *169*, 82–89. https://doi.org/10.1016/j.jpba.2019.02.042.

(26) Choi, Y.; Kim, E.; Piao, Z.; Yun, Y.; Shin, Y. Purification and Characterization Of Chitosanase From Bacillus Sp. Strain KCTC 0377BP And Its Application For The Production Of Chitosan Oligosaccharides. *Appl. Environ. Microbiol.* 2004, *70* (9), 5633-4531. https://doi.org/10.1128/AEM.70.8.4522-4531.2004.

(27) Lenardon, M. D.; Munro, C. A.; Gow, N. A. R. Chitin Synthesis and Fungal Pathogenesis. *Curr Opin Microbiol.* 2010, *13* (4), 416-423. https://doi.org/10.1016/j.mib.2010.05.002

(28) Singh, D. K.; Ray, A. R. Biomedical Applications of Chitin, Chitosan, and Their Derivatives. *Journal of Macromolecular Science, Part C: Polymer Reviews* 2000, *40* (1), 69–83. https://doi.org/10.1081/MC-100100579.

(29) Rinaudo, M. Chitin and Chitosan: Chemistry, Properties and Applications. *J. Sci. Ind. Res.* 2004, *63* (1), 20-31. https://doi.org/10.1016/j.progpolymsci.2006.06.001

(30) Beaudry, F.; Vachon, P. Determination of Glucosamine in Horse Plasma by Liquid Chromatography Tandem Mass Spectrometry. *Biomed Chromatogr* 2008, *22* (1), 1-4. https://doi.org/10.1002/bmc.906.

(31) Song, M.; Hang, T.; Wang, C.; Yang, L.; Wen, A. Precolumn Derivatization LC–MS/MS Method for the Determination and Pharmacokinetic Study of Glucosamine in Human Plasma and Urine. *J Pharm Anal* 2012, *2* (1), 19-28. https://doi.org/10.1016/j.jpha.2011.08.003.

(32) Persiani, S.; Rotini, R.; Trisolino, G.; Rovati, L. C.; Locatelli, M.; Paganini, D.; Antonioli, D.; Roda, A. Synovial and Plasma Glucosamine Concentrations in Osteoarthritic Patients Following Oral Crystalline Glucosamine Sulphate at Therapeutic Dose. *Osteoarthritis Cartilage* 2007, *15* (7), 764-772. https://doi.org/10.1016/j.joca.2007.01.019.

(33) Zhong, S.; Zhong, D; Chen, X. Improved and Simplified Liquid Chromatography/Electrospray Ionization Mass Spectrometry Method for the Analysis of Underivatized Glucosamine in Human Plasma. *Journal of Chromatography B* 2007, *854* (1-2), 291-298. https://doi.org/10.1016/j.jchromb.2007.04.043.

(34) Roda, A.; Sabatini, L.; Barbieri, A.; Guardigili, M.; Locatelli, M.; Violante, F. S.; Rovati, L. C.; Persiani, S. Development and Validation of a Sensitive HPLC-ESI-MS/MS Method for the Direct Determination of Glucosamine in Human Plasma. *Journal of*

Chromatography B 2006, *844* (1), 119-126. https://doi.org/10.1016/j.jchromb.2006.07.013.

(35) Pastorini, E.; Vecchiotti, S.; Colliva, C.; Persiani, S.; Rotini, R.; Roatti, G.; Zaccarelli, L.; Rovati, L. C.; Roda, A. Identification and Quantification of Glucosamine in Rabbit Cartilage and Correlation of Plasma Levels by High Performance Liquid Chromatography-Electrospray Ionization-Tandem Mass Spectrometry. *Anal Chim Acta* 2011, *695* (1-2), 77-83. https://doi.org/10.1016/j.aca.2011.04.003.

(36) Kim, J.; Kim, J.; Hong, J.; Lee, S.; Park, S.; Lee, J.; Kim, J. LC–MS/MS Analysis Of Chitooligosaccharides. *Carbohyd Res* 2013, *372*, 23-29. https://doi.org/10.1016/j.carres.2013.02.007

(37) Guan, Y.; Tian, Y.; Li, Y.; Yang, Z.; Jia, Y.; Hang, T.; Wen, A. Application of a Liquid Chromatographic/Tandem Mass Spectrometric Method to a Kinetic Study of Derivative Glucosamine in Healthy Human Urine. *J Pharm Biomed Anal* 2011, *55* (1), 181-186. https://doi.org/10.1016/j.jpba.2011.01.012.

(38) MassHunter Optimizer Software for Automated MRM Method Development Using the Agilent 6400 Series Triple Quadrupole Mass Spectrometers. https://www.agilent.com/cs/library/technicaloverviews/Public/5990-9011en_lo%20CMS.pdf (accessed Apr 5, 2021).

(39) Barkovich, M. High Performance Liquid Chromatography. https://chem.libretexts.org/Courses/BethuneCookman_University/BCU%3A_CH-346_Instrumental_Analysis/Chromatography_High_Performance_Liquid_Chromatography (accessed Apr 5, 2021)

(40) Dolan, J.; Snyder, L.; Kirkland, J. Introduction to Modern Liquid Chromatography; Wiley: 2013; pp 304-317, 879-886.

(41) Sterling, H. J.; Batchelor, J. D.; Wemmer, D. E.; Williams, E. R. Effects of Buffer Loading for Electrospray Ionization Mass Spectrometry of a Noncovalent Protein Complex That Requires High Concentrations of Essential Salts. *J Am Soc Mass Spectrom* 2010, *21* (6) 1045-1049. https://doi.org/10.1016/j.jasms.2010.02.003.

(42) Konermann, L. Addressing a Common Misconception: Ammonium Acetate as Neutral Ph "Buffer" for Native Electrospray Mass Spectrometry. *J Am Soc Mass Spectrom* 2017, *28* (9), 1827-1835. https://doi.org/10.1007/s13361-017-1739-3.

(43) Greco, G.; Letzel, T. HILIC Mobile Phase: Solvents. https://learning.sepscience.com/hubfs/Technical%20Blogs/HILIC_4.pdf (accessed Apr 5, 2021).

(44) Boyes, B. E.; Dong, M. W. Modern Trends and Best Practices in Mobile-Phase Selection in Reversed-Phase Chromatography. *LCGC North America* 2018, *36* (10), 752-768.

(45) Legido-Quigley, C.; Zheng, L.; Han, P.; Kim, M. Determination of glucosamine in food supplements by HILIC-ESI-MS. *European Pharmaceutical Review* 2017, No. 5.

CHAPTER 3

Detection of Glucosamine in Diagnostically Relevant Media

3.1 Overview

In this chapter, I discuss further method validation for the clinical application of the methods described in Chapter 2. Artificial sputum medium and artificial bronchioalveolar lavage fluid were used to determine the matrix effects of clinical samples on the method previously described. These tests included a negative control to determine the glucosamine content of degraded media, a positive control to determine matrix effects of media inoculated with glucosamine, and a combined method where media was inoculated with *Aspergillus niger* and degraded to determine the glucosamine concentration. A solid phase extraction method was also tested to potentially separate glucosamine from the biological matrices. Unfortunately, the results of the degradations and inoculations were inconsistent and did not lend themselves to a quantified measure of the matrix effects of the media on the samples. The method of separation was also unsuccessful. The results detailed in this chapter show that the method developed in Chapter 2 requires further validation before it can be implemented on clinical samples.

The liquid chromatography mass spectrometry method used in this chapter was developed and constructed by Madeline Schwarz. Biological media experiments were performed using the acid degradation protocol developed by Chris Allison[1] and were carried out by Madeline Schwarz. Melissa M. Reynolds was the advisor on this project.

3.2 Introduction

In order for a bioanalytical method to be applied in a clinical setting, it must undergo rigorous development and validation. Reliability of analytical findings is crucial for many reasons, including to ensure appropriate treatment of patients.[2] The US Food and Drug Administration (FDA) has published and updated guidelines for bioanalytical method validation, with criteria such as selectivity, accuracy, prevision, recovery, calibration curve, and limits of quantification.[3] These guidelines are shown in Table 3.1. These method development standards can initially be applied to "neat" standards (standards of the analyte of interest dissolved in solvent instead of the biological matrix) but should eventually be moved to the biological matrix of interest. Assessing the compound of interest in the proposed sample matrix is important to ensure the validity of the calibration curve, assess matrix effects, and determine if any additional sample preparation steps are needed.[2]

When diagnosing cases of invasive pulmonary aspergillosis (IPA), physicians primarily take samples from a variety of locations, depending on the diagnostic technique to be used. For tissue culture, the gold standard for diagnosis of IPA, samples are collected by fine needle aspiration, open biopsy, or blood.[4-8] When performing non-culture tests for IPA (PCR, ELISA, etc.), the most common sample types are cerebrospinal fluid, serum, bronchioalveolar lavage fluid (BALF), and sputum.[6-8] Bronchioalveolar lavage alone is, when compared to biopsy, a safer and simpler procedure, and is a very reliable sample type for currently used assays.[7,9] Sputum for diagnosis if IPA is a recent development in the field, as it is also easy to collect as bronchioalveolar lavage is an invasive procedure that may not be feasible for some patients.[7,8]

Table 3.1: FDA Bioanalytical Method Validation Recommendation for Chromatographic Assays[3]

Parameter	Elements	Acceptance Criteria
Calibration Curve	• A blank (no analyte), and at least 6 non-zero calibrator levels covering the quantitation range, including LLOQ in every run. • All blanks and calibrators should be in the same matrix as the study samples • The concentration-response relationship should be fit with the simplest regression model.	• Non-zero calibrators should be ±15%, except at LLOQ where the calibrator should be ±20% of nominal concentrations in each run • 75% and a minimum of 6 non-zero calibrator levels should meet the above criteria in each validation run
Quality Controls	• **For A&P Runs:** 4 QC's, including LLOQ, low (L: 3x LLOQ), mid (M: mid-range), and high (H: high-range) from at least five replicates in at least 3 runs • **For other validation runs:** L,M, and H QC's in duplicates	• Refer to A&P Runs, Other Validation Runs, and Stability Evaluations
Selectivity/Specificity	• Analyze blank samples of the appropriate biological matrix from at least six individual sources. • The method should be assessed for interference by cross-reacting molecules, concomitant medications, bio-transformed species, etc.	• Blanks should be free of interference at the retention times of the analyte(s). • Spikes samples should be ±20% LLOQ
Carryover	• The impact of carryover on the accuracy of the study sample concentrations should be assessed	• Carryover should not exceed ±20% LLOQ
Sensitivity	• The lowest non-zero standard on the calibration curve defines the sensitivity (LLOQ)	• The analyte response at the LLOQ should be ≥5 times the analyte response of the zero calibrator. • The accuracy should be ±20% of nominal concentration (from ≥5 replicates from at least 3 runs)

		• The precision should be at least ±25% CV (from ≥3 replicates in at least 6 runs)
Accuracy & Precision (A&P)	• A&P should be established with at least 3 independent A&P runs, 4 QC levels per run (LLOQ, L, M, H) and ≥5 replicates per QC level	• The run should meet the calibration curve acceptance criteria and should include the LLOQ calibrator. • This run has no QC acceptance criteria. • *Accuracy*: ±15% of nominal concentrations, ±20% at LLOQ • *Precision*: ±15% CV, ±20% at LLOQ • Both accuracy and precision must be determined within and between runs
Other Validation Runs	• ≥3 QC Levels (L, M, H) in at least duplicates in each run	• Meet the calibration acceptance criteria. • ≥67% of QC's should be ±15% of the nominal values, ≥50% of QC's per level should be ±15% of their nominal concentrations

In this chapter, artificial sputum medium (ASM) and artificial BALF (ABALF) are used to test the clinical viability of the method developed in Chapter 2. Samples of ASM and ABALF were inoculated with glucosamine (GlcN) and/or fungal cells to evaluate the matrix effects and viability of the method.

3.3 Experimental

3.3.1 Materials

D-Glucosamine HCl was obtained from MP Biomedicals (Santa Ana, CA). ACS-grade acetone, Optima LC-MS grade formic acid, Optima LC-MS acetonitrile, Optima LC-MS water, and ammonium acetate (>98.0%) were obtained from Fisher Chemical (Waltham, MA). Hydrochloric acid was obtained from Ward's Science (Rochester, NY). 0.2-µm Captiva

Econofilters were obtained from Agilent (Palo Alto, CA). ASM and ABALF were obtained from Biochemazone (Leduc, Alberta, Canada) *A. niger* fungi were obtained from domestic cat hair samples and cultured on an agar medium for 14 days. Solid phase extraction columns were obtained from Phenomenex (Torrance, CA).

3.3.2 Sample preparation

A. niger was grown and maintained on potato dextrose agar at 25 °C until harvesting. Fungal cells were transferred into 15-mL centrifuge tubes containing 5 mL chilled acetone (-20 °C) in a biosafety hood. To promote cell lysis, samples were incubated at -20 °C for 60 minutes. Samples were then centrifuged for 10 min at 1300 kxg. The supernatant was decanted, and the sample was dried under vacuum to determine the weight of the lysed fungal cells. To each of the dried pellets, 2 mL of respective media was added and vortexed to suspend the lysed fungal cells. The mixtures were then transferred to a 50 mL round bottom flask and degraded in 5 mL of 10 M HCl in a hot oil bath (90 °C) for approximately 3 hours, or until all HCl was evaporated. The degraded samples were reconstituted in 5 mL of Millli-Q grade water (18.2 MΩ·cm) and stirred at 90°C for 30 minutes. The reconstituted samples were then passed through 0.2-µm filters and analyzed via the LC-QQQ method developed in Chapter 2.

3.3.3 LC-QQQ Methods

LC-QQQ analyses were carried out on an Agilent 6470 triple quadrupole mass spectrometer coupled to a 1290 high speed liquid chromatograph. Separations were performed using a Thermo Fisher Acclaim HILIC-10 column with dimensions of 4.6x150 mm and 5-µm particle size. Mobile phase A was composed of LC-MS grade water with 10 mM ammonium acetate and 0.1% (v/v) formic acid. Mobile phase B was acetonitrile (ACN) with 0.1% (v/v) formic acid. The flow rate was 0.500 mL/min, and a 20-minute runtime was used. The elution

was isocratic at 80:20 for the duration of the separation. Electrospray ionization source was used in positive ionization mode. Ion source conditions were as follows: capillary voltage 1500 V; drying gas flow rate 6 L/min; desolvation line temperature 350 °C; nebulizer gas flow rate 55 L/min; nozzle voltage 2000 V; shielding gas flow 11 L/min; shielding gas temperature 400 °C.

3.3.4 Calculations

All values are reported as an average ± standard deviation unless otherwise indicated. All samples were run with an n=3 unless otherwise indicated

3.4 Results and Discussion

3.4.1 Detection of Glucosamine in media – before and after degradation

First, a negative control test was performed to determine if GlcN was present in the degraded artificial media samples to establish a baseline of detection if needed. As shown in Figure 3.1, no signal above baseline was detected using the LC-QQQ method, meaning no GlcN was detectable.

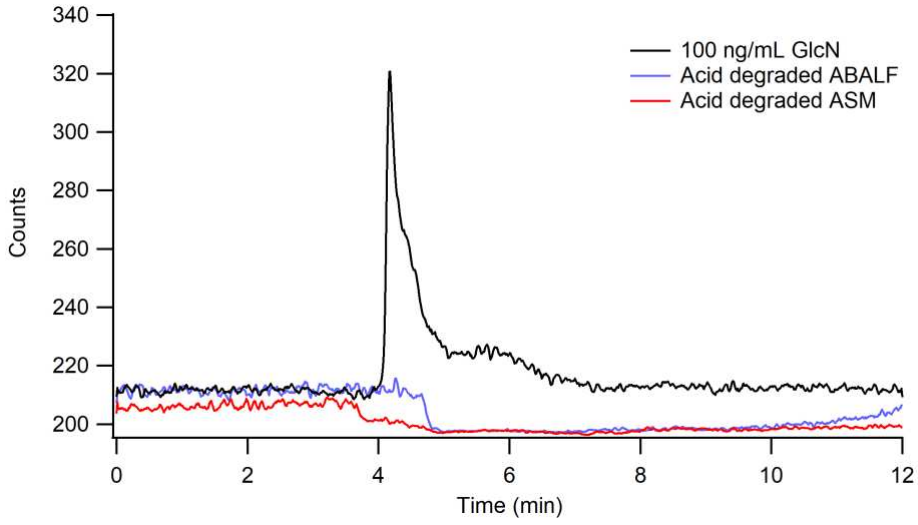

Figure 3.1: Degraded ASM and ABALF samples without GlcN inoculation compared to a neat GlcN standard.

Next, known concentrations of GlcN were spiked into 5 mL of the ASM and ABALF. The final concentration of GlcN in both solutions was calculated to be 9.98 µg/mL. No acid degradations were performed for this step, but the solutions were passed through the 2-micron filters to ensure no large particles entered the mass spectrometer. The resulting chromatograms are shown in Figure 3.2. It was determined that GlcN was detectable in both ASM (Figure 3.2A) and in ABALF (Figure 3.2B), with significant matrix effects. ASM caused a slight shift in retention time but a consistent peak shape, while ABALF caused no shift in retention time, but caused the peak shape to change drastically. The change caused in the ASM matrix is likely due to matrix effects associated with the sample medium.[10,11] ASM contains the primary components of human sputum, including lipids, micronutrients, amino acids, mucin, proteins, and DNA.[12] These components could change the retention time, as they could be effecting the interaction between the column and the analyte.[10] The change in ABALF signal is also likely due to interactions between the analyte interacting with the matrix. BALF, prior to running through the upper respiratory system, is comprised of normal saline (9 g NaCl per 1 L water),[13] which may be coupling with the glucosamine and causing slight changes in the retention times.

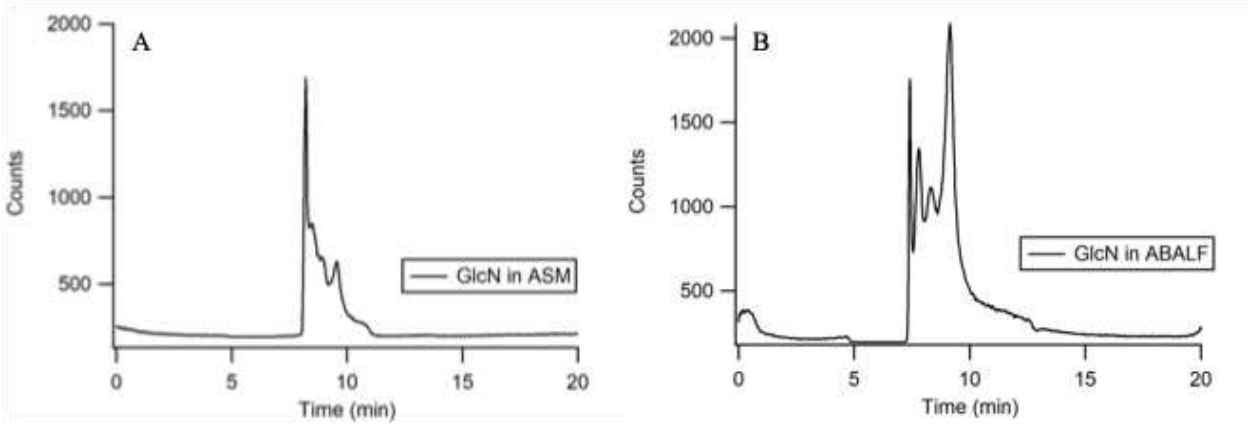

Figure 3.2: GlcN inoculated A: ASM and B: ABALF

To further examine the matrix effects of the chosen degradation method in media, samples of *Aspergillus niger* were added to both ASM and ABALF as described in the methodology. In short, samples were lysed, dried, and added to their respective media. Then, the fungal sample and media were subjected to the acid degradation protocol, and samples were tested on the LC-QQQ using the methods developed in Chapter 2. Surprisingly, the chromatographs produced from this experiment, shown in Figure 3.3, do not mimic the chromatographs depicted when analyzing GlcN in undegraded media.

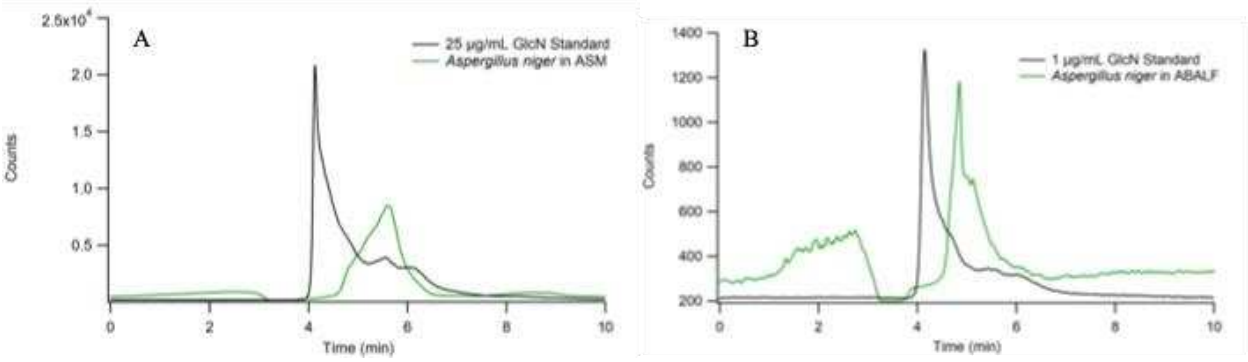

Figure 3.3: *Aspergillus niger* degraded in A: ASM and B: ABALF compared to a neat GlcN standard at A: 25 µg/mL and B: 1 µg/mL.

This change could be due to a variety of factors. First, the acid degraded media and undegraded media may have different chemical compositions that have different matrix effects on the glucosamine samples. Next, due to logistical constraints, not all experiments took place at the same time, so there may have been some degradation of the artificial media. This may have led to the variation in peak shape shown. Further testing would be needed to confirm either of these hypotheses. These future tests would include inoculating degraded media with known amounts of glucosamine to confirm peak shape and matrix effects, and either MS2 scans or trials

on a TOF-MS to determine the identity of the compounds. Further discussion of these future tests can be found in Chapter 6 of this work.

3.4.2 Solid Phase Extraction of Glucosamine

Solid phase extraction (SPE) is an effective way to prepare samples, very similar to liquid-liquid extraction. SPE extracts analytes of interest from the sample matrix by binding the analytes to a solid column prior to elution.[14] As shown in Figure 3.4, there are four main steps to solid phase extraction. First, the column is conditioned to better interact with the analytes for retention. Then, the sample is loaded onto the column. At this point, the liquid sample is allowed to pass through the column and the analytes of interest retain on the column. Next, the sample is washed, removing unwanted analytes and any remaining sample matrix from the column. Lastly, the analyte of interest is eluted. Solid phase extraction not only allows for the lessening of matrix effects, but also allows for samples to be concentrated if necessary.[14]

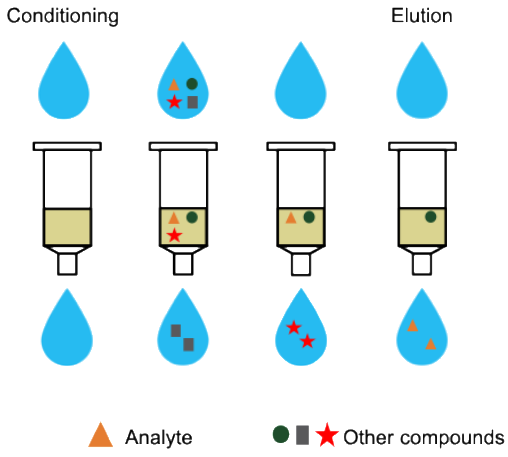

Figure 3.4: Solid Phase Extraction process

For the solid phase extraction, a Strata-X-C column was used (Phenomenex, Torrance, CA). The Strata-X-C column contains a strong cation-exchange polymeric sorbent that allows for retention of basic compounds with a pK_a≥10.5.[15] GlcN has a pK_a=7.58, making it nearly neutral,

but technically an extremely weak base.[16] This, theoretically, makes glucosamine an ideal candidate for elution from this column.

When tested, the elution scheme was as follows: first, the column was conditioned with 1 mL acetonitrile, then 1 mL of water. Then, the sample (10 µg/mL GlcN in water) was added and passed through the column. Next, the column was washed with 1 mL acetonitrile and dried for five minutes. Finally, the sample was eluted with 1 mL of acidified water (0.1% formic acid in water).

Unfortunately, after the above procedure was performed and the samples were tested using the method developed in Chapter 2, no GlcN was observed. This could be due to a couple of factors. First, the GlcN may not be retained on the column as previously thought. Elution of analytes during wash steps is a common problem with SPE method development.[17] Further, the elution solvent may not have been strong enough to fully elute the analyte of interest. This is also a common problem with SPE method development.[17] Further troubleshooting of the method is needed to understand how to best elute GlcN on the SPE column.

3.5 Conclusions

In this chapter, GlcN was tested in biological media to determine possible matrix effects. Samples of *A. niger* were also degraded in biological media to assess the viability of the method proposed in Chapter 2 for clinical samples. ASM and ABALF were chosen as sample media due to their relevancy in current testing for IPA. No GlcN was detected in ASM or ABALF, but when GlcN was added to undegraded ASM and ABALF, the peak shape changed drastically. When *A niger* was added to ASM and ABALF, the peak shape from GlcN was different from both the neat standard and the undegraded sample. The tests performed in this chapter show that further

work needs to be performed with this method and biological media before it can be applied in a clinical context.

CHAPTER 3 – REFERENCES

(1) Allison, C. L.; Moskaluk, A.; VandeWoude, S.; Reynolds, M. M. Detection of Glucosamine as a Marker for Aspergillus Niger: A Potential Screening Method for Fungal Infections. *Anal Bioanal Chem* 2021, *413* (11), 2933-2941. https://doi.org/10.1007/s00216-021-03225-7.

(2) Tiwari, G.; Tiwari, R. Bioanalytical Method Validation: An Updated Review. *Pharm Methods* 2010, *1* (1), 25-38. https://doi.org/10.4103/2229-4708.72226.

(3) FDA. *Bioanalytical Method Validation Guidance for Industry*; 2018. https://www.fda.gov/media/70858/download (accessed 2024-09-30).

(4) *About Fungal Diseases*. CDC. https://www.cdc.gov/fungal/about/?CDC_AAref_Val=https://www.cdc.gov/fungal/about-fungal-diseases.html (accessed 2024-09-30).

(5) Ledoux, M.-P.; Herbrecht, R. Invasive Pulmonary Aspergillosis. *Journal of Fungi* 2023, *9* (2), 131. https://doi.org/10.3390/jof9020131.

(6) Donnelly, J. P.; Chen, S. C.; Kauffman, C. A.; Steinbach, W. J.; Baddley, J. W.; Verweij, P. E.; Clancy, C. J.; Wingard, J. R.; Lockhart, S. R.; Groll, A. H.; Sorrell, T. C.; Bassetti, M.; Akan, H.; Alexander, B. D.; Andes, D.; Azoulay, E.; Bialek, R.; Bradsher, R. W.; Bretagne, S.; Calandra, T.; Caliendo, A. M.; Castagnola, E.; Cruciani, M.; Cuenca-Estrella, M.; Decker, C. F.; Desai, S. R.; Fisher, B.; Harrison, T.; Heussel, C. P.; Jensen, H. E.; Kibbler, C. C.; Kontoyiannis, D. P.; Kullberg, B.-J.; Lagrou, K.; Lamoth, F.; Lehrnbecher, T.; Loeffler, J.; Lortholary, O.; Maertens, J.; Marchetti, O.; Marr, K. A.; Masur, H.; Meis, J. F.; Morrisey, C. O.; Nucci, M.; Ostrosky-Zeichner, L.; Pagano, L.; Patterson, T. F.; Perfect,

J. R.; Racil, Z.; Roilides, E.; Ruhnke, M.; Prokop, C. S.; Shoham, S.; Slavin, M. A.; Stevens, D. A.; Thompson, G. R.; Vazquez, J. A.; Viscoli, C.; Walsh, T. J.; Warris, A.; Wheat, L. J.; White, P. L.; Zaoutis, T. E.; Pappas, P. G. Revision and Update of the Consensus Definitions of Invasive Fungal Disease From the European Organization for Research and Treatment of Cancer and the Mycoses Study Group Education and Research Consortium. *Clinical Infectious Diseases* 2020, *71* (6), 1367–1376. https://doi.org/10.1093/cid/ciz1008.

(7) Nuh, A.; Ramadan, N.; Shah, A.; Armstrong-James, D. Sputum Galactomannan Has Utility in the Diagnosis of Chronic Pulmonary Aspergillosis. *Journal of Fungi* 2022, *8* (2), 188. https://doi.org/10.3390/jof8020188.

(8) Xiao, W.; Gong, D.; Mao, B.; Du, X.; Cail, L.-L.; Wang, M.; Fu, J. Sputum Signatures for Invasive Pulmonary Aspergillosis in Patients with Underlying Respiratory Diseases (SPARED): Study Protocol for a Prospective Diagnostic Trial. *BMC Infect Dis* 2018, *18* (1), 271. https://doi.org/10.1186/s12879-018-3180-z.

(9) Levy, H.; Horak, D. A.; Tegtmeier, B. R.; Yokota, S. B.; Forman, S. J. The Value of Bronchoalveolar Lavage and Bronchial Washings in the Diagnosis of Invasive Pulmonary Aspergillosis. *Respir Med* 1992, *86* (3), 243–248. https://doi.org/10.1016/S0954-6111(06)80062-4.

(10) Fang, N.; Yu, S.; Ronis, M. J.; Badger, T. M. Matrix Effects Break the LC Behavior Rule for Analytes in LC-MS/MS Analysis of Biological Samples. *Exp Biol Med* 2015, *240* (4), 488–497. https://doi.org/10.1177/1535370214554545.

(11) Nasiri, A.; Jahani, R.; Mokhtari, S.; Yazdanpanah, H.; Daraei, B.; Faizi, M.; Kobarfard, F. Overview, Consequences, and Strategies for Overcoming Matrix Effects in LC-MS

Analysis: A Critical Review. *Analyst* 2021, *146* (20), 6049–6063. https://doi.org/10.1039/D1AN01047F.

(12) *Artificial Sputum Medium*. Biochemazone. https://biochemazone.com/product/artificial-sputum-medium/?attribute_ml=100+mL (accessed 2024-10-14).

(13) Dawlett, M.; Gonzalez, A. Common Crystalloid Intravenous Fluids. In *Core Concepts of Pediatrics, 2nd ed*; 2021.

(14) Badawy, M. E. I.; El-Nouby, M. A. M.; Kimani, P. K.; Lim, L. W.; Rabea, E. I. A Review of the Modern Principles and Applications of Solid-Phase Extraction Techniques in Chromatographic Analysis. *Anal Sci* 2022, *38* (12), 1457–1487. https://doi.org/10.1007/s44211-022-00190-8.

(15) *Strata-X-C SPE Products*. Phenomenex. https://www.phenomenex.com/products/strata-x-solid-phase-extraction-products/strata-x-c#overview (accessed 2024-10-14).

(16) National Center for Biotechnology Information. *PubChem Compound Summary for CID 439213; D-Glucosamine*. PubChem. https://pubchem.ncbi.nlm.nih.gov/compound/D-Glucosamine (accessed 2024-10-14).

(17) Raynie, D. E.; Watson, D. W. Understanding and Improving Solid-Phase Extraction. *LCGC North America* 2014, *32* (12), 908–915.

CHAPTER 4

Development of Separation and LC-QQQ Methods for the Detection of CBD, THC, and Metabolites in Human Plasma Samples

4.1 Overview

In this chapter, I develop a method for LC-QQQ to detect CBD, THC, and the major metabolites in human plasma samples. Cannabinoids and their metabolites are of major interest to the medical community, especially due to the major decriminalization of *Cannabis* in the United States. The results depicted in this chapter lay the groundwork for a quantitative and repeatable detection method for CBD, THC, THC-COOH, and 11-OH-THC in plasma samples. More work is needed before the method can be applied to clinical samples.

The liquid chromatography mass spectrometry method used in this chapter was developed and constructed by Jamie Cuchiaro and Madeline Schwarz. Blank plasma samples were collected by Eleftherios "Lefty" Hetelekides. Calibrations and quality control experiments were performed by Madeline Schwarz. Data analysis was performed by Madeline Schwarz. Melissa M. Reynolds was the advisor on this project.

4.2 Introduction

Historians currently date the first evidence of *Cannabis* use by humans at the end of the Ice Age in ancient Japan and China. The earliest archaeobotanical evidence dates back to Japan approximately 10,000 years ago, while materials made from *Cannabis* fibers have been found in a site in China from 4000 BCE.[1-3] Evidence shows that *Cannabis* was used for fibers, a food source, and for medicinal functions. *Cannabis* was likely introduced to European countries

around 450 BCE, where remnants of plants have been found in graves, and Herodotus from Halicarnassus recorded the uses of hemp in funeral proceedings, in saunas for relaxation, and as a fiber.[1-4] In the first century CE, the writings of Greek and Latin physicians recorded the uses for hemp as a medicinal plant.[1,3-6]

The first modern study on *Cannabis* for pharmacological and toxicological properties was performed by William Brooke O'Shaughnessy, who realized that *Cannabis* cultivated in India, *C. indica*, was different than what was produced in Europe, *C. sativa*.[1,4,7] O'Shaughnessy also noted the effects of *Cannabis* as an analgesic and proposed it as a remedy for seizures.[4,7] French psychiatrist Jacques-Joseph Moreau later studied the psychoactive effects of *Cannabis* by trying it himself and noting the acute effects.[1,4,7] Due to these works, along with other studies performed around the world, the 19th century saw a progressive rise in *Cannabis* use in medicine for a variety of purposes. The fall of *Cannabis* began in the early 19th century, when it was discovered that there was a variability in efficacy and therapeutic doses, and other analgesic and anti-inflammatory drugs became available that did not have psychoactive effects and had known pharmacological profiles.[1] During the second International Opium Convention in 1925, *Cannabis* was proposed to be restricted along with opium, cocaine, and other drugs.[1,4,8] In 1937, the "Marijuana Tax Act" was passed in the United States adding taxes to business deals regarding *Cannabis*, interrupting major research efforts about its medical use.[1,9] *Cannabis* was removed from the US National Formulary and form Pharmacopeia in 1941 and was formally added to US federal law as a Schedule 1 substance pursuant to the Controlled Substances Act of 1970.[1,10]

Currently, *Cannabis* is being decriminalized globally either for strictly medical use, or for recreational purposes as well. In fact, the Department of Justice has recently proposed transferring marijuana from a Schedule 1 substance to a Schedule 3 substance, changing

restrictions in the US.[11,12] Colorado, one of the first US states to legalize recreational *Cannabis* use in 2014, has reported over 15 billion dollars in sales since legalization, with the sales in calendar year 2023 at 1.5 billion dollars.[13]

Cannabis plants biosynthesize a type of compound called phytocannabinoids, molecules that interact with the body's endocannabinoid system.[14-17] The two most abundant phytocannabinoids are cannabidiol (CBD) and Δ^9-tetrahydrocannabinol (THC). CBD (Figure 1) is a non-psychotropic compound, meaning it does not produce psychoactive effects when consumed. THC (Figure 4.1) is a psychotropic compound, meaning it does produce psychoactive effects when consumed.[14,15]

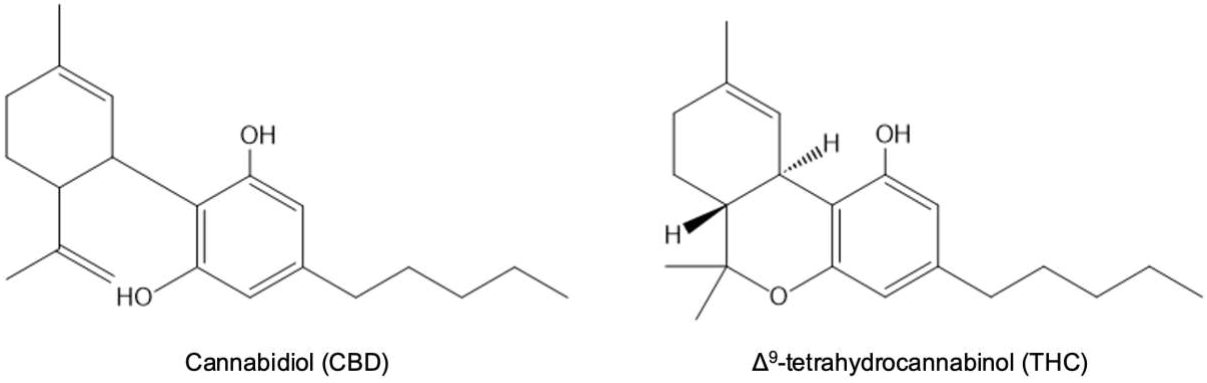

Cannabidiol (CBD) Δ^9-tetrahydrocannabinol (THC)

Figure 4.8: Chemical Structure of CBD and THC

There are four main receptors in the endocannabinoid system: cannabinoid type 1 receptors (CB1Rs), cannabinoid type 2 receptors (CB2Rs), transient receptor potential vanilloids (TRPV1s), and G-protein-couple receptor 55 (GPR55).[14,15] CBD is a noncompetitive negative allosteric modulator of CB1Rs.[14] This means that CBD binds to a site on the receptor that is not where agonists (molecules/drugs of interest) typically bind to the receptor (noncompetitive), and this binding causes an interaction to the receptor that diminishes the ability of agonists to bind to the primary site.[18] THC is an agonist of CB1Rs, which means that THC binds to the primary site on the receptor and activates it.[14,18] CB1Rs main function is to mediate inhibition of transmitter

release at nerve endings, and are found in the brain, lungs, vasculature, muscles, GI tract, heart, lymphocytes, and adipose tissue.[14,19,20] CBD is an inverse agonist of CB2Rs.[14] This means that CBD binds to the receptor binding site and produces an effect opposite to that of an agonist.[18] THC is a partial agonist of CB2Rs, which indicates that THC does not produce full activation of the receptors.[14,18] CB2Rs are responsible for expressing only when there is active inflammation or injury and are found on the surface of immune system cells, tonsils, GI tract lymphocytes, bone, peripheral nerve endings, and blood cells.[14,19,20] CBD is an agonist for TRPV1, meaning CBD binds to and activates TRPV1.[14,18] TRPV1 is responsible for detection and regulation of body temperature.[21] Lastly, CBD is an antagonist of GPR55, meaning CBD reduces the effect of agonists bound to GPR55.[14,18] CBD bound to GPR55 reduces glutamate release and neuro-excitability in the central nervous system.[22]

The metabolism of THC and CBD depends on how they are consumed. THC and CBD are consumed in a variety of ways, including smoking dried plant flower (the most common form of consumption), or by ingestion via infused edibles. When ingested, THC and CBD travel to the liver. THC is then either eliminated or metabolized into other molecules, namely 11-hydroxy-Δ^9-tetrahydrocannabinol (11-OH-THC, Figure 4.2). 11-OH-THC is then later further metabolized into 11-nor-9-carboxy-Δ^9-tetrahydrocannabinol (THC-COOH, Figure 4.2). THC's bioavailability after ingestion is between 4 and 12% but is a highly lipid soluble compound. THC is readily taken up by fat tissues where it is slowly released back into the body, which leads to an estimated plasma half-life of 1-3 days in occasional users.[23,24] CBD is also either eliminated or metabolized by the liver into several metabolites. The two most common metabolites of CBD are 7-hydroxycannabidiol (7-OH-CBD, Figure 4.2), and 7-carboxycannabidiol (7-COOH-CBD, Figure

4.2). After ingestion, CBD's bioavailability is approximately 6%, which is rapidly distributed to organ tissues where it is used quickly. CBD's estimated plasma half-life is 18-32 hours.[23]

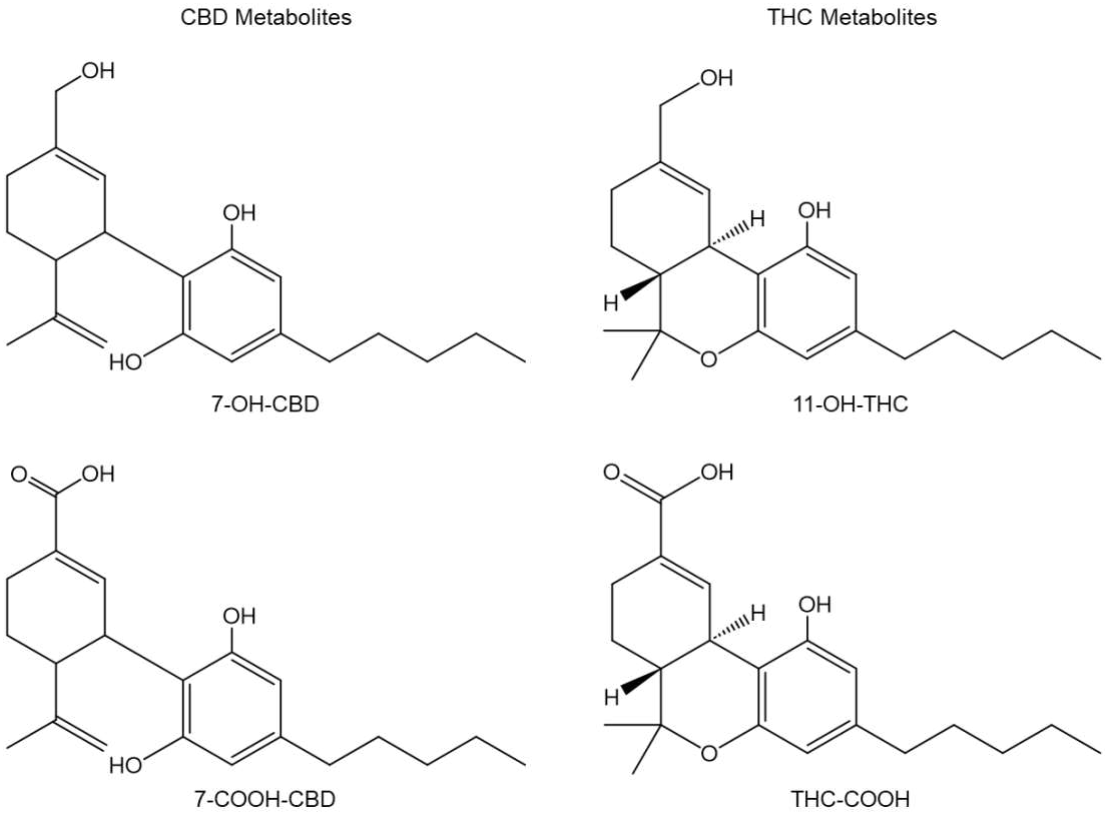

Figure 4.9: Major metabolites of CBD and THC

Due to the widespread criminalization of THC and CBD since the 1970's, research on their medical effects have been slowed. However, in recent years legal access to phytocannabinoids derived from *Cannabis* is increasing. *Cannabis* is currently legal for medical use in 38 states, 5 US territories, and the District of Columbia (DC). In 24 of those 38, three territories, and DC, *Cannabis* is also legal for recreational use.[25] CBD specific products are conditionally legal in all 50 states, with conditions including requiring medical licenses, the percent THC available in the plant or product, etc.[25,26] These further legalizations have warranted research into the use, effects, and metabolism of THC and CBD. For example, CBD is now known as an anti-convulsant agent, reducing seizure frequency and severity in pharmacoresistant

epileptic patients with few to no adverse effects.[4,15,27-29] In fact, CBD is FDA approved to treat strongly drug-resistant epileptic syndromes, namely Dravet syndrome and Lennox-Gestalt syndrome.[30] CBD may also be useful in treatment and/or prevention of movement disorders like Parkinson's disease, Dystonic movement disorders, and Huntington's disease, but more testing is needed. THC is known to create a "high" due to its interactions with CB1Rs, but human studies on its effects to the endocrine system are only beginning.[14] Currently, analysis of THC, CBD, and their major metabolites are warranted, including detection of these compounds in blood plasma. Detection of compounds and their metabolites can lead to information about the rate of metabolism, if concentration varies based on oral dosage, localization in the body, etc.[31-33]

High performance liquid chromatography (HPLC) is a physical separation technique conducted using a solid phase (stationary phase) and a liquid phase (mobile phase). A sample/mixture is separated into its component parts by interacting with the stationary and mobile phases.[34-37] A general schematic for HPLC is shown in Figure 4.3. The stationary phase typically consists of a stainless steel tube filled with small, spherical, porous particles, otherwise known as a column.[34-39] The mobile phase consists of one or more solvents that interact with the analytes and move the analyte through the system.[34-37] The mobile phase is often a mixture either held at a constant ratio throughout the elution of the sample (isocratic analysis) or changed with time during the elution (gradient analysis). Mobile phase is pumped from the solvent bottles into a solvent mixer where gas is removed by a degasser and the ratio programmed by the user is mixed and pumped along. The mobile phase then passes through the autosampler, where the sample is injected onto the flow path. After injection, the sample and mobile phase pass through the column, where analytes can interact with the stationary phase and separate. After separation, the analytes and mobile phase pass through the detector.

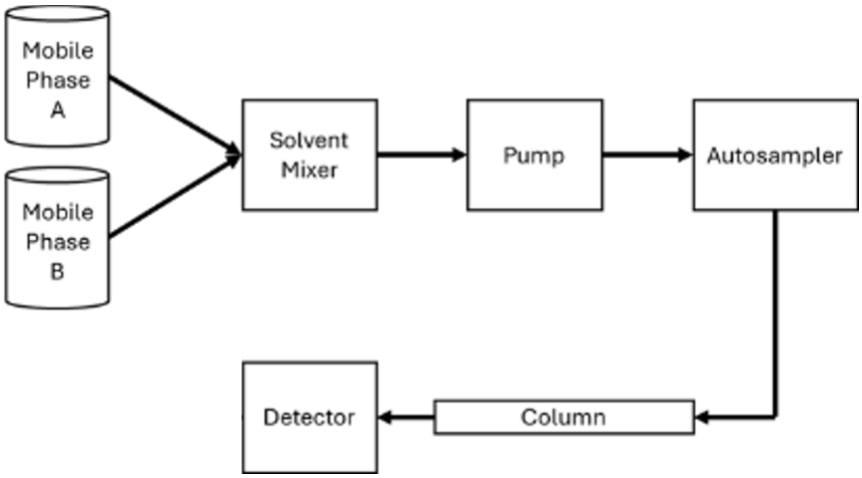

Figure 4.3: General schematic showing the flow path for HPLC. A mobile phase carries sample through a column containing stationary phase, and to a detector.

The mechanism of separation for an analyte from a mixture depends on the compositions of the mobile phase and stationary phase.[34-40] The most common mixture of components for HPLC separation, and what is utilized in this chapter, is called "Reversed-phase chromatography" (RPC). RPC consists of a nonpolar stationary phase and a mobile phase mixture of water and an organic solvent (methanol, acetonitrile, etc.). This study also utilizes gradient analysis with linear gradients. Gradient analysis works well for samples whose retention ranges exceed the preferred goal for isocratic separation.[41] The change in the polarity of the mobile phase allows for decreased retention of non-polar molecules, meaning the non-polar molecules will move more quickly through the column.[36,39,41]

A combination of HPLC and triple quadrupole mass spectrometry (LC-QQQ) is very common for measuring small quantities of molecules of interest. When compared to diode array detection (DAD), a very common detector used for analysis of cannabinoids, LC-QQQ provides an ease in workflow and higher throughput. Due to the unique nature of the triple quadrupole detector, LC-QQQ is also much (approx. 100x) more sensitive than LC-DAD methods. Due to these factors, LC-QQQ was chosen over LC-DAD for these methods. In this chapter, methods

developed to detect CBD, THC, and their major metabolites from blood plasma using LC-QQQ are described.

4.3 Experimental

4.3.1 Materials

Optima LC-MS grade formic acid, Optima LC-MS grade acetonitrile, Optima LC-MS grade methanol, and Optima LC-MS water were obtained from Fisher Chemical (Waltham, MA). 0.2-µm Captiva Econofilters were obtained from Agilent (Palo Alto, CA). Zinc sulfate heptahydrate (≥99.0%) was obtained from Sigma-Aldrich (St. Louis, MO). CBD (1000 µg/mL in MeOH) and THC (1 mg/mL in MeOH) were obtained from Restek (Bellefonte, PA). THC-COOH (1 mg/mL in MeOH) was obtained from Cayman Chemicals (Ann Arbor, MI). 11-OH-THC (1 mg/mL in MeOH), 7-COOH-CBD (1 mg/mL in MeOH), and 7-OH-CBD (1 mg/mL in MeOH) were obtained from Neta Scientific (Marlton, NJ).

4.3.2 Calibration Curve and Quality Control Sample Preparation

Solutions used for calibration curves were prepared using serial dilutions with methanol from the purchased standards. The working solutions of CBD, THC, 11-OH-THC, THC-COOH, 7-OH-CBD, and 7-COOH-CBD were diluted in methanol immediately before use for calibration curves. The concentrations of these working solutions were 5000, 1000, 500, 100, 50, 10, and 5 ng/mL.

Plasma quality control samples were prepared after initial calibration had been performed. As further discussed in the results and discussion section, 7-OH-CBD and 7-COOH-CBD were not pursued in this step of the analysis. Aliquots of CBD, THC, 11-OH-THC, and THC-COOH were added to 0.5 mL of plasma in appropriate amounts to make a final working

solution (compounds in plasma) dependent on the test being performed. These solutions were subjected to the various plasma precipitation methods discussed in later sections.

4.3.3 LC-QQQ Methods

LC-QQQ analyses were carried out on an Agilent 6470 triple quadrupole mass spectrometer coupled to a 1290 high speed liquid chromatograph. Separations were performed using an Agilent Poroshell 120 EC-C18 column with dimensions of 4.6x150 mm and particle size of 2.7 μm. Mobile phase A was composed of LCMS-grade water with 0.1% (v/v) formic acid. Mobile phase B was LCMS-grade acetonitrile with 0.1% (v/v) formic acid. The gradient elution, shown in Figure 4.4, began with 25% A and 75% B. The gradient was held for 1 minute, then ramped for 1.75 minutes to 20% A and 80% B, and then further ramped for 5 minutes to 0% A and 100% B. The mobile phase of 100% B was held for 1.75 minutes. The mobile phase was then ramped down to 40% A and 60% B over 1 minute, and held there until the end of the run, for a total run time of 12.75 minutes. The flow rate was constant during the entire process at 0.75 mL/min. Electrospray ionization source was used in positive ionization mode. Ion source conditions were as follows: capillary voltage 3000 V; drying gas flow rate 12 L/min; desolvation line temperature 350 °C; nebulizer gas flow rate 25 L/min; nozzle voltage 1800 V; shielding gas flow 12 L/min; shielding gas temperature 350 °C.

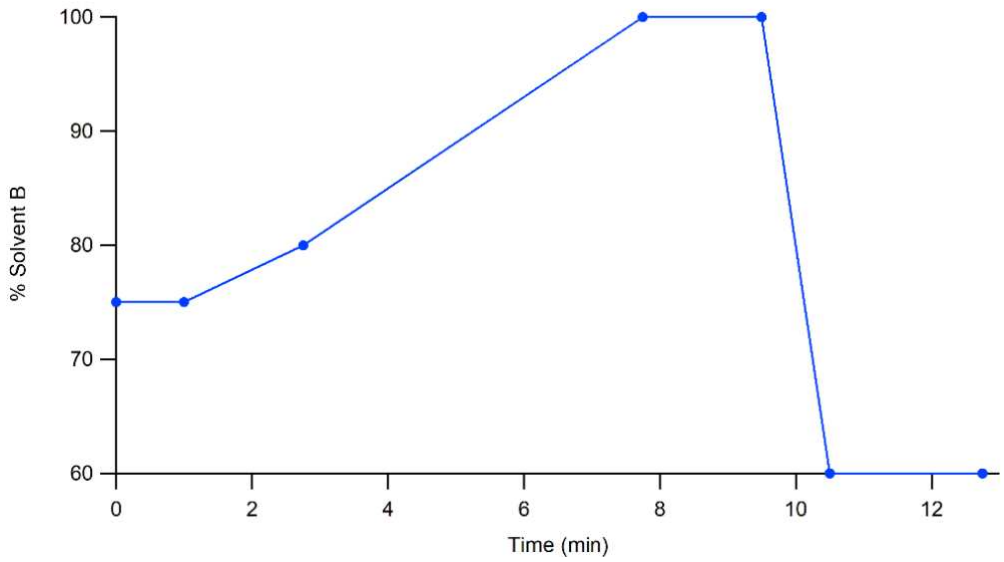

Figure 4.4: Mobile phase B composition (%) throughout the developed method

4.3.4 Calculations

The line of best fit for the calibration curve described in this work was calculated using the method of least squares regression model. All values are reported as an average ± standard deviation unless otherwise indicated. Unless otherwise indicated, n=5 for all samples.

Peak areas taken for analysis were taken from extracted multiple reaction monitoring (MRM) peaks. These quantifier peaks were determined using the most abundant fragment during neat calibration steps. An example comparison between the total ion chromatogram and an extracted fragment peak is shown in Figure 4.5. The transitions used for each analyte are shown in Table 4.1.

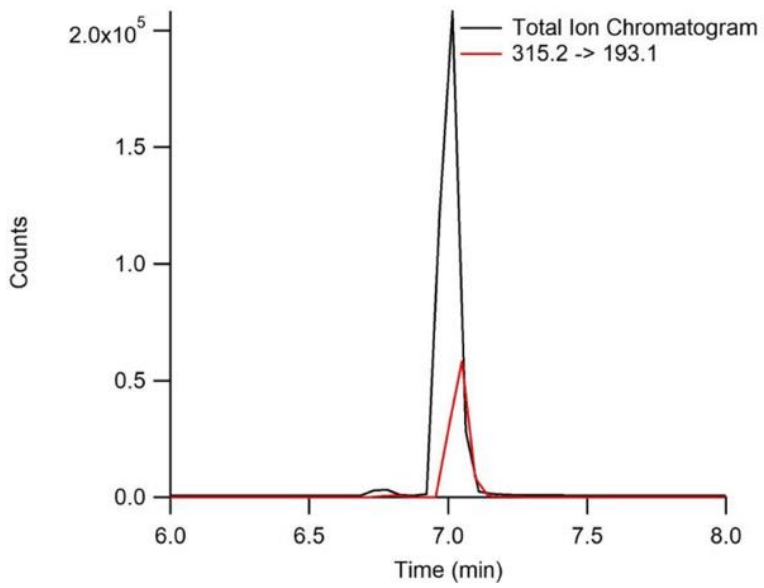

Figure 4.5: Total ion chromatogram of THC (black) compared to the extracted ion chromatogram (red) used for quantification.

Table 4.1: Quantifying mass-to-charge ratio transitions used for each analyte in this chapter

Compound	Starting Mass → Ending Mass
THC	315.2 → 193.1
11-OH-THC	331.2 → 77.1
THC-COOH	345.2 → 193.2
CBD	315.2 → 193.1
7-OH-CBD	331.2 → 77.1
7-COOH-CBD	345.2 → 193.2

4.4 Results and Discussion

4.4.1 Method Validation

The analytical method validation for this method was based on the guidelines published online by the United States Food and Drug Administration (FDA). An LC method previously developed for the detection of cannabinoids was used as is described in the methods section.[42] Three quality control (QC) samples were prepared to cover the calibration curve range and to determine precision and accuracy. Accuracy was calculated as the percent error between the nominal and measured concentrations of standards, while precision was calculated as the

coefficient of variation (CV) within a standard level. The lower limit of quantification (LLOQ) was experimentally determined. FDA guidelines recommend that the precision and accuracy for LLOQ should be ±20%. All calibration levels and quality control samples were run with an n=5 unless otherwise indicated.

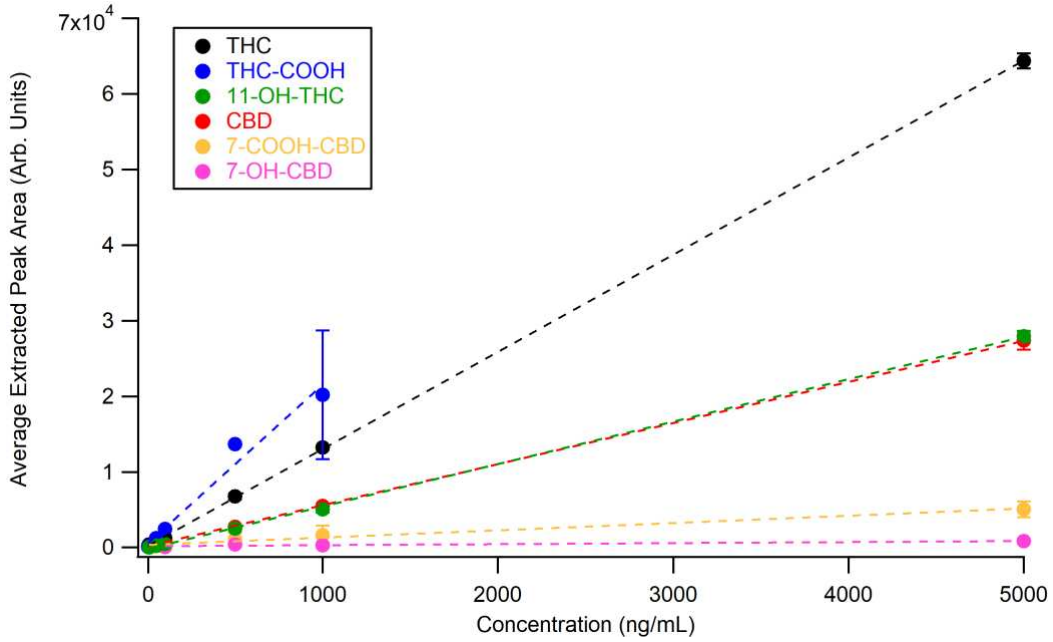

Figure 4.6: Neat Calibration curve for all compounds of interest (n=5)

Neat calibration curves for each molecule of interest were prepared and are shown in Figure 4.6. To ensure the validity of the neat calibration curve, the precision of each point in the calibration curves are shown in Table 4.2. With this evaluation, it was determined that the calibrations of 7-OH-CBD and 7-COOH-CBD do not meet the FDA's standards for bioanalytical methods. This is due to their high CV values in the desired calibration range. 11-OH-THC was determined to meet the criteria above 100 ng/mL. As recommended by the FDA's standards, the lowest level that meets the criteria (100 ng/mL) was determined to be the limit of detection for the method. THC-COOH met the criteria between 500 and 5 ng/mL, but not at 1000 ng/mL. This was determined to be the working calibration range as recommended by the FDA's standards.

Finally, CBD and THC met all FDA criteria throughout the calibration range. Due to these factors, 7-OH-CBD and 7-COOH-CBD were not evaluated for quality control purposes. Individual calibration curves for the remaining compounds used for this chapter can be found in Appendix II.

Table 4.2: Coefficient of variance (CV) for each calibration point and compound. A yellow highlight indicates the level not meeting the FDA guidelines.

Calibration Concentration (ng/mL)	THC CV (%)	CBD CV (%)	11-OH-THC CV (%)	THC-COOH CV (%)	7-COOH-CBD CV (%)	7-OH-CBD CV (%)
5000	2	4	3	--	21	12
1000	1	4	9	42	78	95
500	6	10	10	2	72	7
100	8	8	23	1	53	31
50	9	3	26	4	10	--
10	2	8	27	9	16	--
5	9	11	--	19	--	--

Using the limit of least squares, the calibration curves for the four molecules of interest selected after initial vetting were evaluated, and limits of detection and quantification were determined. These values can be found in Table 4.3.

Table 4.3: Calculated limits of detection and quantification for the molecules of interest that met FDA criteria.

Compound	LLOD (ng/mL)	LLOQ (ng/mL)
CBD	0.03	0.08
THC	0.01	0.03
THC-COOH	0.03	0.1
11-OH-THC	0.03	0.1

One characteristic of note for the separation method used is the coelution of two compounds of interest. In the total ion chromatogram, THC-COOH and 11-OH-THC coelute, meaning they elute off the column at the same time. In a method using HPLC, this would cause a major issue for quantification. This is shown in Figure 4.7. Luckily, with LC-QQQ this becomes a non-issue. THC-COOH and 11-OH-THC have different parent masses and fragment ions,

meaning they can be separated in the extracted ion chromatogram. This is shown in Figure 8, which is a zoomed-in portion of Figure 4.7 showing the two separate peaks that were used for quantification purposes.

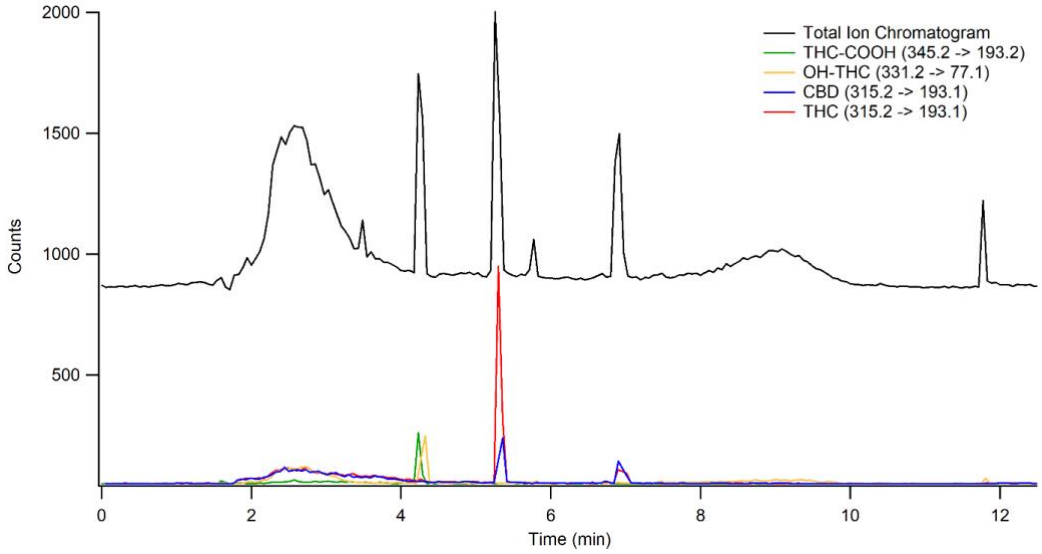

Figure 4.7: Total ion chromatogram and MRM transitions of a plasma quality-control run.

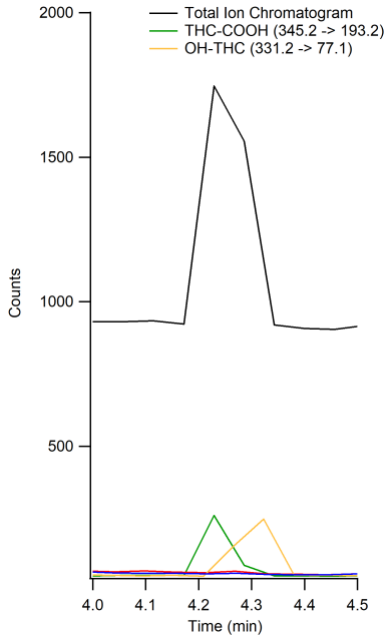

Figure 4.8: Zoomed in portion of Figure 7 showing from 4-4.5 min. As shown here, the total ion chromatogram is one peak, with two compounds coeluting, but the two compounds are separated in the extracted ion chromatograms, allowing for quantification.

4.4.2 Protein Precipitation 1 Method Development

To properly perform quality controls of the compounds in the appropriate matrix, the compounds of interest needed to be added to plasma. Unfortunately, a mixture of plasma and cannabinoids could not be directly added to the instrument, as the matrix effects from the plasma would be harmful to the instrument. To rectify this, a separation method between the larger components in the plasma, such as proteins, needed to be implemented for the samples. Previous studies have shown that a simple one-step protein precipitation can be implemented to separate cannabinoids from plasma samples.[43-45] The first protein precipitation method tested for this analysis was as simple as possible, aiming for ease of implementation in clinical laboratories. LC-MS grade acetonitrile was kept at -20°C and was added to the plasma in a 2:1 ACN to plasma ratio. The resulting mixture was then centrifuged for 10 minutes at 1100 xg. The supernatant was then passed through a 2-micron filter and added to an LC-MS vial, where analysis was performed. Quality control samples were generated by adding known concentrations of the analytes of interest to blank plasma to generate a working solution of 5000 ng/mL and performing the precipitation. The quality control samples were replicated for n=3 samples and run at n=5. An example of the quality control sample results generated is shown in Figure 4.9 (one sample at n=5). This quality control was performed to determine the percent loss of the molecules of interest using this method. To evaluate the method, the CV was compared to the FDA's standard. Results of the first protein precipitation can be seen in Table 4.4.

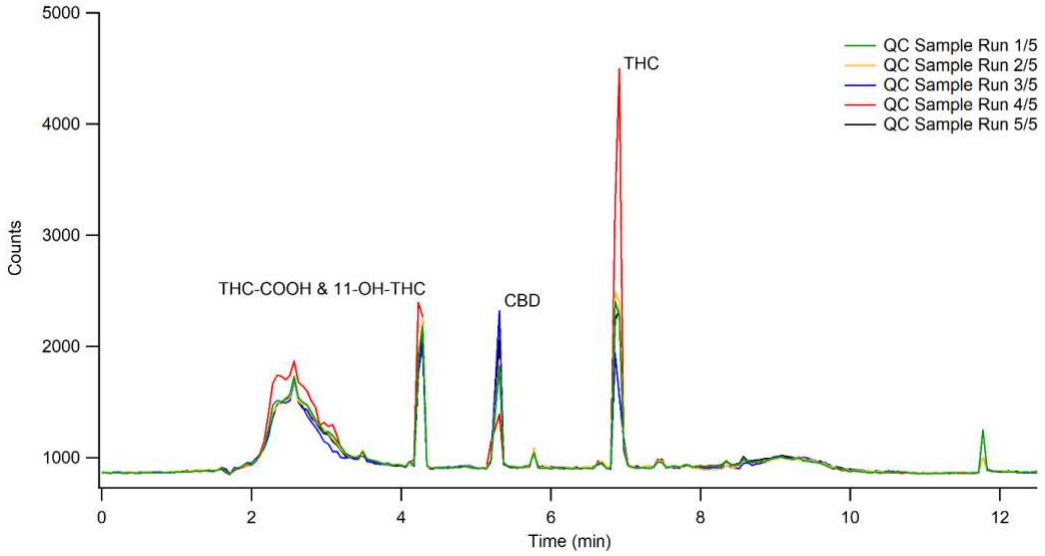

Figure 4.9: Example total ion chromatogram showing the quality control samples after protein precipitation. The injections in this figure represent 1 sample with 5 separate injections.

Table 4.4: Representative results of first quality control tests (QC sample 1, n=5)

Compound	Average extracted peak area ± standard deviation	Coefficient of variation	Calculated concentration (based on average)
THC	15000 ± 5000	33%	1168.9 ng/mL
11-OH-THC	100 ± 30	30%	46.5 ng/mL
THC-COOH	5000 ± 2000	51%	208.9 ng/mL
CBD	40000 ± 20000	62%	7675.8 ng/mL

The first FDA standard evaluated for the QC samples was the CV's. As described in Chapter 3 of this dissertation, when evaluating precision CV values should be ±15%. All the CV values from the quality controls performed had more than double the desired variance. The percent loss is also at issue in this method. While the FDA does not have standards for recovery (other than it should be documented and consistent), 100% recovery is the most desirable for all bioanalytical methods. While achieving 100% recovery is rare, recovery as close to 100% as possible is often considered satisfactory. Currently, the recovery percent is very low for all

compounds except CBD, which experienced an increase in signal. Due to these factors, an alternative protein precipitation method was explored.

4.4.3 Protein Precipitation 2 Method Development

The second protein precipitation method explored for this work was derived from a study performed by Sempio et. al. in 2022.[43] To the plasma, a mixture of 70% methanol and 30% water with 0.2 M $ZnSO_4$ was added (4:1 mixture to plasma). The solvent mixture and plasma combination were centrifuged for 10 minutes at 1100 xg. The supernatant was then filtered and analyzed using the LC-QQQ methods described. The concentration of cannabinoids in the plasma was 50 ng/mL. This concentration was chosen instead of the 5000 ng/mL used in the previous step primarily because 5000 ng/mL is outside the calibration range for THC-COOH, and 50 ng/mL is approximately in the middle of the calibration range. The quality control samples were performed at n=3 samples and run at n=5. Results of this protein precipitation are shown in Table 4.5. The CV values for this method were also outside the FDA's acceptability standards. The recovery percents also vary widely, with most being over the initial concentration.

Table 4.5: Representative results of second quality control tests (n=5)

Compound	Average extracted peak area ± standard deviation	Coefficient of variation	Calculated concentration (based on average)
THC	1600 ± 300	16%	111.5 ng/mL
11-OH-THC	1700 ± 700	41%	323.7 ng/mL
THC-COOH	600 ± 500	78%	4.5 ng/mL
CBD	4000 ± 3000	73%	669.5 ng/mL

The information gathered from these experiments show that further analysis of separation methods is needed for successful analysis of the target molecules in plasma. Current methods are sufficient for detection of neat standards, but more work needs to implement the analysis to human plasma samples.

4.5 Conclusions

Due to the decriminalization of cannabinoids globally, they will continue to be a molecule of interest for the near future. The rate of metabolism of cannabinoids when consumed in a variety of methods is also of interest, specifically when ingested orally. This chapter describes the beginning of a method to detect cannabinoids and their metabolites. The method developed was optimized for the detection of CBD, THC, THC-COOH, and 11-OH-THC in neat samples. Further work to separate the compounds from plasma is needed to optimize the method for use on clinical samples.

CHAPTER 4 – REFERENCES

(1) Pisanti, S.; Bifulco, M. Medical Cannabis : A Plurimillennial History of an Evergreen. *J. Cell. Physiol.* 2019, *234* (6), 8342–8351. https://doi.org/10.1002/jcp.27725.

(2) Li, H.-L. An Archaeological and Historical Account of Cannabis in China. *Econ. Bot.* 1974, *28* (4), 437–448.

(3) Long, T.; Wagner, M.; Demske, D.; Leipe, C.; Tarasov, P. E. Cannabis in Eurasia: Origin of Human Use and Bronze Age Trans-Continental Connections. *Veg. Hist. Archaeobot.* 2017, *26* (2), 245–258. https://doi.org/10.1007/s00334-016-0579-6.

(4) Fankhauser, M. History of Cannabis in Western Medicine. In *Cannabis and cannabinoids: pharmacology, toxicology, and therapeutic potential*; Grotenhermen, F., Russo, E., Eds.; Haworth Integrative Healing Press: New York, 2002; pp 37–51.

(5) Pliny the Elder. Book XX. In *Natural History vol VI*; Jones, W. H. S., Ed.; Harvard University Press, 1951; pp 152–153.

(6) Pliny the Elder Book XIX. In *Natural History vol V*; Rackham, H., Ed.; Harvard University Press, 1950; pp 530–533.

(7) O'Shaughnessy, W. B. On the Preparations of the Indian Hemp, or Gunjah, (Cannabis Indica) Their Effects on the Animal System in Health, and Their Utility in the Treatment of Teatnus and Other Convulsive Diseases. *Prov. Med. J. Retrosp. Med. Sci.* 1843, *5* (123), 363–369.

(8) Kendell, R. Cannabis Condemned: The Proscription of Indian Hemp. *Addiction* 2003, *98* (2), 143–151. https://doi.org/10.1046/j.1360-0443.2003.00273.x.

(9) Musto, D. F. The 1937 Marijuana Tax Act. *Arch. Gen. Psychiatry* 1972, *26* (2), 101–108.

(10) Health, N. I. of. *About Cannabis Policy*. NIH. https://alcoholpolicy.niaaa.nih.gov/about/about-cannabis-policy

(11) Administration, D. E. *Schedules of Controlled Substances: Rescheduling of Marijuana [Docket No. DEA-1362; A.G. Order No. 5931-2024]*. Department of Justice. https://www.federalregister.gov/documents/2024/05/21/2024-11137/schedules-of-controlled-substances-rescheduling-of-marijuana.

(12) Miller, Z.; Goodman, J.; Mustian, J.; Whitehurst, L. *US poised to ease restrictions on marijuana in historic shift, but it'll remain controlled substance*. Associated Press. https://apnews.com/article/marijuana-biden-dea-criminal-justice-pot-f833a8dae6ceb31a8658a5d65832a3b8.

(13) Colorado Department of Revenue. *Marijuana Sales Reports*. State of Colorado. https://cdor.colorado.gov/data-and-reports/marijuana-data/marijuana-sales-reports.

(14) Meah, F.; Lundholm, M.; Emanuele, N.; Amjed, H.; Poku, C.; Agrawal, L.; Emanuele, M. A. The Effects of Cannabis and Cannabinoids on the Endocrine System. *Rev. Endocr. Metab. Disord.* 2022, *23* (3), 401–420. https://doi.org/10.1007/s11154-021-09682-w.

(15) Cifelli, P.; Ruffolo, G.; De Felice, E.; Alfano, V.; van Vliet, E. A.; Aronica, E.; Palma, E. Phytocannabinoids in Neurological Diseases: Could They Restore a Physiological GABAergic Transmission? *Int. J. Mol. Sci.* 2020, *21* (3), 723. https://doi.org/10.3390/ijms21030723.

(16) Brenneisen, R. Chemistry and Analysis of Phytocannabinoids and Other Cannabis Constituents. In *Marijuana and the Cannabinoids*; ElSohly, M. A., Ed.; Humana Press: Totowa, 2007; pp 17–49.

(17) Gertsch, J.; Pertwee, R. G.; Di Marzo, V. Phytocannabinoids beyond the Cannabis Plant – Do They Exist? *Br. J. Pharmacol.* 2010, *160* (3), 523–529. https://doi.org/10.1111/j.1476-5381.2010.00745.x.

(18) Tocris. *Pharmacological Glossary*. Tocris Biosciences Resources. https://www.tocris.com/resources/pharmacological-glossary (accessed 2024-05-06).

(19) Borowska, M.; Czarnywojtek, A.; Sawicka-Gutaj, N.; Woliński, K.; Płazińska, M. T.; Mikołajczak, P.; Ruchała, M. The Effects of Cannabinoids on the Endocrine System. *Endokrynol. Pol.* 2018, *69* (6), 705–719. https://doi.org/10.5603/EP.a2018.0072.

(20) Pertwee, R. G. Sites and Mechanisms of Action. In *Cannabis and cannabinoids: pharmacology, toxicology, and therapeutic potential*; Grotenhermen, F., Russo, E., Eds.; Haworth Integrative Healing Press: Binghamton, 2002; pp 73–87.

(21) Rosenbaum, T.; Simon, S. A. TRPV1 Receptors and Signal Transduction. In *TRP Ion Channel Function in Sensory Transduction and Cellular Signaling Cascades*; Liedtke, W. B., Heller, S., Eds.; CRC Press/Taylor & Francis: Boca Raton, 2007.

(22) Lauckner, J. E.; Jensen, J. B.; Chen, H.-Y.; Lu, H.-C.; Hille, B.; Mackie, K. GPR55 Is a Cannabinoid Receptor That Increases Intracellular Calcium and Inhibits M Current. *Proc. Natl. Acad. Sci.* 2008, *105* (7), 2699–2704. https://doi.org/10.1073/pnas.0711278105.

(23) Chayasirisobhon, S. Mechanisms of Action and Pharmacokinetics of Cannabis. *Perm. J.* 2021, *25* (1), 1–3. https://doi.org/10.7812/TPP/19.200.

(24) Huestis, M. A. Pharmacokinetics and Metabolism of the Plant Cannabinoids, Δ 9-Tetrahydrocannibinol, Cannabidiol and Cannabinol; 2005; pp 657–690. https://doi.org/10.1007/3-540-26573-2_23.

(25) Legislatures, N. C. of S. *State Medical Cannabis Laws*. https://www.ncsl.org/health/state-medical-cannabis-laws.

(26) Laurence, E. *Your Guide to CBD Legalization By State*. Forbes Health. https://www.forbes.com/health/cbd/cbd-legalization-by-state/ (accessed 2024-05-06).

(27) Pisanti, S.; Bifulco, M. Modern History of Medical Cannabis: From Widespread Use to Prohibitionism and Back. *Trends Pharmacol. Sci.* 2017, *38* (3), 195–198. https://doi.org/10.1016/j.tips.2016.12.002.

(28) de Carvalho Reis, R.; Almeida, K. J.; da Silva Lopes, L.; de Melo Mendes, C. M.; Bor-Seng-Shu, E. Efficacy and Adverse Event Profile of Cannabidiol and Medicinal Cannabis for Treatment-Resistant Epilepsy: Systematic Review and Meta-Analysis. *Epilepsy Behav.* 2020, *102*, 106635. https://doi.org/10.1016/j.yebeh.2019.106635.

(29) Grotenhermen, F. Review of Therapeutic Effects. In *Cannabis and cannabinoids: pharmacology, toxicology, and therapeutic potential*; Grotenhermen, F., Russo, E., Eds.; Haworth Integrative Healing Press: Binghamton, 2002; pp 123–142.

(30) FDA. *FDA Approves First Drug Comprised of an Active Ingredient Derived from Marijuana to Treat Rare, Severe Forms of Epilepsy*. US Food and Drug Administration. https://www.fda.gov/news-events/press-announcements/fda-approves-first-drug-comprised-active-ingredient-derived-marijuana-treat-rare-severe-forms (accessed 2024-05-06).

(31) Müller-Vahl, K. R.; Kolbe, H.; Schneider, U.; Emrich, H. M. Movement Disorders. In *Cannabis and cannabinoids: pharmacology, toxicology, and therapeutic potential*; Grotenhermen, F., Russo, E., Eds.; Binghamton, 2002; pp 205–214.

(32) Peres, F. F.; Lima, A. C.; Hallak, J. E. C.; Crippa, J. A.; Silva, R. H.; Abílio, V. C. Cannabidiol as a Promising Strategy to Treat and Prevent Movement Disorders? *Front. Pharmacol.* 2018, *9*. https://doi.org/10.3389/fphar.2018.00482.

(33) Kim, H.; Zhang, S.; Sin, M.-K. Cannabidiol (CBD) Consideration in Parkinson Disease. *J. Nurse Pract.* 2022, *18* (6), 611–613. https://doi.org/10.1016/j.nurpra.2022.04.006.

(34) Zotou, A. An Overview of Recent Advances in HPLC Instrumentation. *Open Chem.* 2012, *10* (3), 554–569. https://doi.org/10.2478/s11532-011-0161-0.

(35) Dong, M. W. *HPLC and UHPLC for Practicing Scientists*, 2nd ed.; Wiley & Sons: Hoboken, New Jersey, 2019.

(36) Snyder, L. R.; Kirkland, J. J.; Dolan, J. W. Basic Concepts and the Control of Separation. In *Introduction to Modern Liquid Chromatography*; Wiley: Hoboken, New Jersey, 2010; pp 19–86. https://doi.org/10.1002/9780470508183.

(37) Kazakevich, Y. V. HPLC Theory. In *HPLC Method Development for Pharmaceuticals*; Ahuja, S., Rasmussen, H., Eds.; Academic Press, 2007; pp 13–44.

(38) Kazakevich, Y. V. High-Performance Liquid Chromatography Retention Mechanisms and Their Mathematical Descriptions. *J. Chromatogr. A* 2006, *1126* (1–2), 232–243. https://doi.org/10.1016/j.chroma.2006.05.022.

(39) Kaliszan, R.; Wiczling, P.; Markuszewski, M. J. PH Gradient Reversed-Phase HPLC. *Anal. Chem.* 2004, *76* (3), 749–760. https://doi.org/10.1021/ac034999v.

(40) Molnár, I. Searching for Robust HPLC Methods – Csaba Horváth and the Solvophobic Theory. *Chromatographia* 2005, *62* (S13), s7–s17. https://doi.org/10.1365/s10337-005-0645-1.

(41) Snyder, L. R.; Kirkland, J. J.; Dolan, J. W. Gradient Elution. In *Introduction to Modern Liquid Chromatography*; John Wiley and Sons Ltd: Hoboken, New Jersey, 2010; pp 403–473. https://doi.org/10.1002/9780470508183.

(42) Cuchiaro, J. H. Adsorptive Separations of Phytocannabinoids and Pesticides in the Liqiud Phase, Colorado State University, 2022.

(43) Sempio, C.; Almaraz-Quinones, N.; Jackson, M.; Zhao, W.; Wang, G. S.; Liu, Y.; Leehey, M.; Knupp, K.; Klawitter, J.; Christians, U.; Klawitter, J. Simultaneous Quantification of 17 Cannabinoids by LC–MS-MS in Human Plasma. *J. Anal. Toxicol.* 2022, *46* (4), 383–392. https://doi.org/10.1093/jat/bkab030.

(44) Antunes, M.; Barroso, M.; Gallardo, E. Analysis of Cannabinoids in Biological Specimens: An Update. *Int. J. Environ. Res. Public Health* 2023, *20* (3). https://doi.org/10.3390/ijerph20032312.

(45) Antunes, M.; Simões, S.; Fonseca, S.; Franco, J.; Gallardo, E.; Barroso, M. Detection and Quantification of Selected Cannabinoids in Oral Fluid Samples by Protein Precipitation and LC-MS/MS. *Forensic Sci. Int.* 2024, *363*, 112174. https://doi.org/10.1016/j.forsciint.2024.112174.

CHAPTER 5

Dissertation Outcomes and Future Directions

5.1 Fungal Detections

In Chapters 2 and 3, I discussed the development of a method for detections of GlcN as a biomarker for pulmonary fungal infections, like IPA. The LC-QQQ method was developed, and the acid degradation of biologically relevant media was explored. The exploration into the degradation of media, however, should be explored further to allow for a method that could be applied to clinical samples.

The first step that should be taken is to further evaluate the matrix effects that degraded media has on glucosamine. This can be completed by performing the acid degradation as outlined in the chapters, then adding known amounts of glucosamine standard to the degraded media. The matrix effects should then be compared to the matrix effects discussed in Chapter 3, and the comparison will provide valuable information about the acid degradation performed and discussed in Chapter 3.

Further evaluation into the SPE method discussed in Chapter 3 is also warranted, to minimize the matrix effects from the biological media, whatever they may be. SPE methods can be difficult to optimize, but various studies have been performed to aid in their optimization.[1] The conditioning and or washing steps of the SPE method used in Chapter 3 may need adjusting to better account for the pK_a of GlcN. It may also be possible that a different SPE column may be needed to retain GlcN, one targeted toward polar neutral molecules rather than weak bases. The SPE method developed would need to be evaluated using the FDA's standards to evaluate the

matrix effects and reproducibility of the method before applications to clinical samples could begin.

5.2 Cannabinoid Detections

In Chapter 4, I discussed methods developed to detect THC, CBD, and their major metabolites in human plasma samples. After the LC-MS method was developed for the target analytes, calibration curves were performed to verify the reproducibility of the method. Quality controls were then performed to determine matrix effects, and to determine the reproducibility of the protein precipitation methods developed to separate the analytes from the plasma. Unfortunately, the methods developed and discussed in Chapter 4 did not meet the FDA's standards for bioanalytical method development.

There are several steps that could be taken to decrease the variation in signal seen in Chapter 4. Firstly, the retention of cannabinoids in the chosen centrifuge vessels should be tested to determine if they are adhering to the plastic. 15 mL polypropylene conical centrifuge tubes were used for the centrifuge portion of the procedure. Some studies have shown that cannabinoids degrade in plastic containers during storage, but others refute that claim.[2,3] Determining if the sample is being lost at this step in the process is crucial to determining the methods to be used for clinical samples. A second step to decrease the variation in signal is to determine the matrix effects of the precipitated plasma samples. This can be done by spiking known concentrations of cannabinoids into the supernatant of a precipitated plasma sample, so a mathematical determination of matrix effects can be better made. Finally, it may be prudent to evaluate another separation method, rather than protein precipitation. Previous work on this project evaluated SPE for the separation of plasma and cannabinoids, and results were highly

variable with low recovery of cannabinoids. Other separation methods for cannabinoids from plasma include liquid-liquid extraction, salting-out assisted liquid-liquid extractions, and QuEChERS (Quick, Easy, Cheap, Effective, Rugged and Safe).[4] The QuEChERS sample preparation approach is commonly used in the food safety industry, and is reportedly well suited for analysis of pesticides, and cannabinoids if modifications to the base method are made.[5] Any of these methods would also be viable options to test for reproducibility and minimization of matrix effects on the desired cannabinoid analytes. Once the separation method is developed, testing on clinical samples of blood plasma can begin.

CHAPTER 5 – REFERENCES

(1) Raynie, D. E.; Watson, D. W. Understanding and Improving Solid-Phase Extraction. *LCGC North America* 2014, *32* (12), 908–915.

(2) Christophersen, A. S. Tetrahydrocannabinol Stability in Whole Blood: Plastic Versus Glass Containers. *J Anaal Toxicol* 1986, *10* (4), 129-131. https://doi.org/10.1093/jat/10.4.129.

(3) Bruno, C.; Paintaud, G.; Darrouzain, F. Sampling and Storage Conditions for Cannabinoid Analysis: Plastic vs. Glass. *Toxicologie Analytique et Clinique* 2019, *31* (2), S69. https://doi.org/10.1016/j.toxac.2019.03.106.

(4) Antunes, M.; Barroso, M.; Gallardo, E. Analysis of Cannabinoids in Biological Specimens: An Update. *Int. J. Environ. Res. Public Health* 2023, *20* (3). https://doi.org/10.3390/ijerph20032312.

(5) Cochran, J.; Rigdon, A.; Kowalski, J.; Fagras, G.; Dahl, J. H.; Laine, D. Evaluation of Modified QuEChERS for Pesticide Analysis in Cannabis. *LCGC Supplements* 2017, *35* (5), 8–22.

APPENDIX I - SUPPLEMENTAL INFORMATION FOR CHAPTER 2

Optimization for the multiple reaction monitoring of glucosamine was performed using the Agilent Optimizer program. The optimizer program automates the process of mass spectrometer optimization by creating methods and worklists to run the optimization for the compound and method specified by the user. All optimization was run using the same glucosamine neat standard in sequence to avoid sample degradation. Table SI1 shows the used optimized parameters, and Figures SI1-5 show the data that lead to the results in Table SI1.

Table SI1. Optimized mass spectrometry parameters used for glucosamine detection. Individual parameter tests are shown in Figures SI1-5

Parent Ion	Fragmentor Voltage	Product Ion	Collision Energy	Abundance
180.09	73 V	162.1	4	56393
		84.1	12	13619
		144.1	8	8824

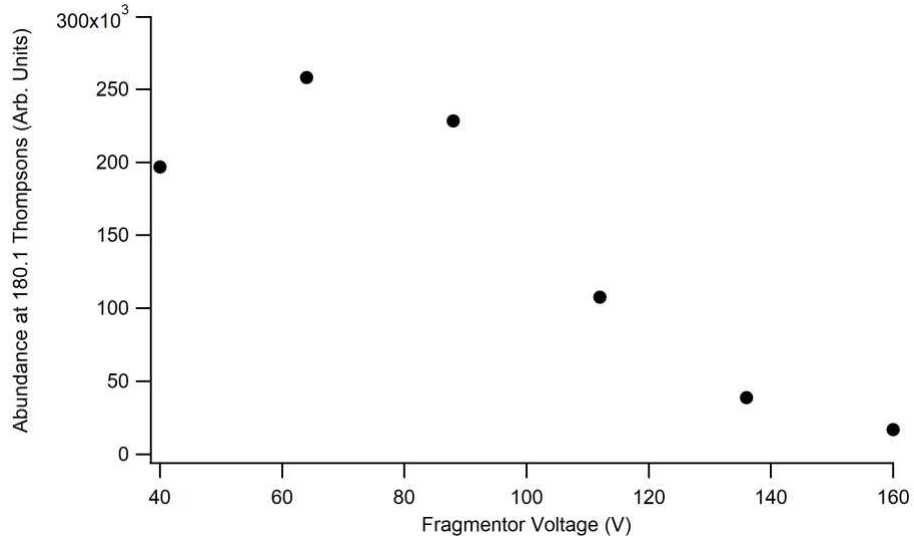

Figure SI1: Optimization of the fragmentor voltages

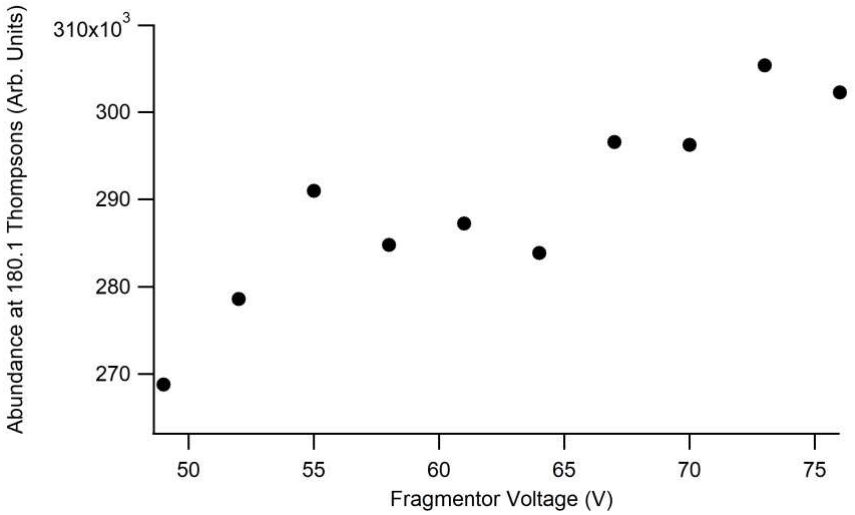

Figure SI2: Narrow range fragmentor voltages tested for optimization

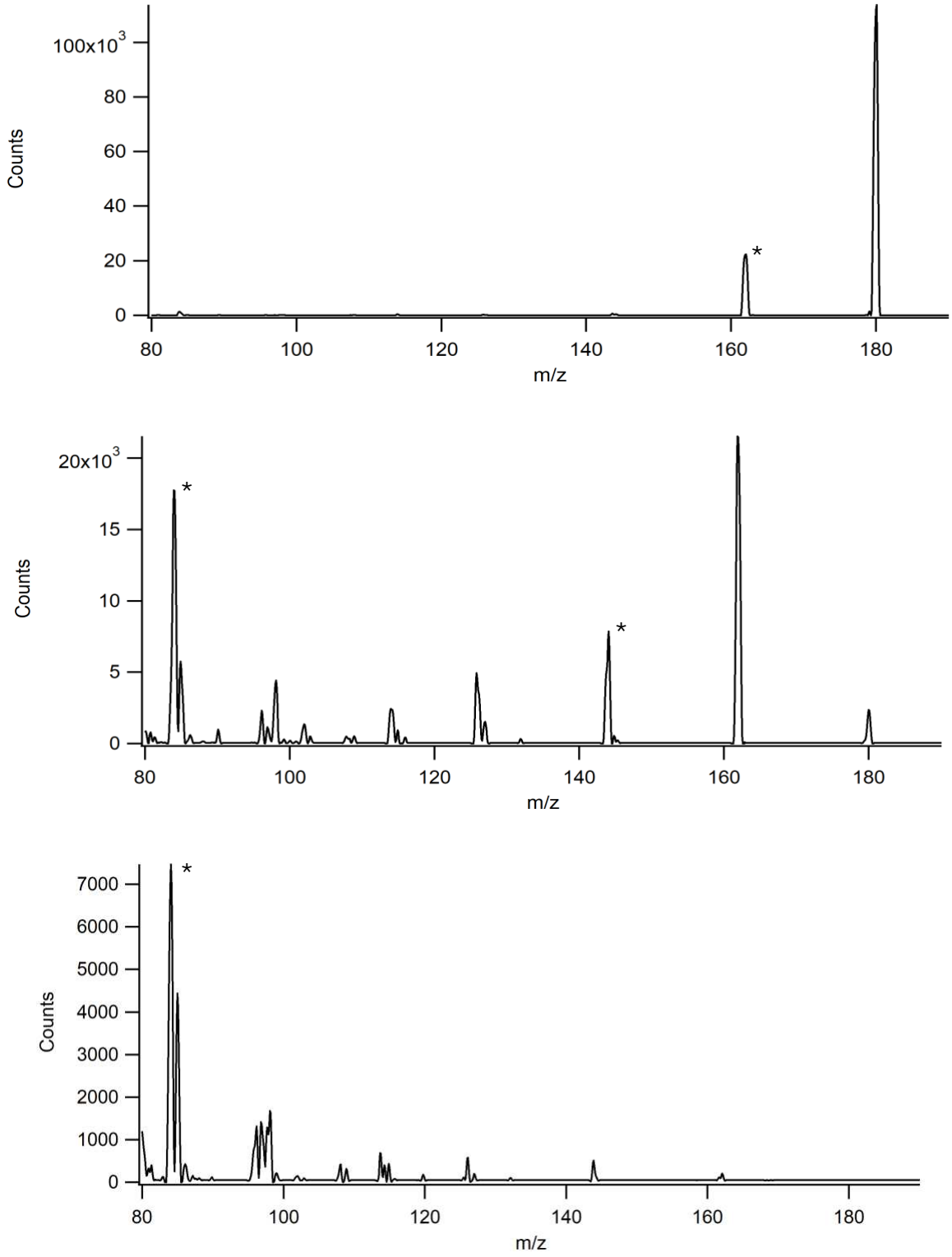

Figure SI3: Scans for product ions. Product ions selected are marked *.

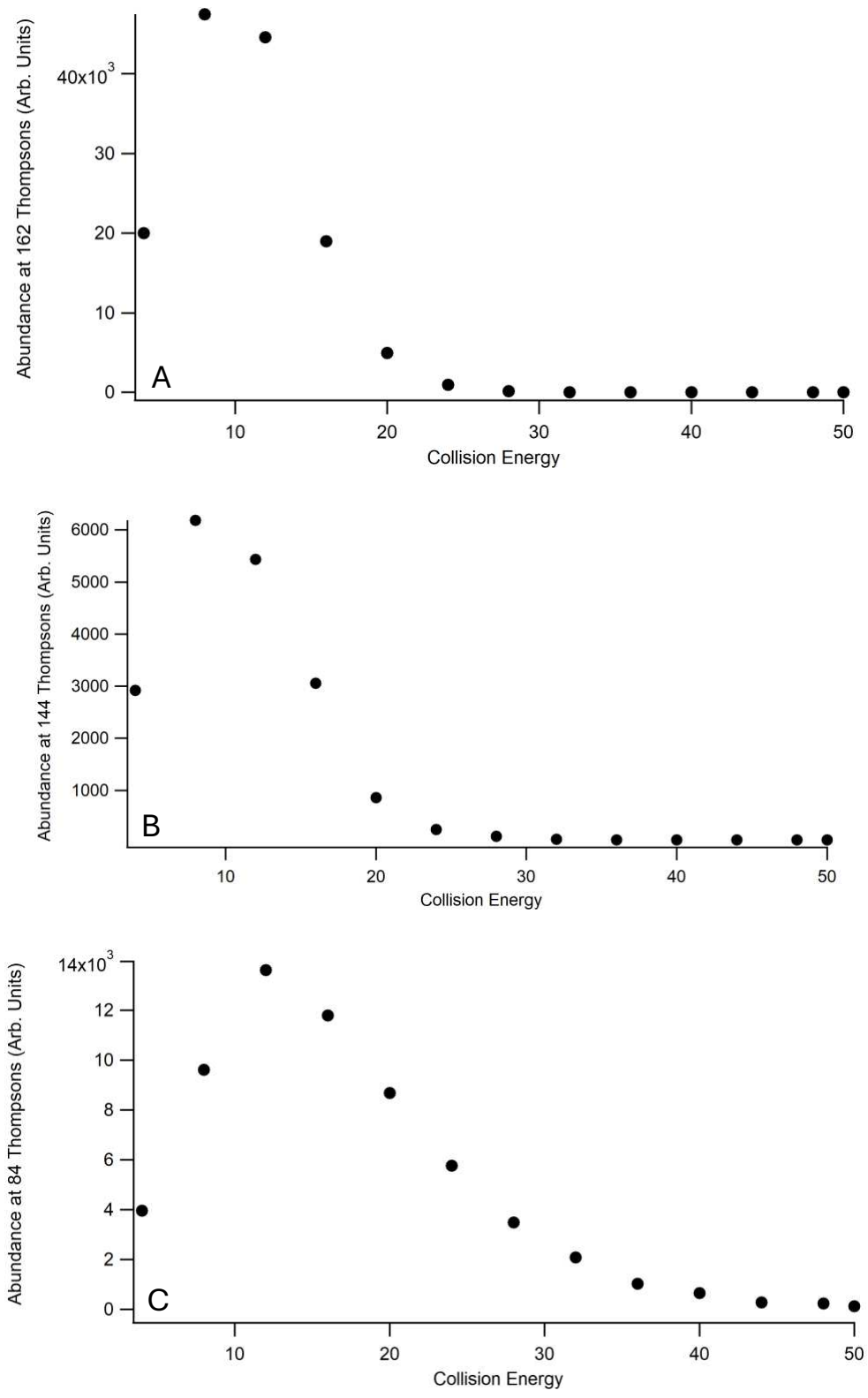

Figure SI4: Collision energy tests for each product ion optimization. A shows the tests for 162, B for 144, and C for 84.

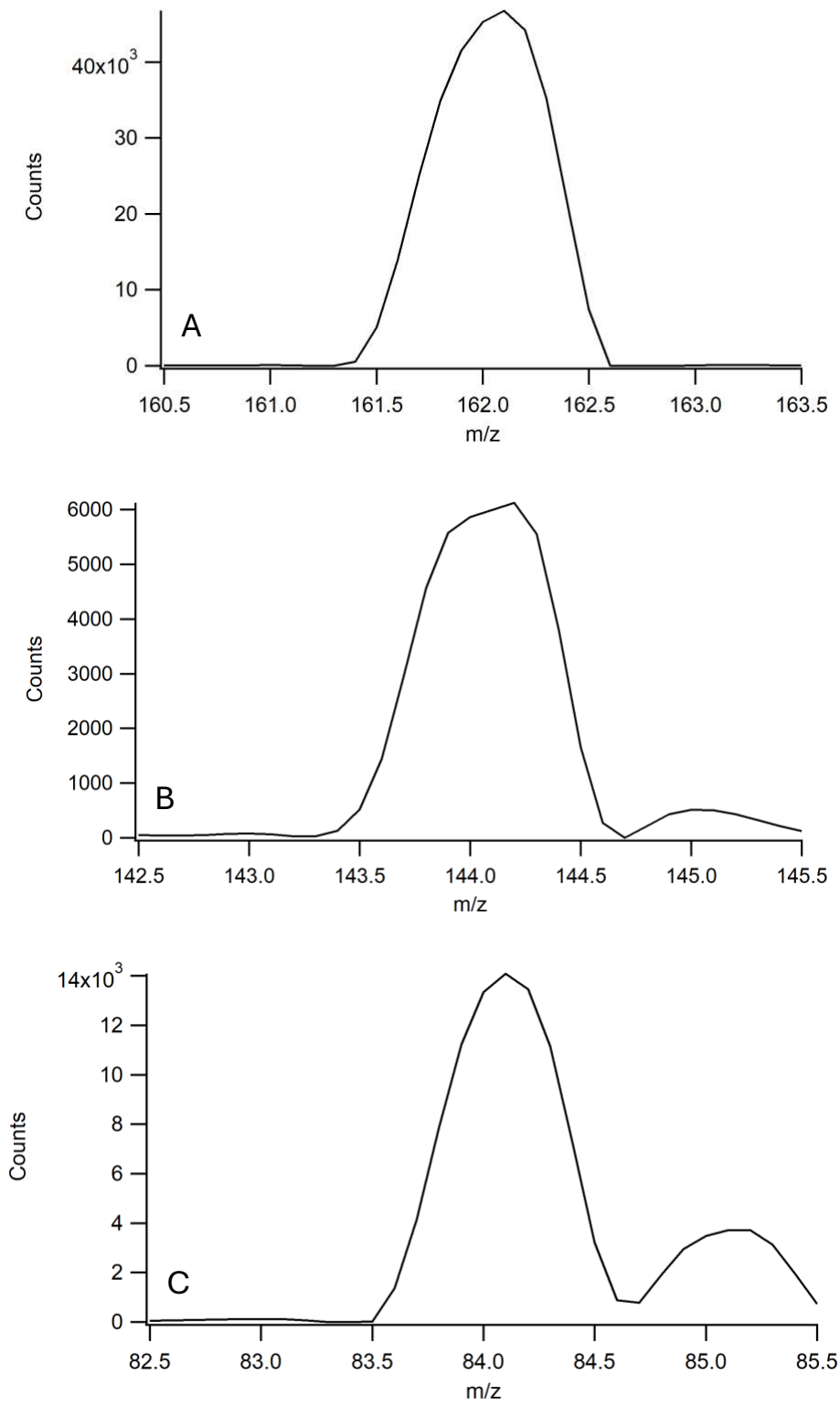

Figure SI5: Narrow mass scans for each product ion at their respective collision energies. A shows the scan for 162, B for 144, and C for 84.

Optimization for the source parameters used for the electrospray ionization of glucosamine was performed using the Agilent Source Optimizer program. The optimizer program automates the process of source optimization by creating methods and worklists to run the optimization for the compound and method specified by the user. All optimization was run using the same glucosamine neat standard in sequence to avoid sample degradation. Table SI2 shows the optimized parameters used in the method described in Chapter 2, and Figures SI6-12 show the data that lead to the results in Table SI1.

Table SI2. Optimized source parameters used for glucosamine detection. Individual parameter tests are shown in Figures SI6-12.

Parameter	Low	High	Interval Size	Optimized Value
Capillary Voltage (V)	1000	6000	500	1500
Drying Gas Flow Rate (L/min)	4	12	2	6
Desolvation Line Temperature (°C)	100	350	50	350
Nebulizer Gas Flow Rate (L/min)	15	60	5	55
Nozzle Voltage (V)	0	2000	300	2000
Shielding Gas Flow (L/min)	6	12	1	11
Shielding Gas Temperature (°C)	150	400	50	400

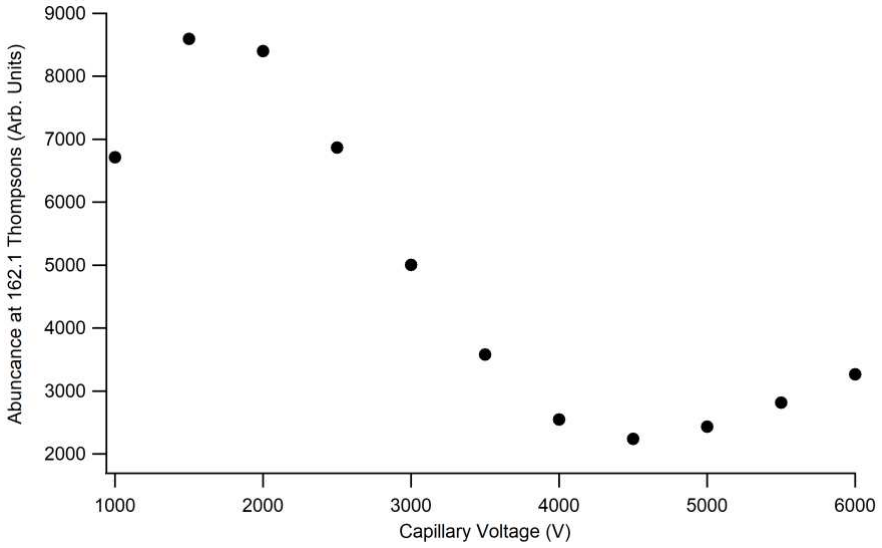

Figure SI6: Optimization of the capillary voltage

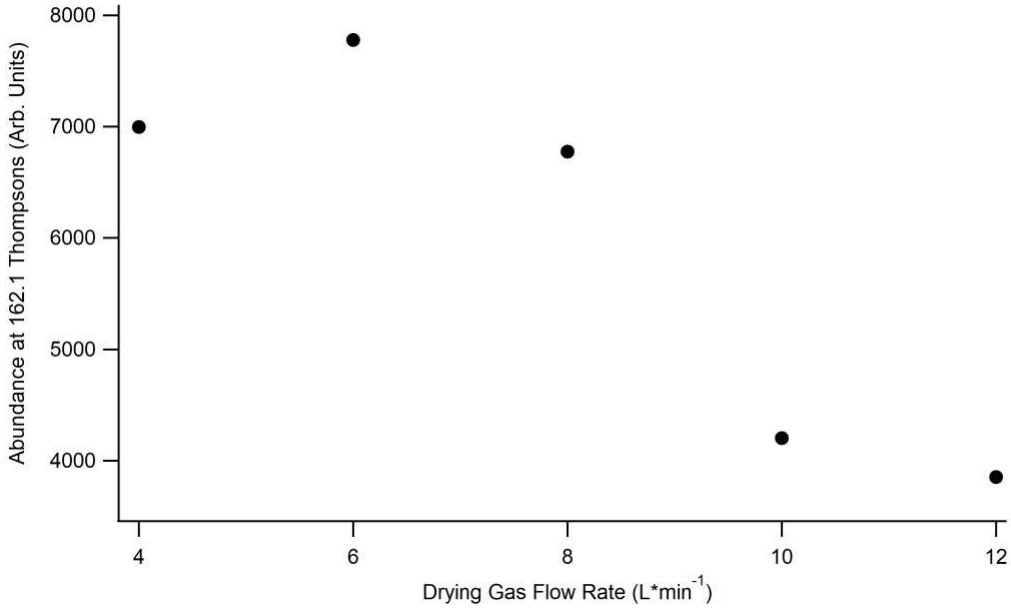

Figure SI7: Optimization of the drying gas flow rate

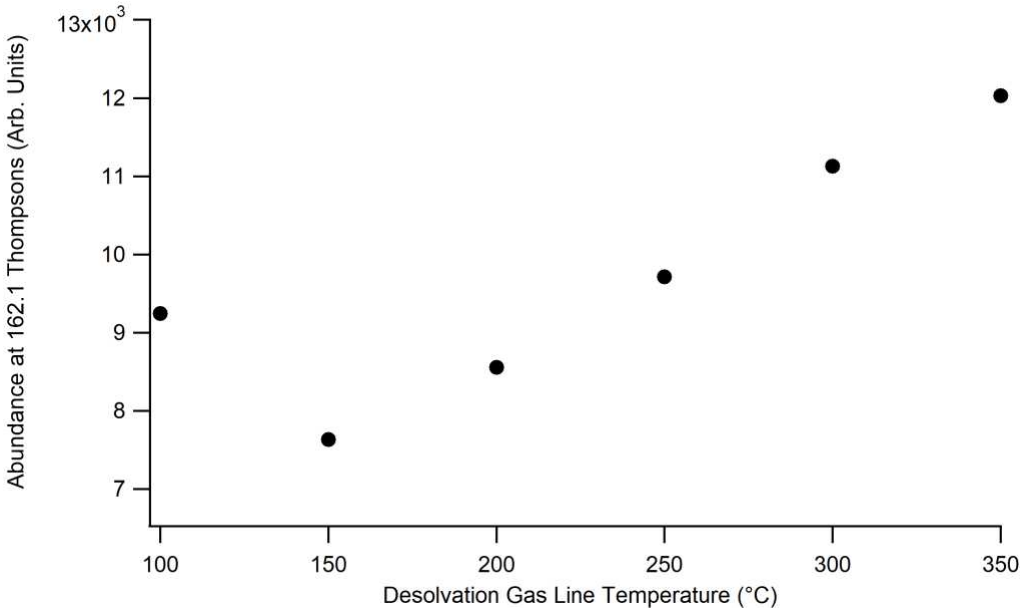

Figure SI8: Optimization of the desolvation gas line temperature

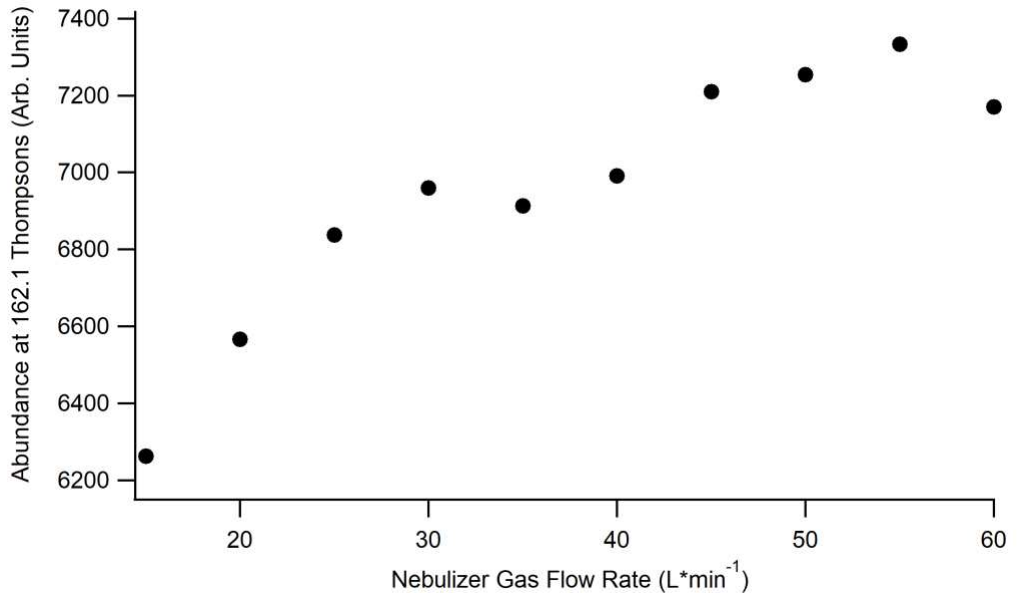

Figure SI9: Optimization of the nebulizer gas flow rate

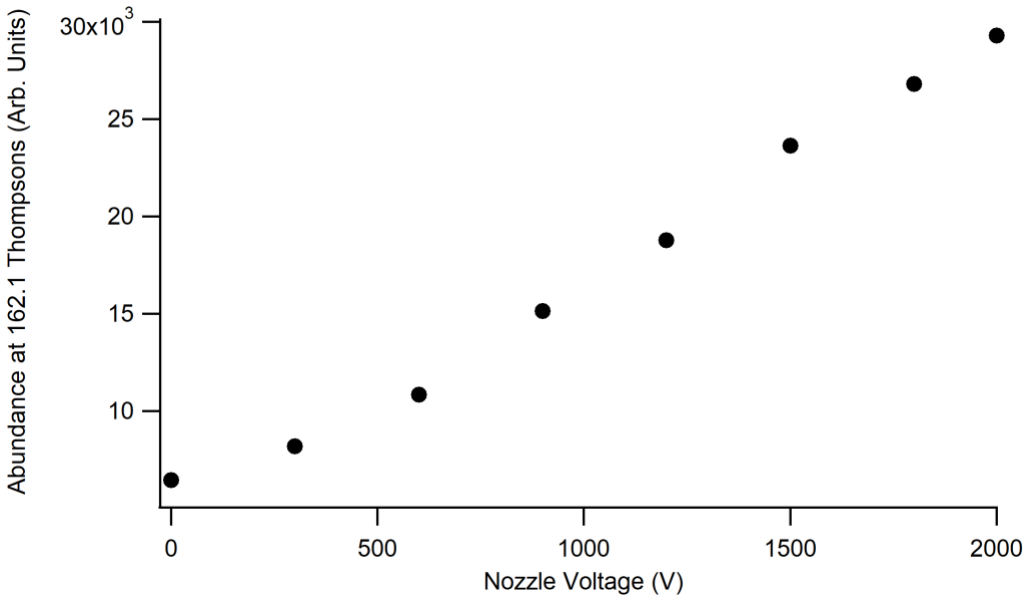

Figure SI10: Optimization of the nozzle voltage

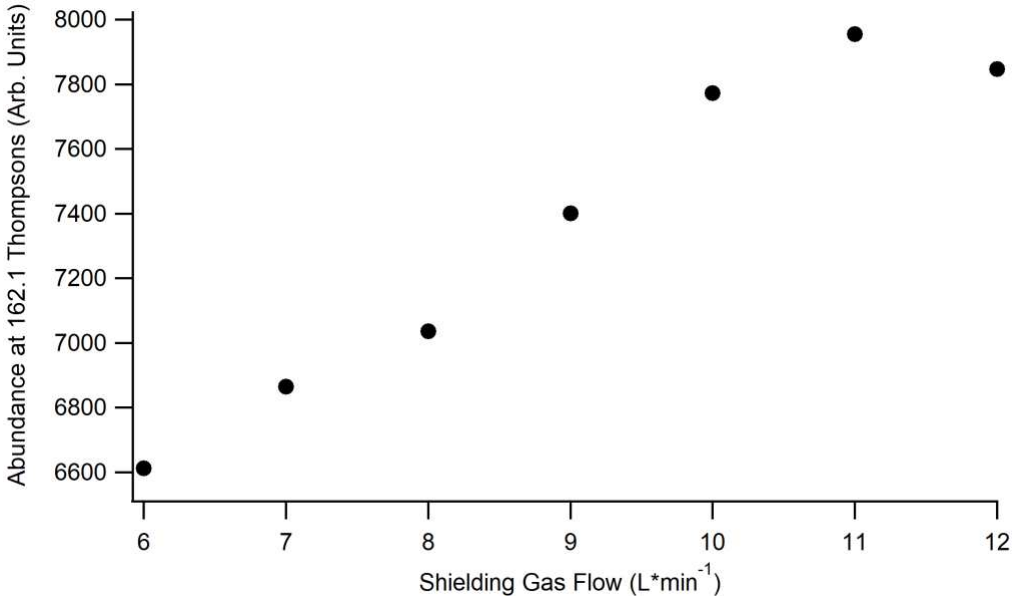

Figure SI11: Optimization of the shielding gas flow rate

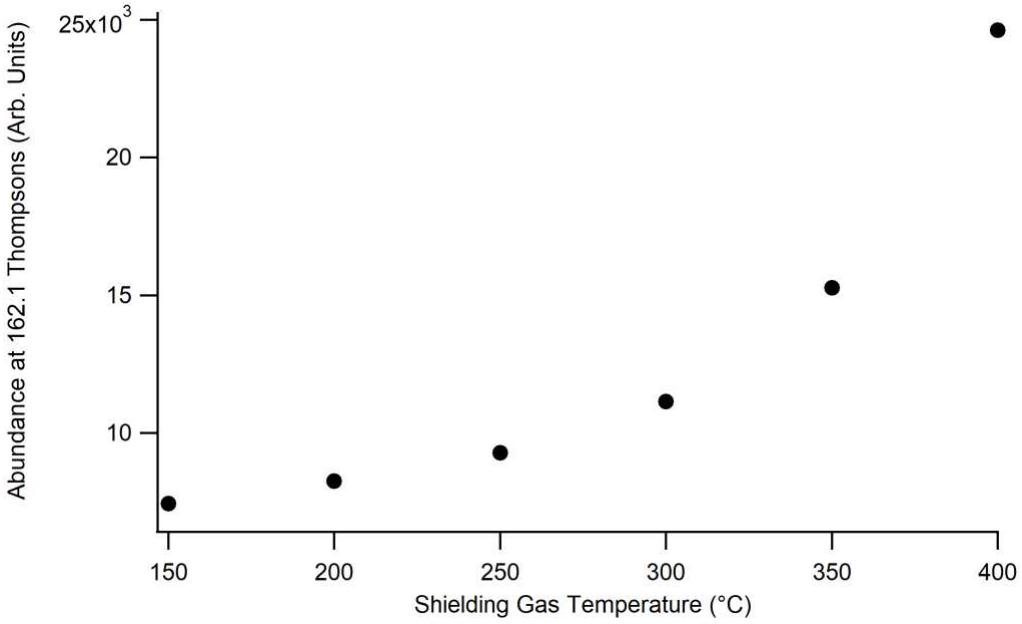

Figure SI12: Optimization of the shielding gas temperature

APPENDIX II: SUPPLEMENTAL INFORMATION FOR CHAPTER 4

Optimization for the multiple reaction monitoring of THC, 11-OH-THC, THC-COOH, CBD, 7-OH-CBD, and 7-COOH-CBD was performed using the Agilent Optimizer program. The optimizer program automates the process of mass spectrometer optimization by creating methods and worklists to run the optimization for the compound and method specified by the user. All optimization was run using the same glucosamine neat standard in sequence to avoid sample degradation. Table SI3 shows the used optimized parameters, and Figures SI13-42 show the data that lead to the results in Table SI3.

Table SI3. Optimized mass spectrometry parameters used for glucosamine detection. Individual parameter tests are shown in Figures SI13-42

Compound	Parent Ion	Fragmentor Voltage (V)	Product Ion	Collision Energy	Abundance
THC	315.2	132.0	193.1	24	10221
			123.0	40	6381
			93.1	28	4052
11-OH-THC	331.2	114.0	105.1	46	80032
			91.1	66	63196
			77.1	98	76743
THC-COOH	345.2	117.0	193.1	30	8331
			91.1	62	5509
			77.1	100	6752
CBD	315.2	111.0	193.1	24	154438
			123.0	40	9393
			93.1	24	5874
7-OH-CBD	311.2	111.0	105.1	46	68647
			91.1	66	54887
			77.1	90	65226
7-COOH-CBD	345.2	117.0	193.2	30	3058
			91.1	70	1966
			77.1	100	2292

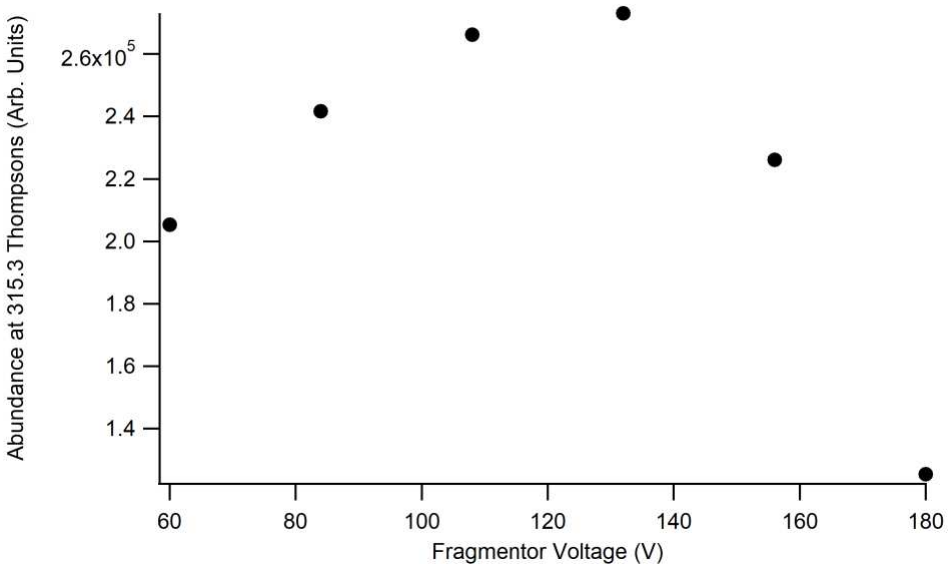

Figure SI13: Optimization of fragmentor voltages for THC

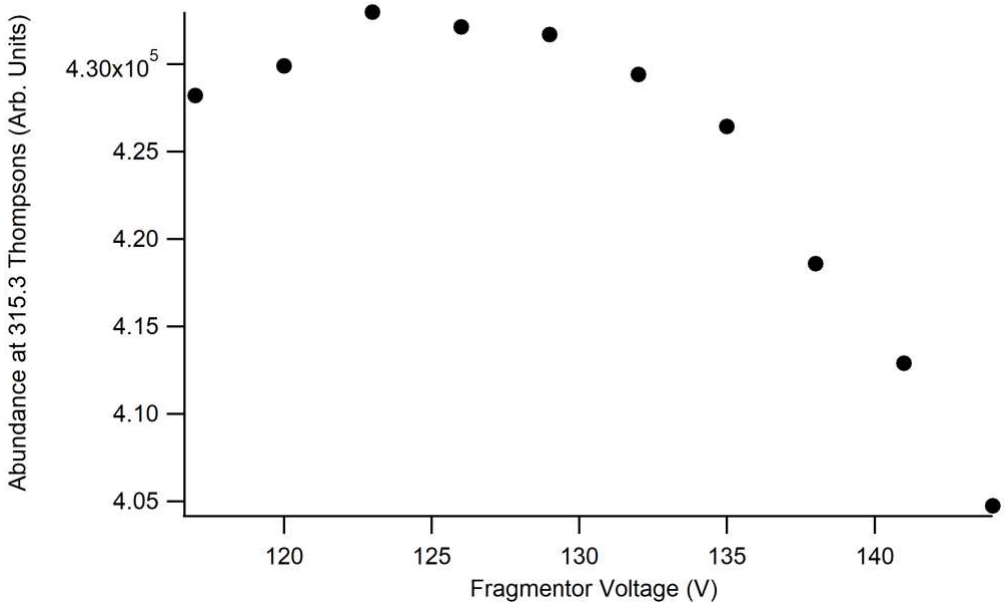

Figure SI14: Narrow range fragmentor voltages tested for THC

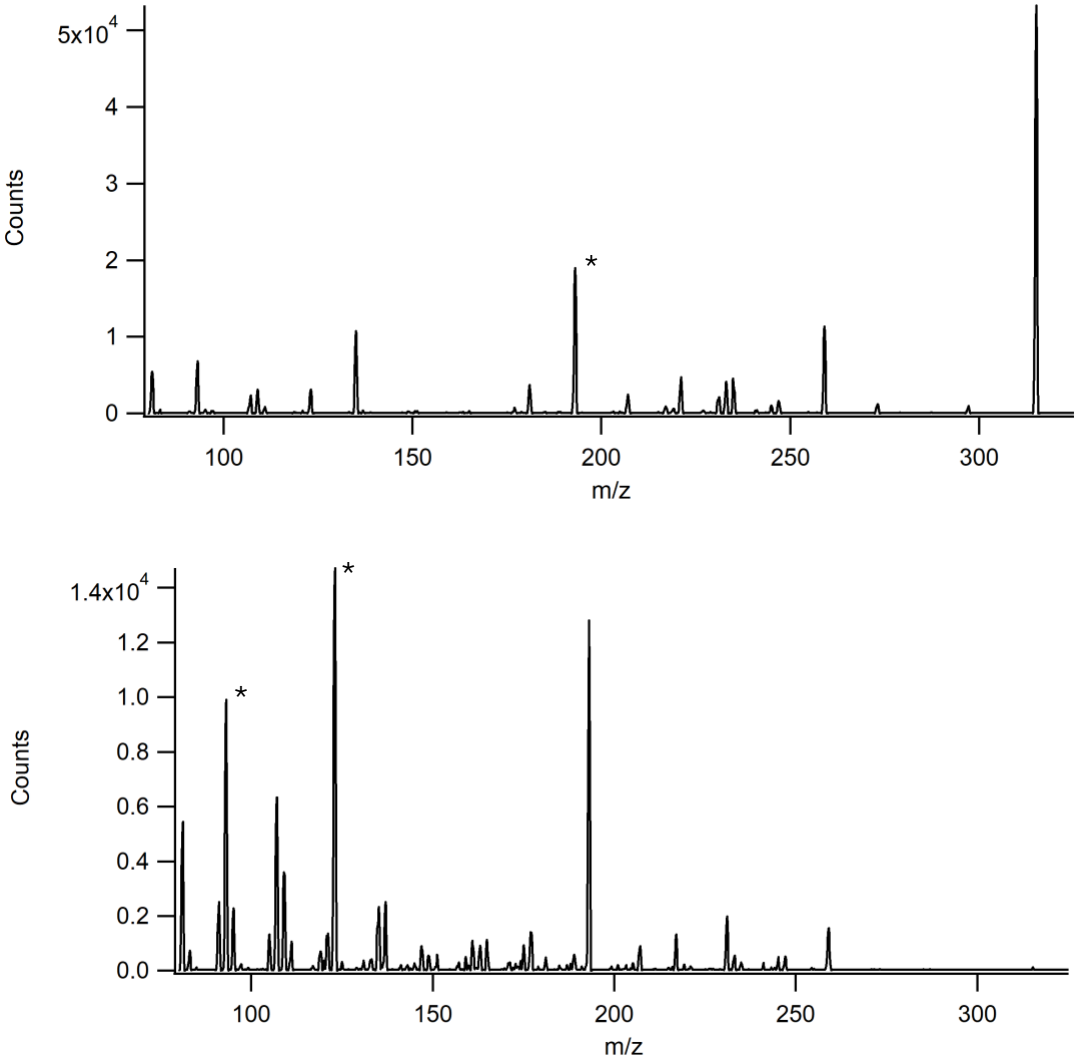

Figure SI15: Scans for Product Ions of THC. Product Ions selected are marked *.

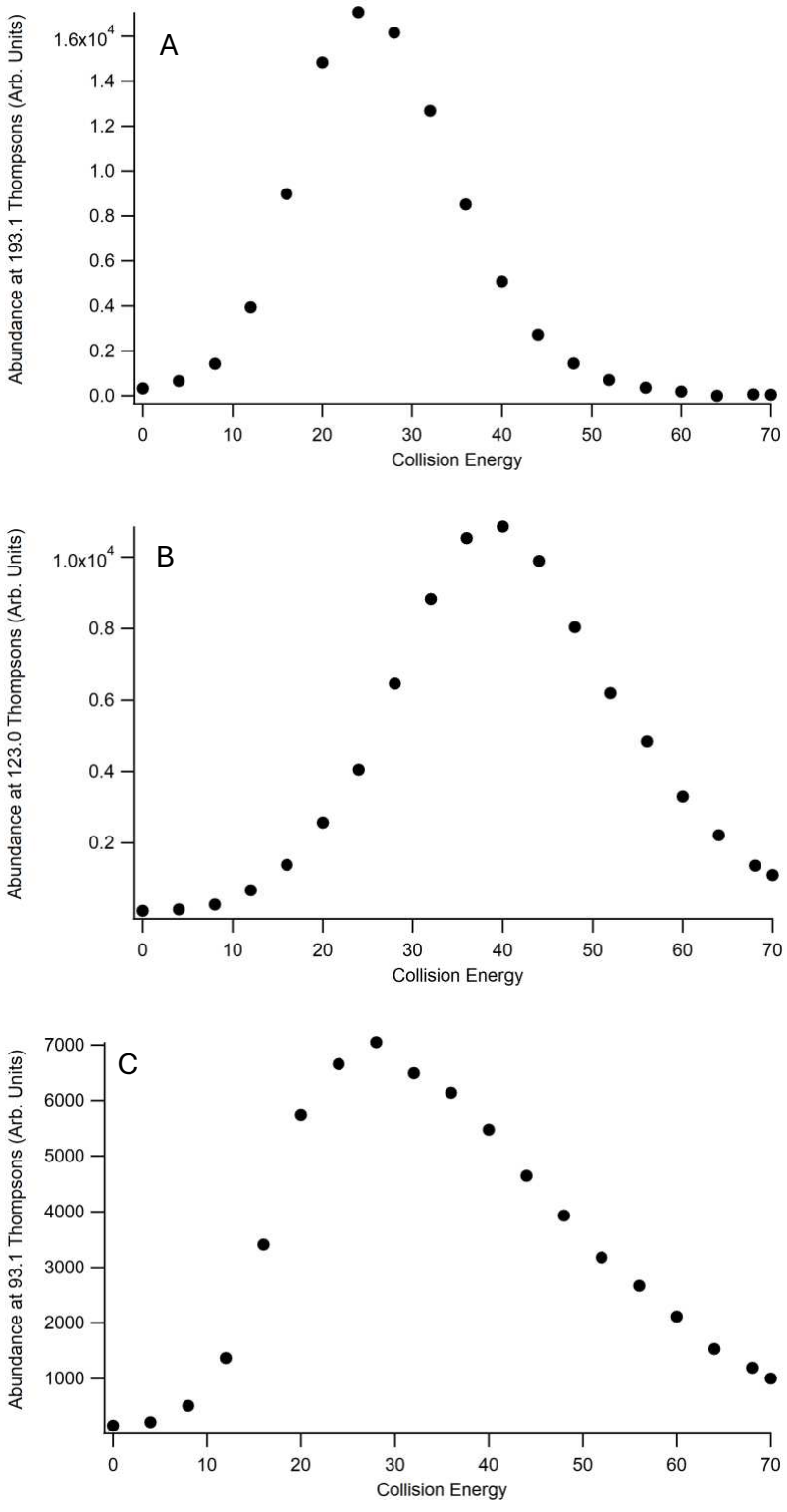

Figure SI16: Collision energy tests for each THC product ion optimization. A shows the tests for 193.1, B for 123.0, and C for 93.1.

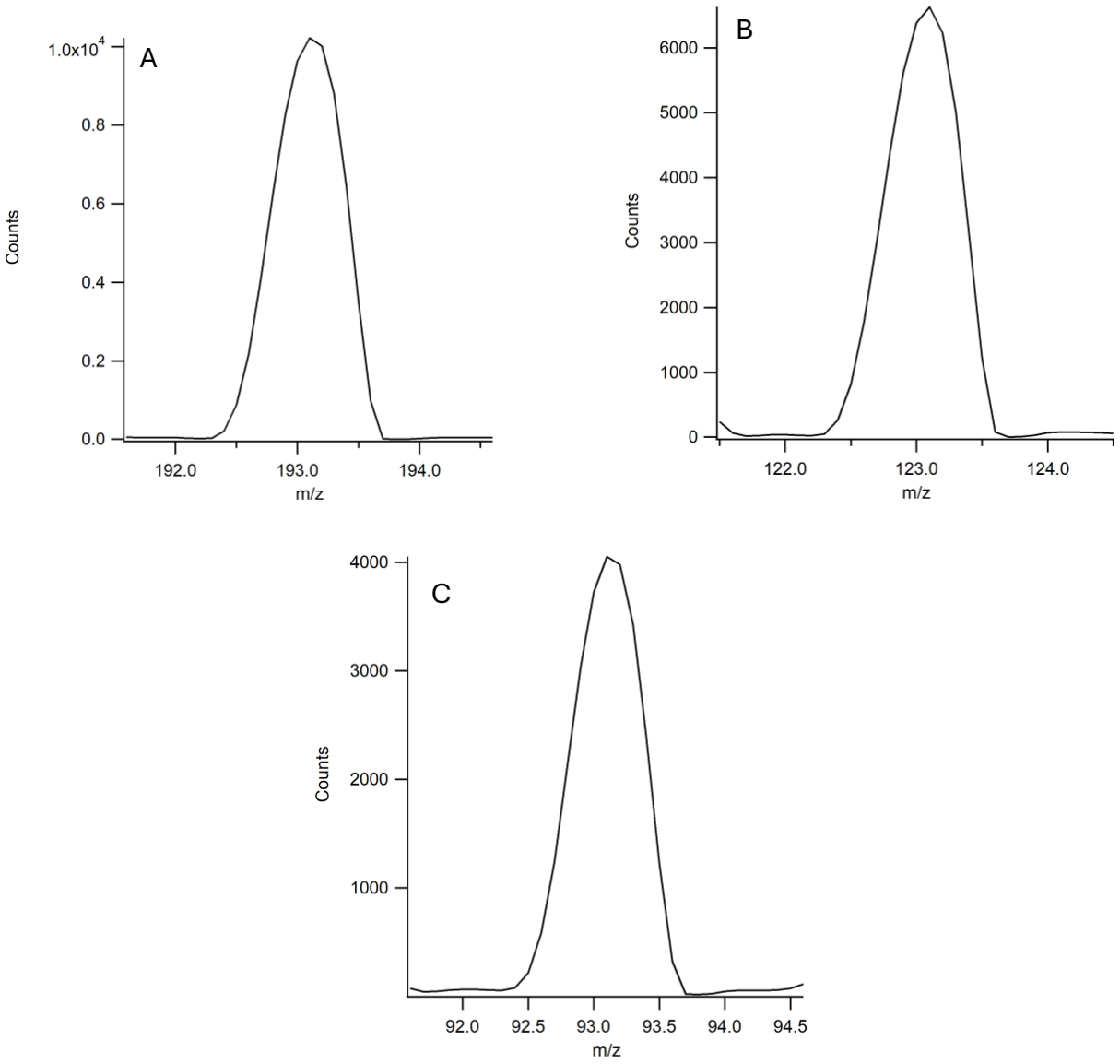

Figure SI17: Narrow Mass Scans for each THC product ion at their respective collision energies. A shows the scan for 193.1, B for 123.0, and C for 93.1.

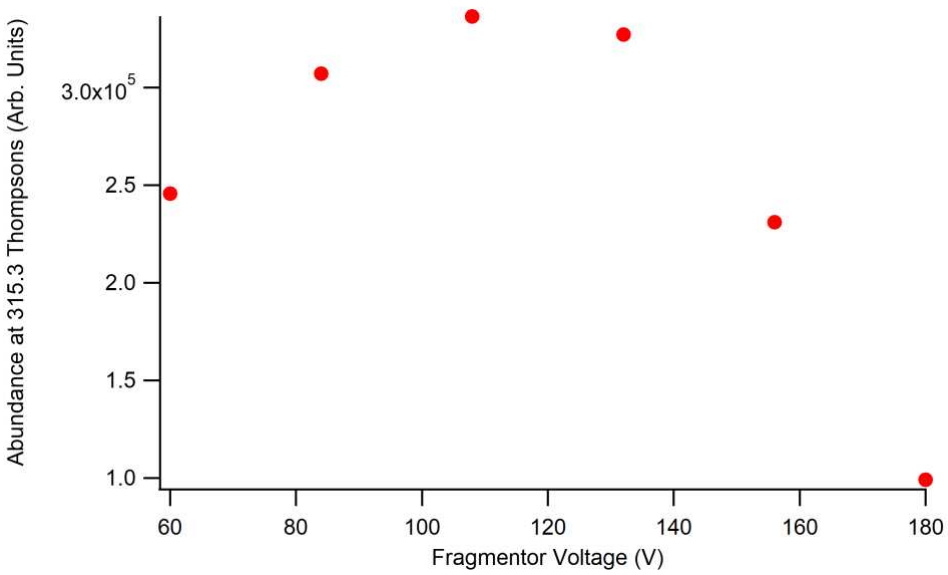

Figure SI18: Optimization of fragmentor voltages for CBD

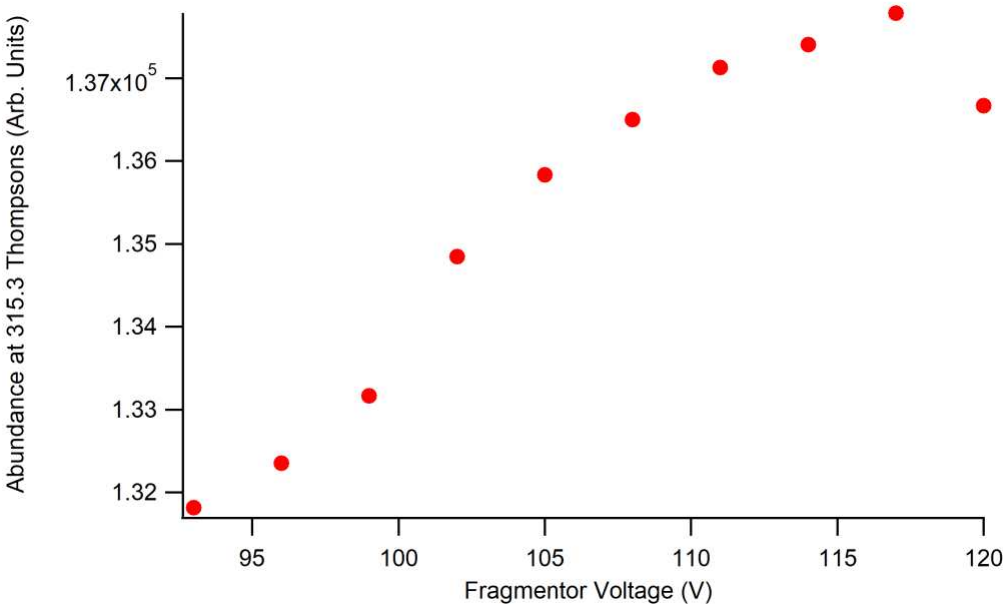

Figure SI19: Narrow range fragmentor voltages tested for CBD

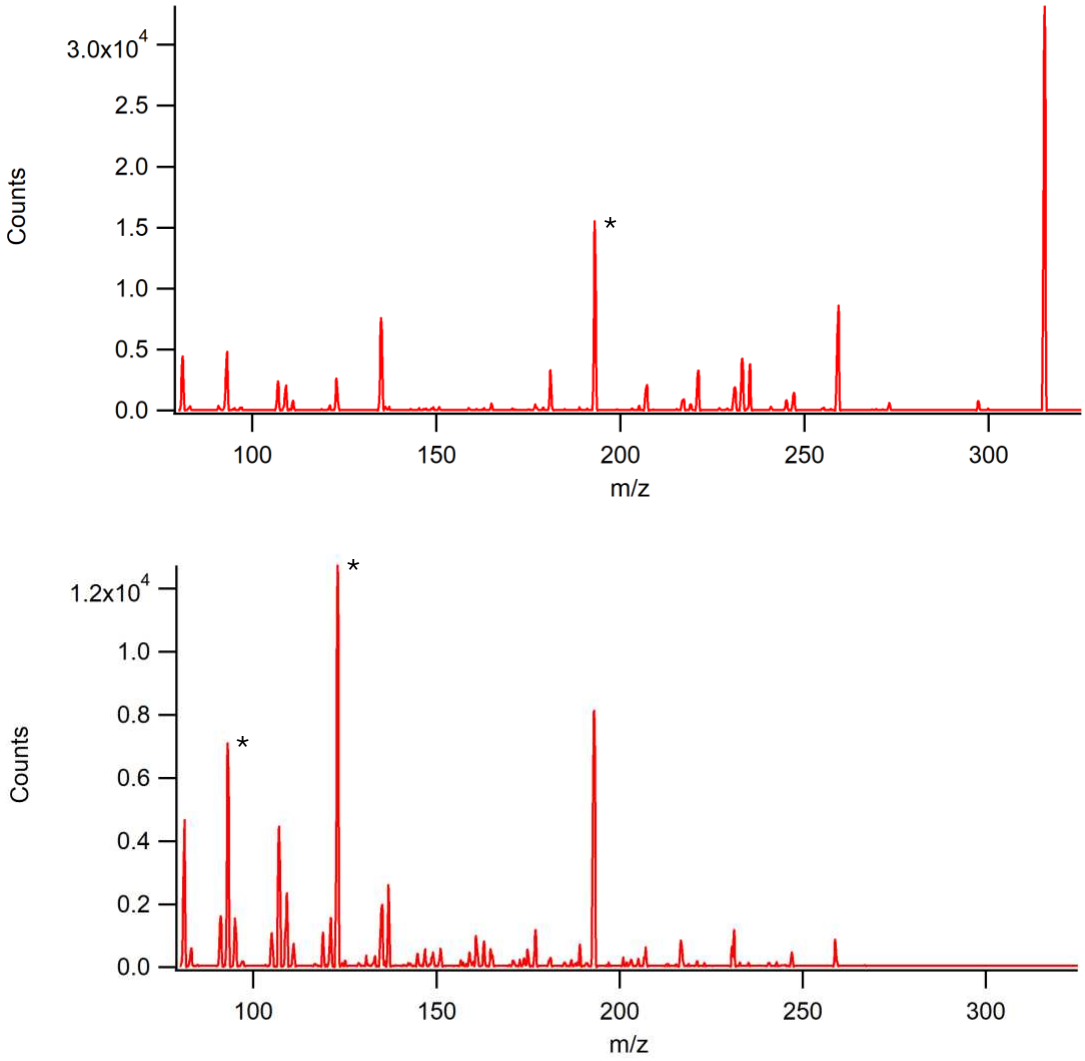

Figure SI20: Scans for CBD Product Ions. Product Ions selected are marked *.

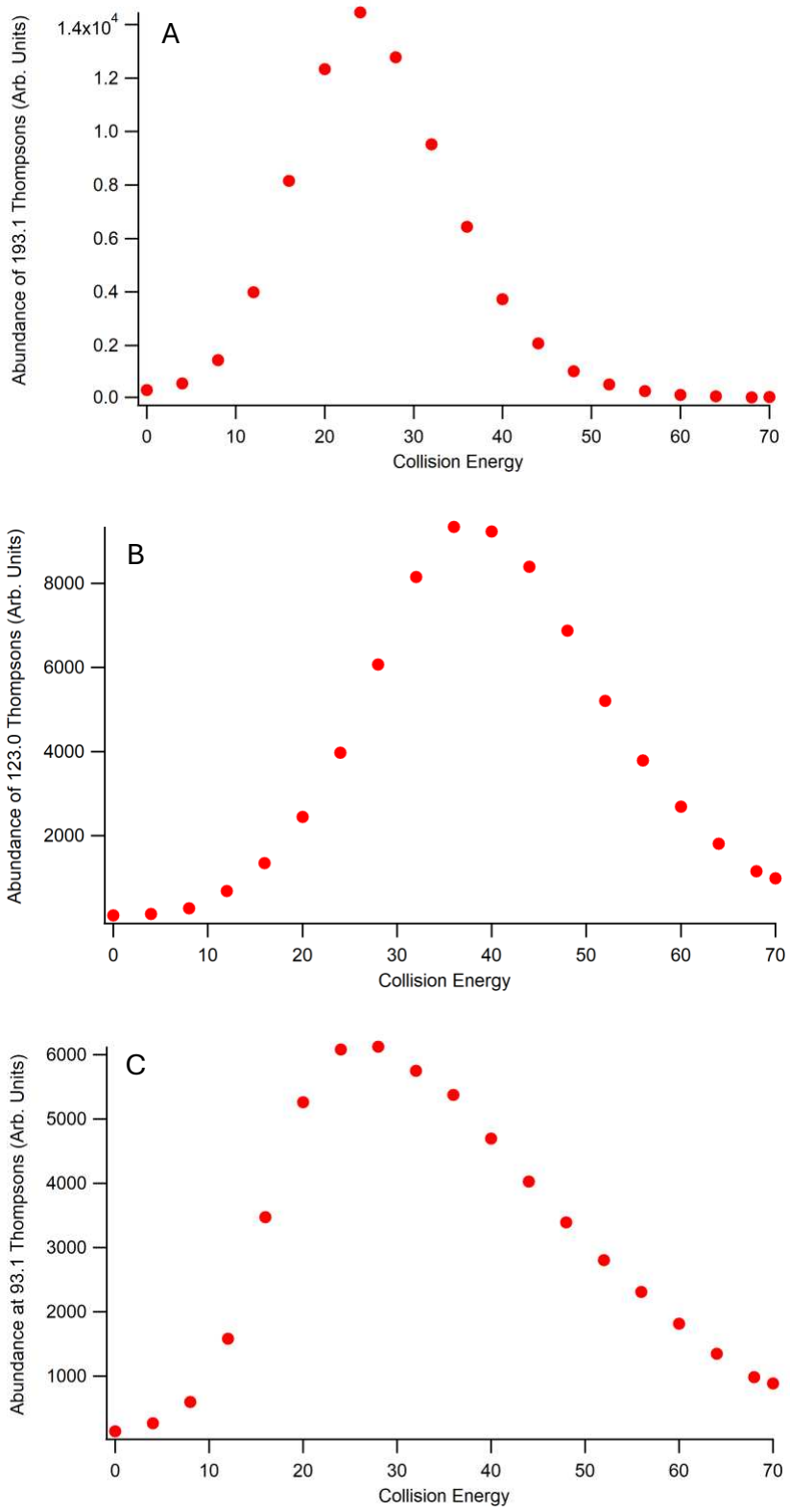

Figure SI21: Collision energy tests for each CBD product ion optimization. A shows the tests for 193.1, B for 123.0, and C for 93.1.

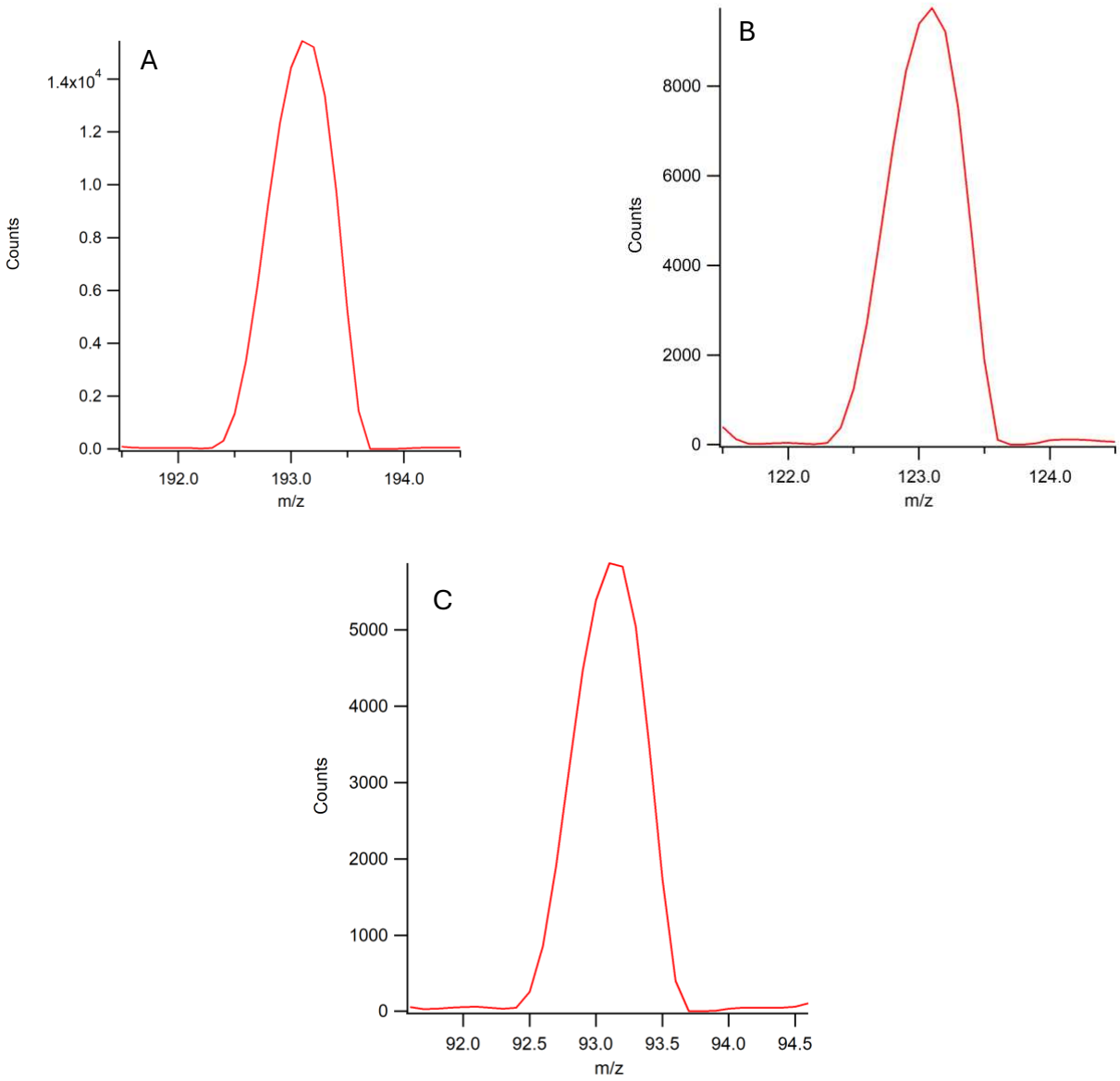

Figure SI22: Narrow Mass Scans for each CBD product ion at their respective collision energies. A shows the scan for 193.1, B for 123.0, and C for 93.1.

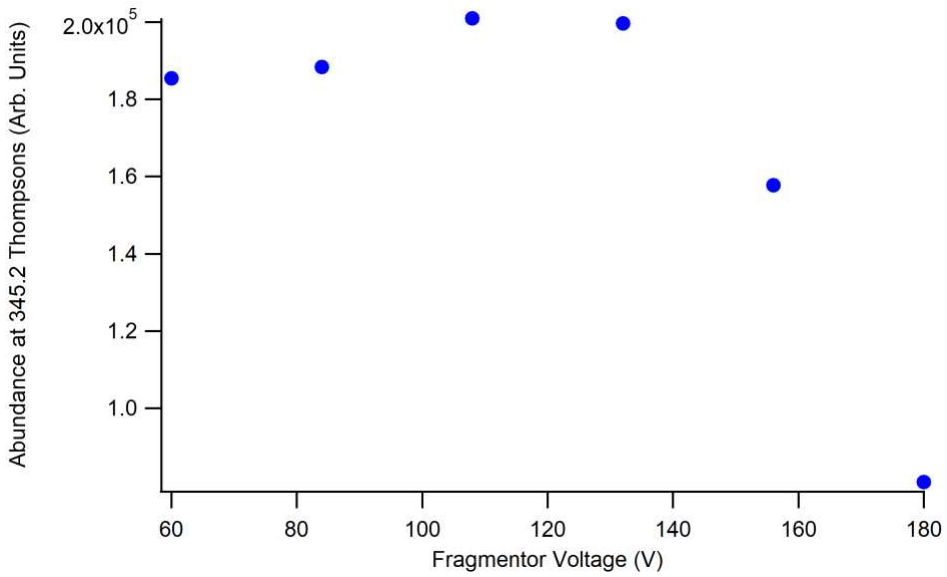

Figure SI23: Optimization of fragmentor voltages for THC-COOH

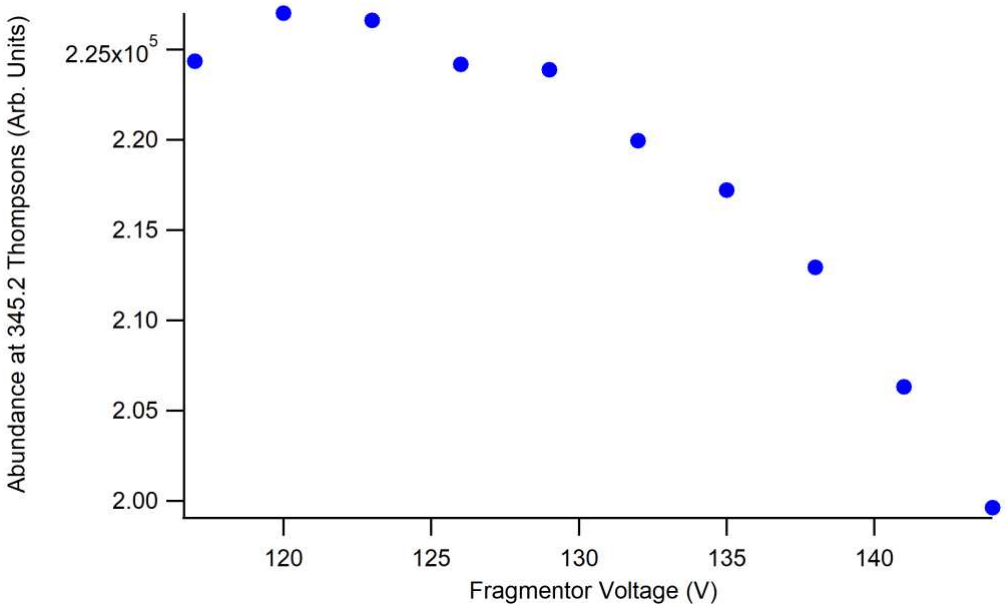

Figure SI24: Narrow range fragmentor voltages tested for THC-COOH

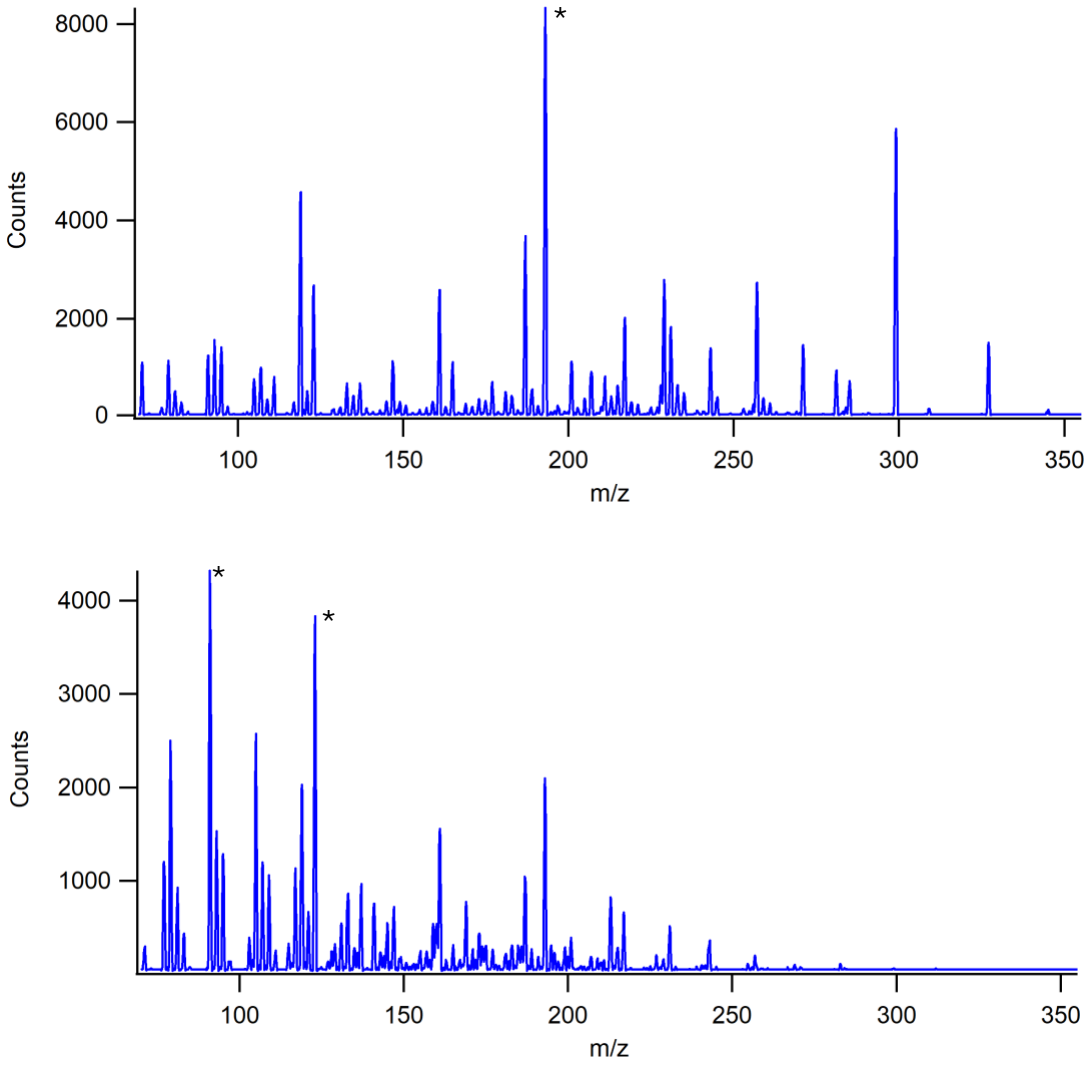

Figure SI25: Scans for Product Ions of THC-COOH. Product Ions selected are marked *.

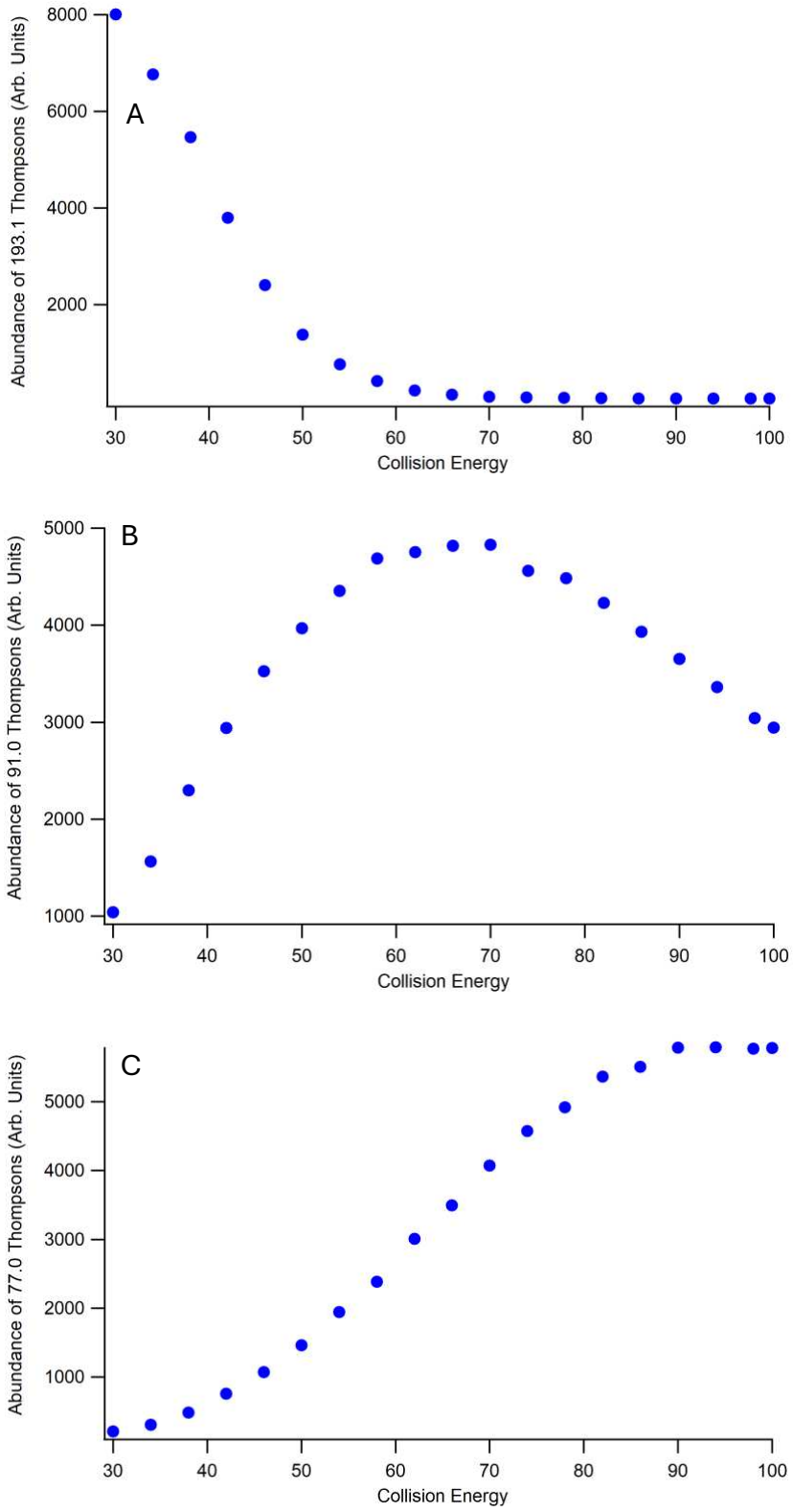

Figure SI26: Collision energy tests for each THC-COOH product ion optimization. A shows the tests for 193.1, B for 91.0, and C for 77.0.

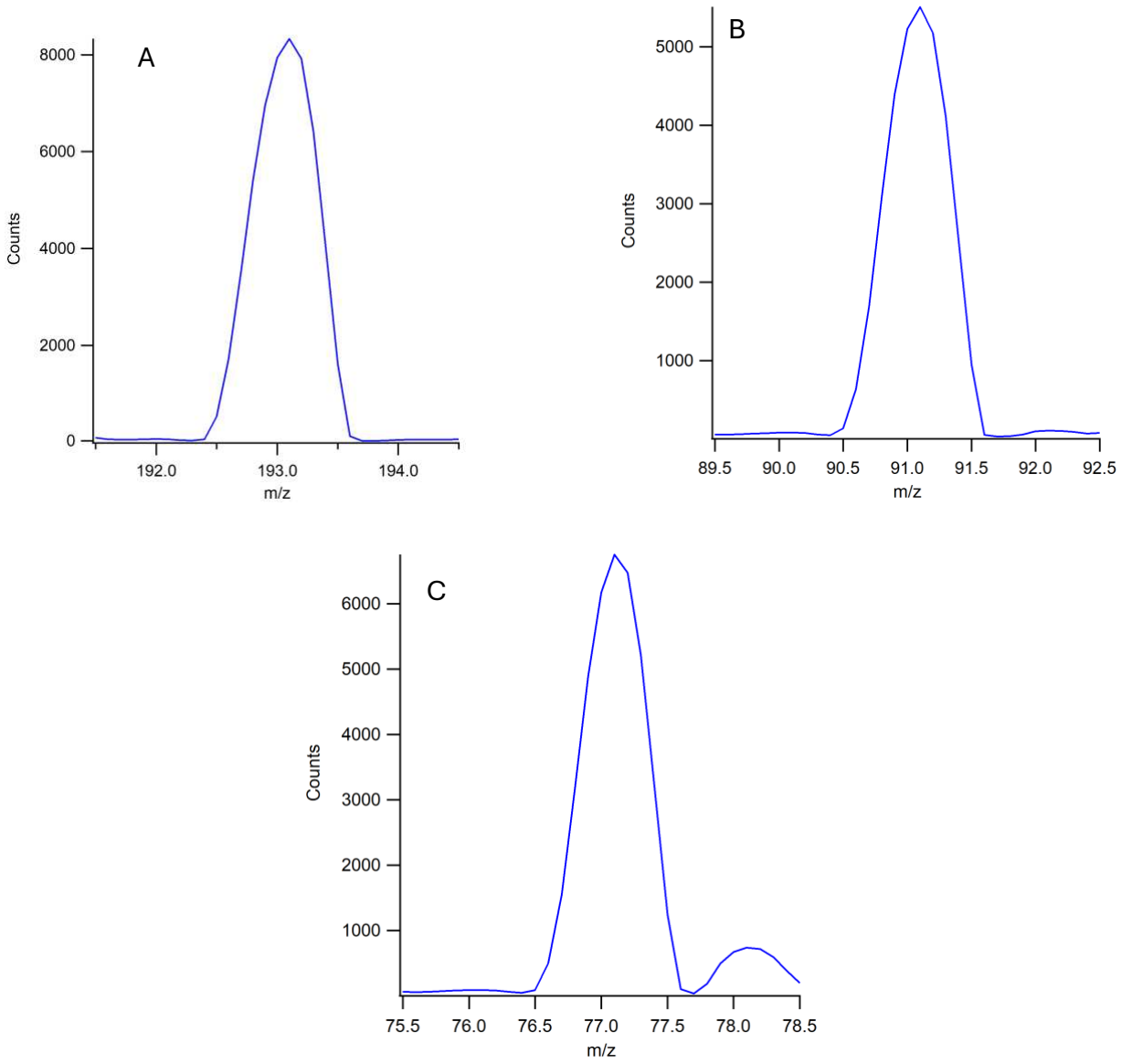

Figure SI27: Narrow Mass Scans for each THC-COOH product ion at their respective collision energies. A shows the scan for 193.1, B for 91.1, and C for 77.0.

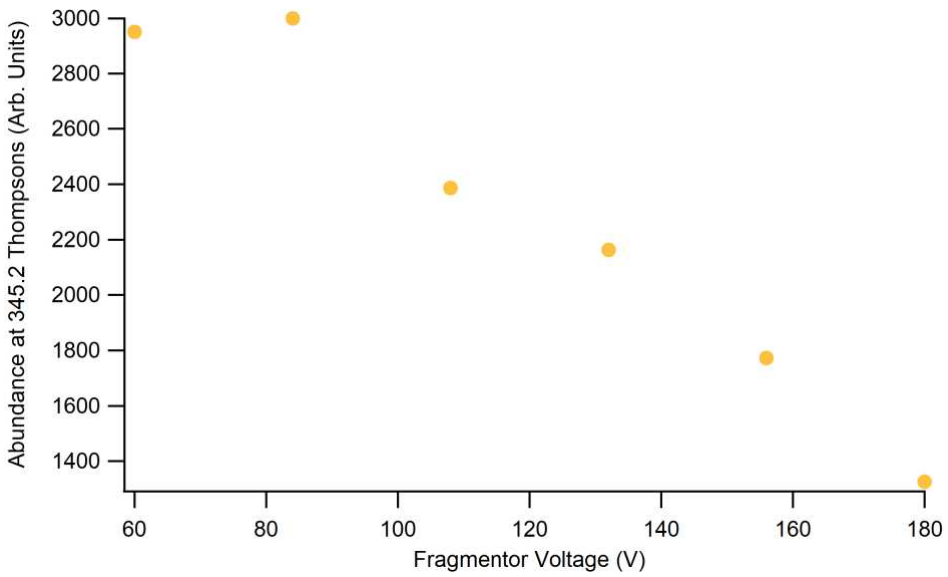

Figure SI28: Optimization of fragmentor voltages for 7-COOH-CBD

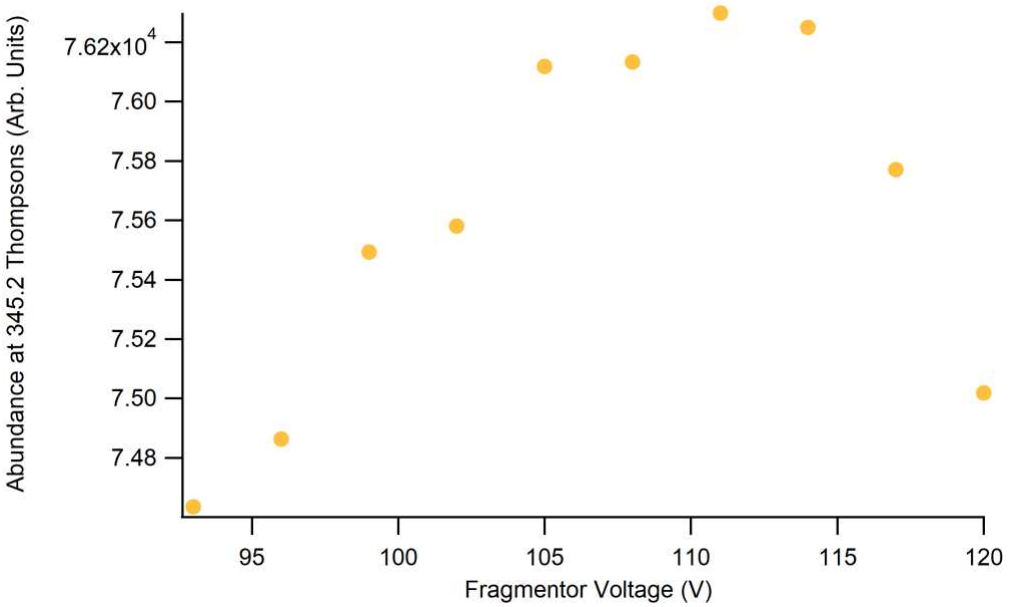

Figure SI29: Narrow range fragmentor voltages tested for 7-COOH-CBD

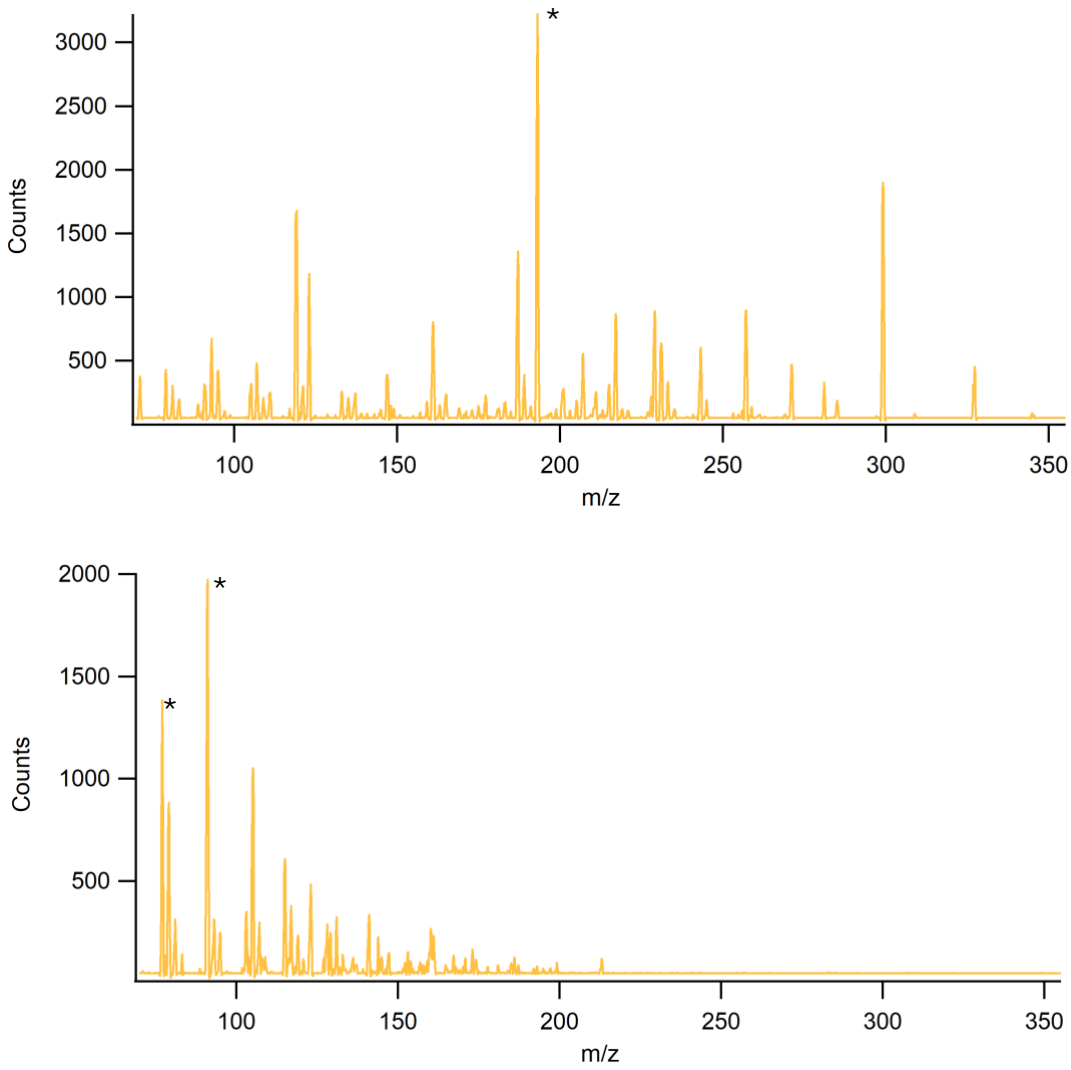

Figure SI30: Scans for 7-COOH-CBD Product Ions. Product Ions selected are marked *.

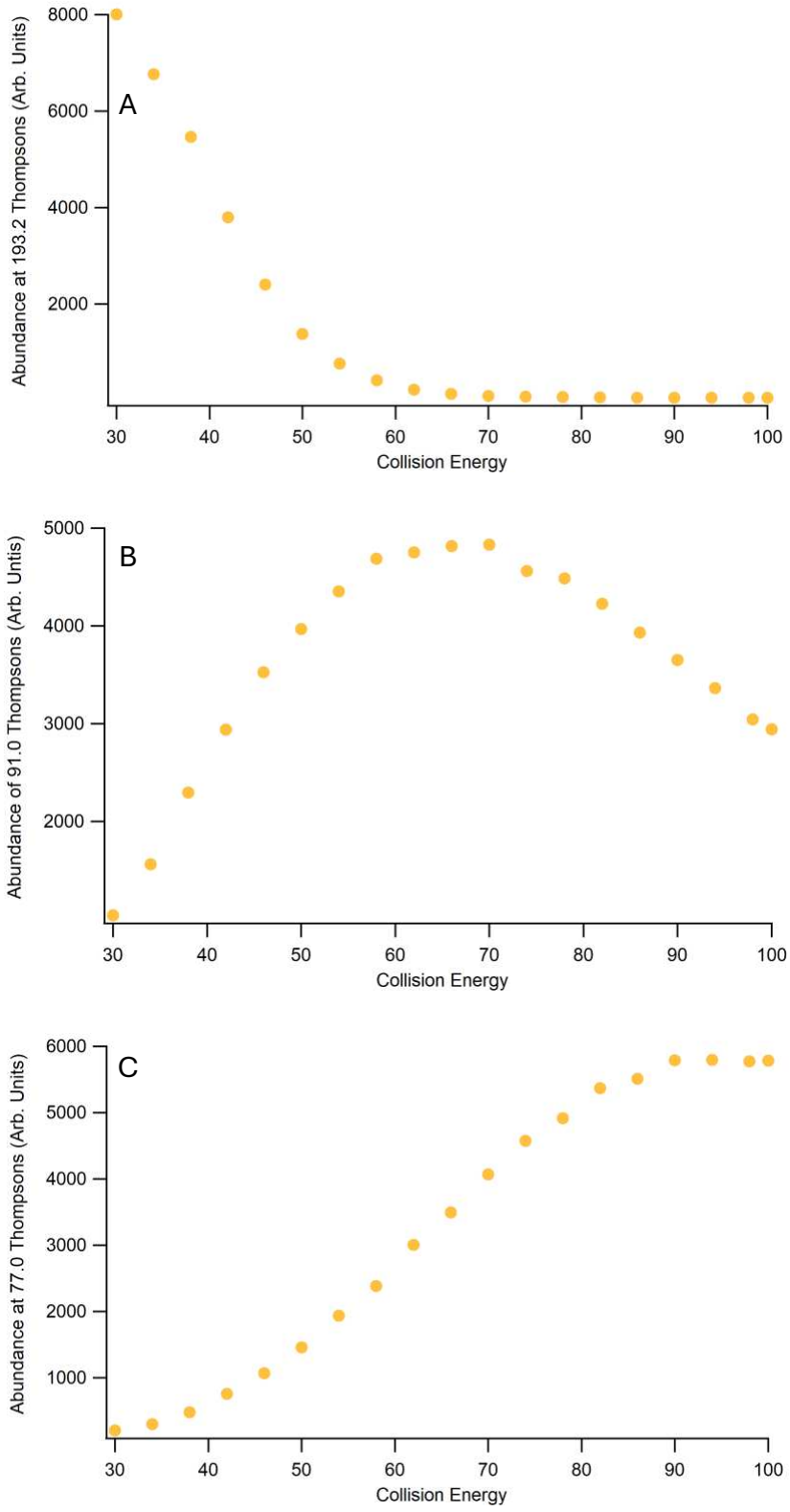

Figure SI31: Collision energy tests for each CBD product ion optimization. A shows the tests for 193.2, B for 91.0, and C for 77.0.

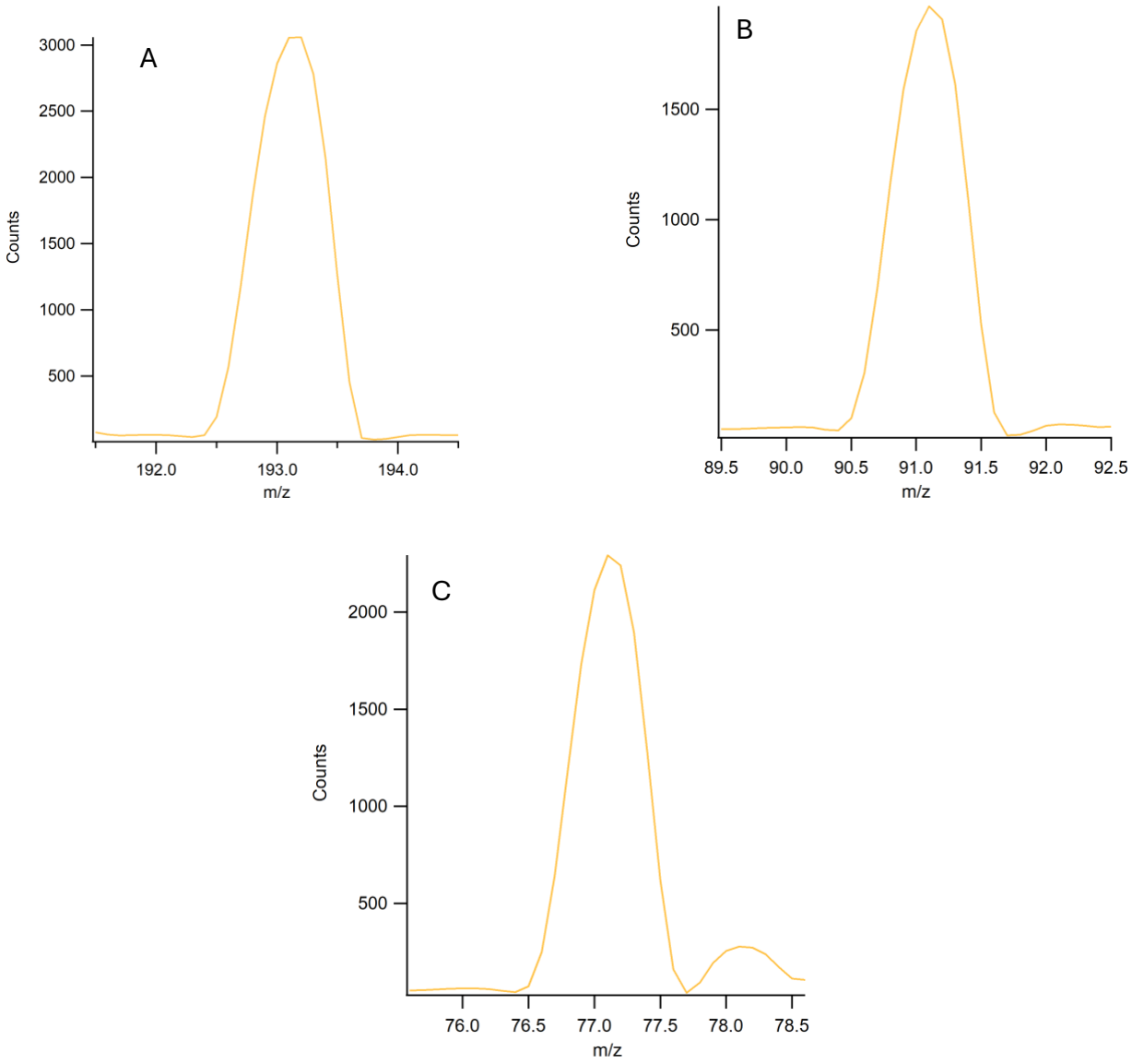

Figure SI32: Narrow Mass Scans for each CBD product ion at their respective collision energies. A shows the scan for 193.1, B for 91.2, and C for 77.0.

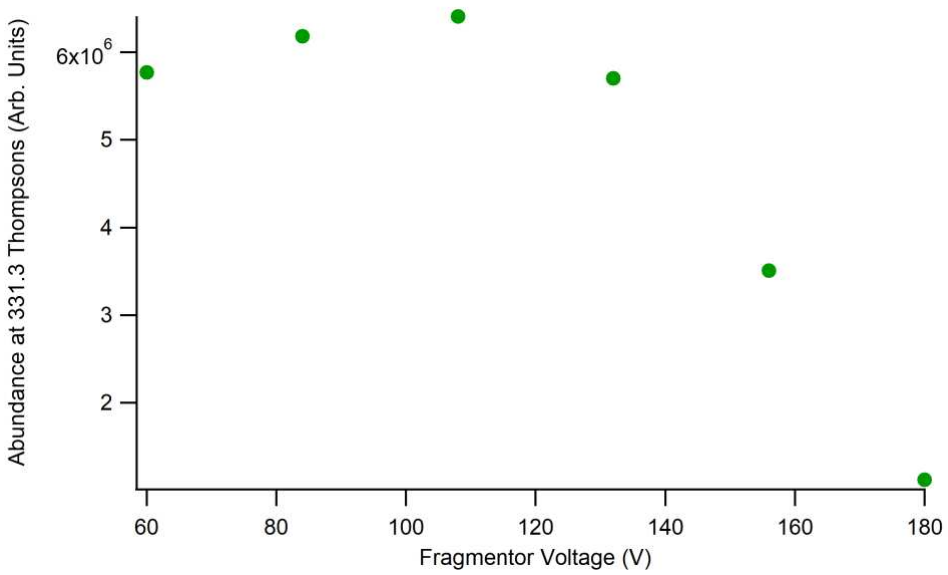

Figure SI33: Optimization of fragmentor voltages for 11-OH-THC

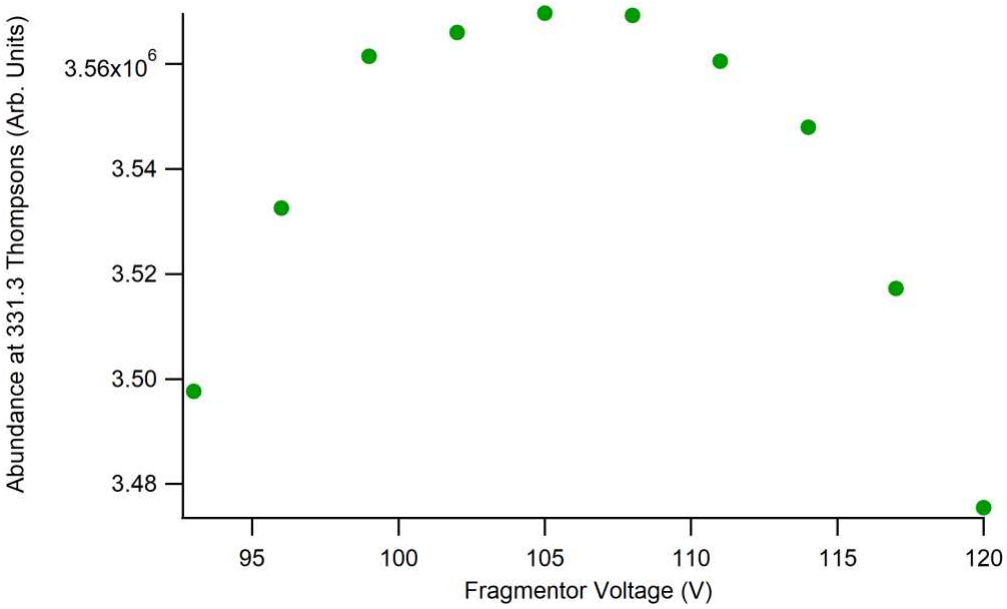

Figure SI34: Narrow range fragmentor voltages tested for 11-OH-THC

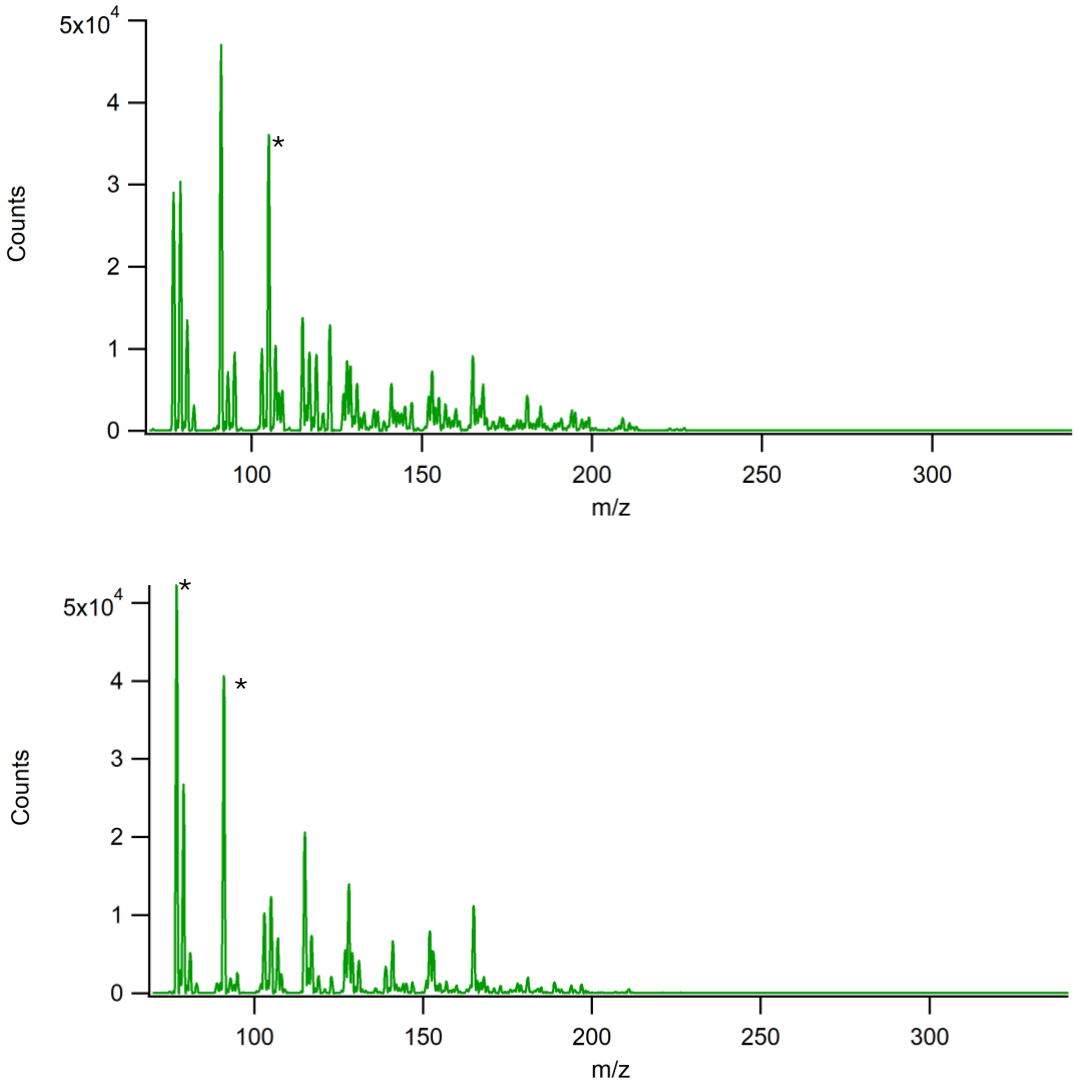

Figure SI35: Scans for Product Ions of 11-OH-THC. Product Ions selected are marked *.

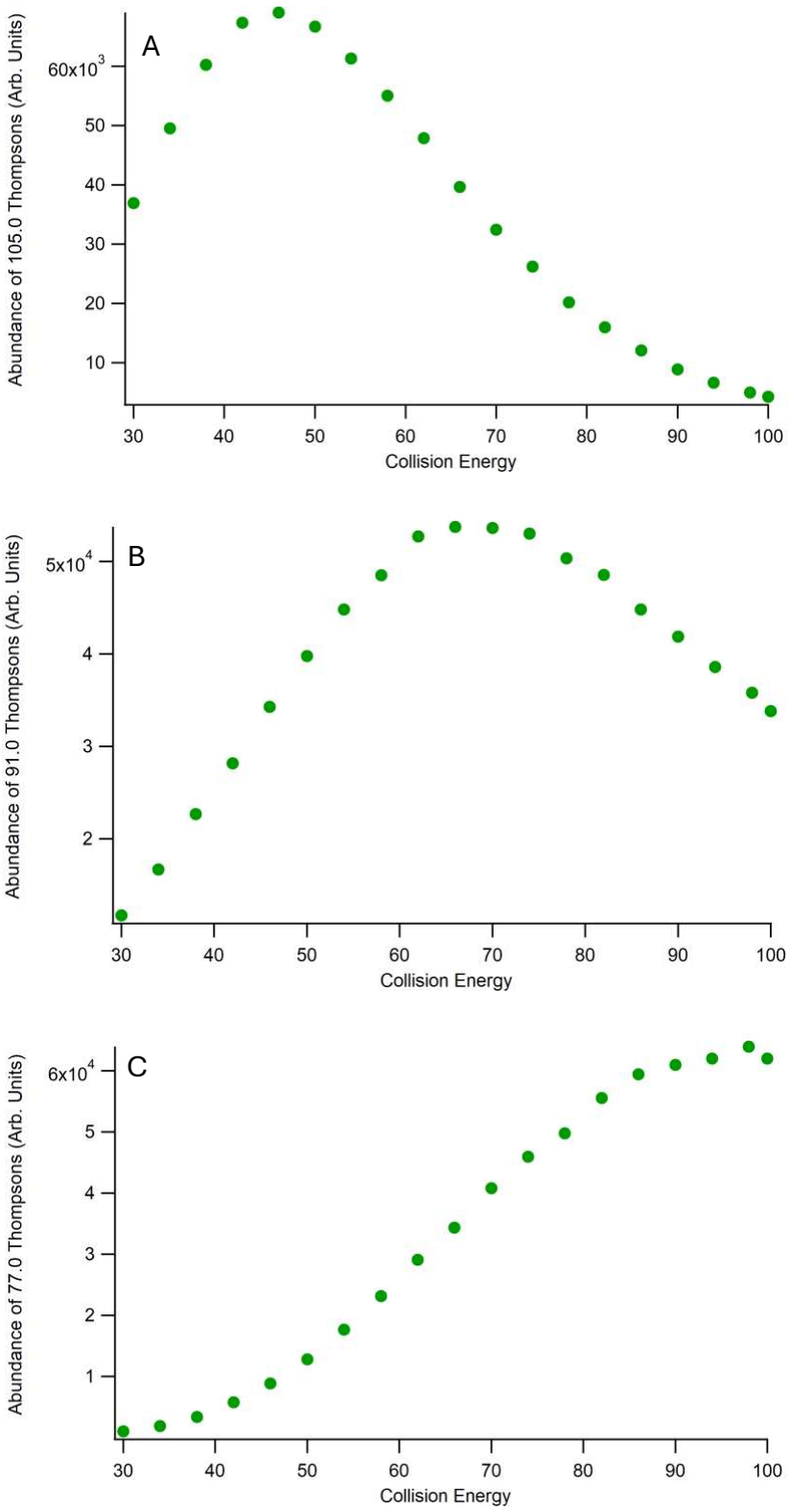

Figure SI36: Collision energy tests for each 11-OH-THC product ion optimization. A shows the tests for 105.0, B for 91.0, and C for 77.0.

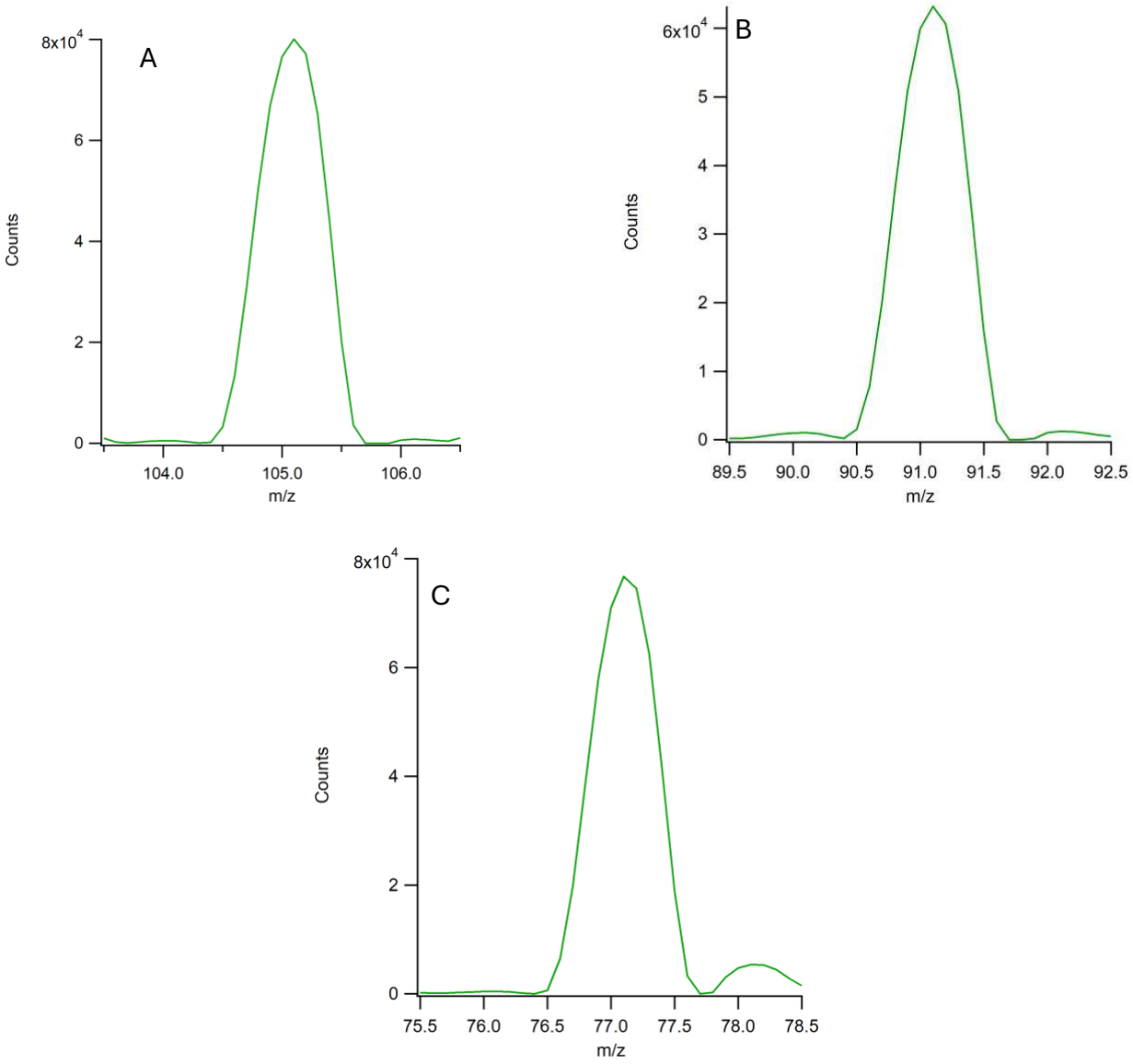

Figure SI37: Narrow Mass Scans for each 11-OH-THC product ion at their respective collision energies. A shows the scan for 105.0, B for 91.0, and C for 77.0.

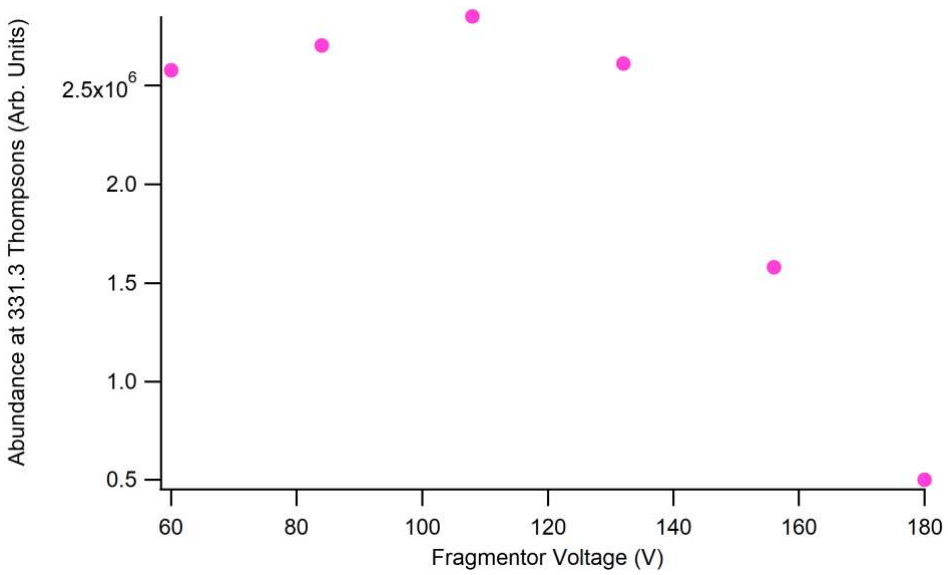

Figure SI38: Optimization of fragmentor voltages for 7-OH-CBD

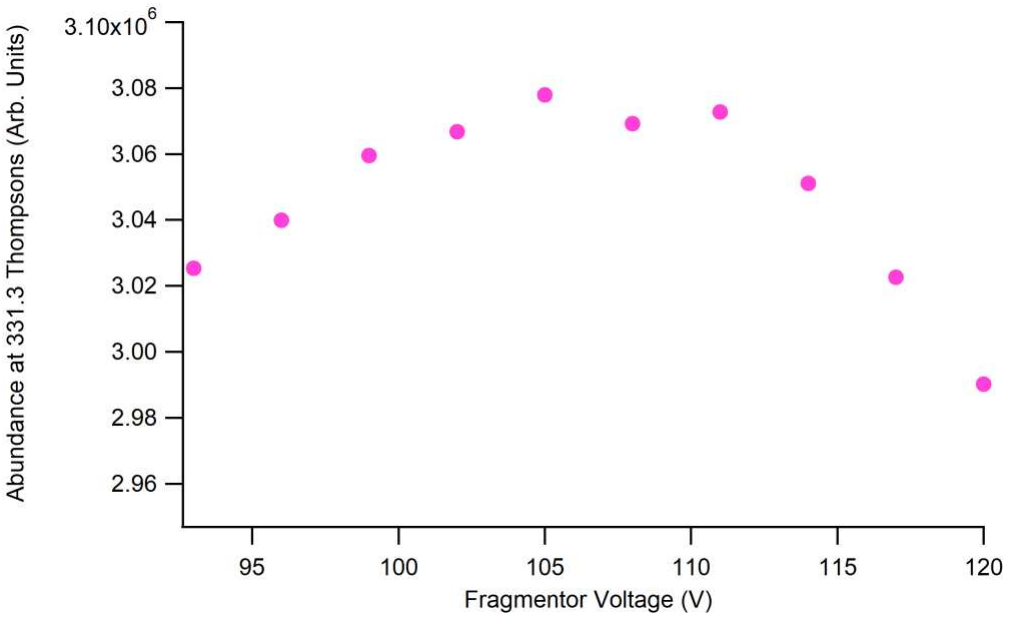

Figure SI39: Narrow range fragmentor voltages tested for 7-OH-CBD

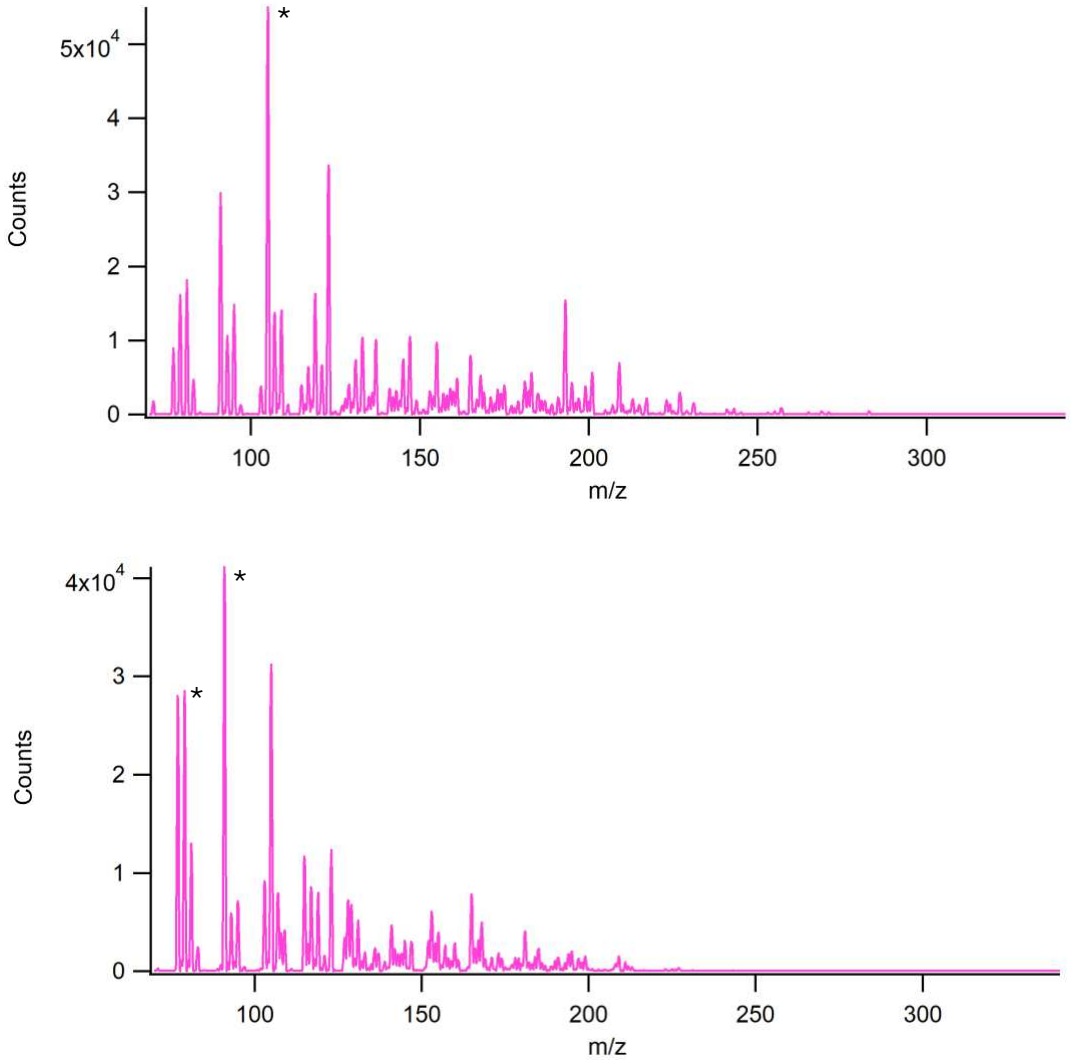

Figure SI40: Scans for 7-OH-CBD Product Ions. Product Ions selected are marked *.

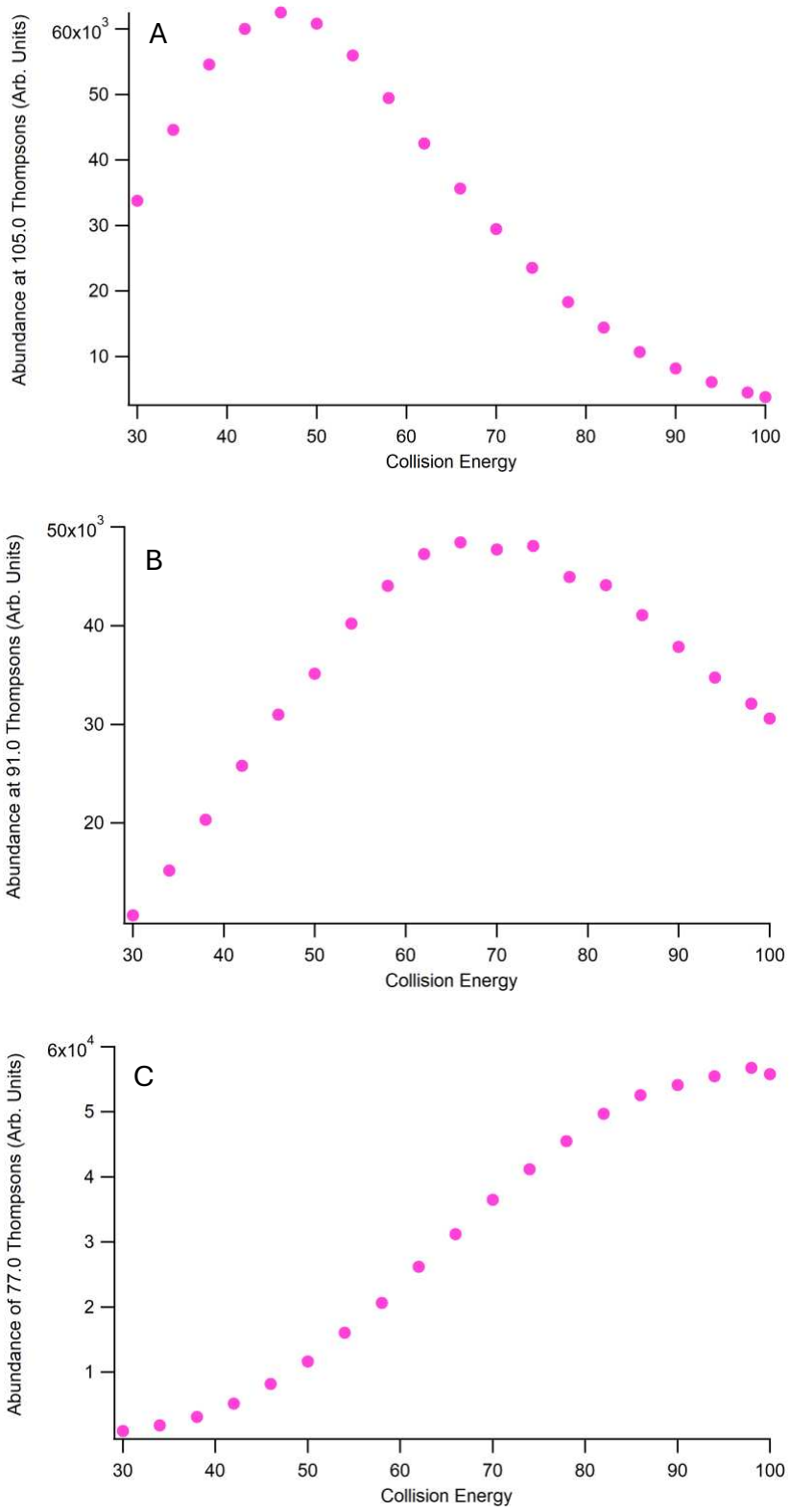

Figure SI41: Collision energy tests for each 7-OH-CBD product ion optimization. A shows the tests for 105.0, B for 91.0, and C for 77.0.

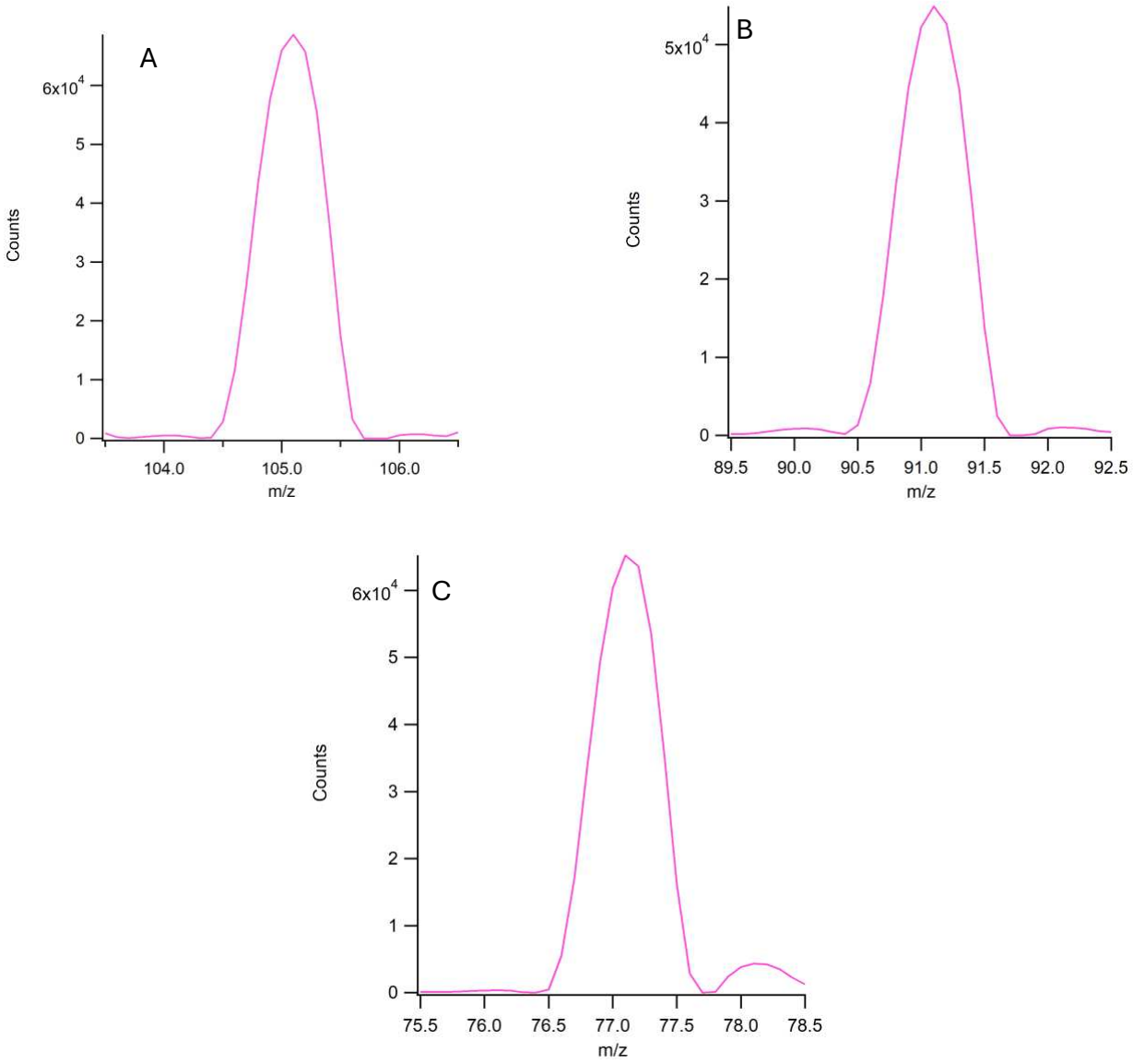

Figure SI42: Narrow Mass Scans for each CBD product ion at their respective collision energies. A shows the scan for 105.0, B for 91.0, and C for 77.0.

Calibration curves were performed for each of the neat standards, and a combination figure for all calibrations is shown in Chapter 4 Figure 6. The four calibration curves used for quantification in the chapter are separated here in Figures SI43-46, to show their individual linear characteristics, lines of best fit, and correlation coefficients.

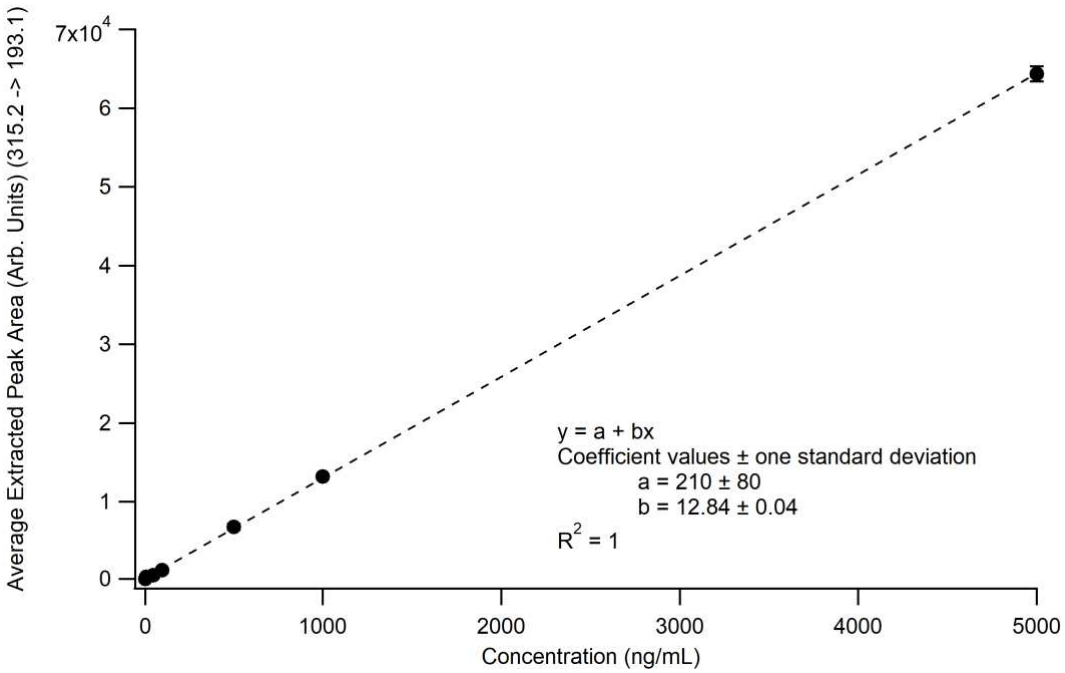

Figure SI43: Calibration curve generated from neat THC standards with n=5 for each level.

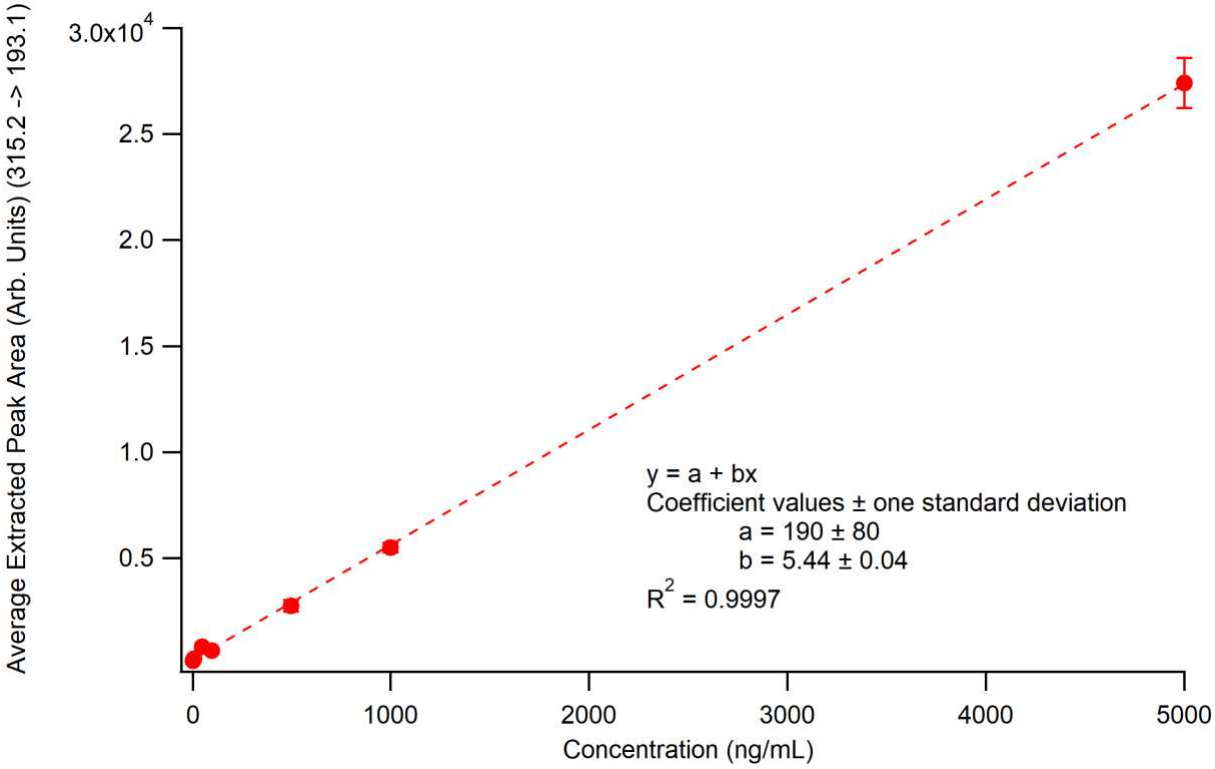

Figure SI44: Calibration curve generated from neat CBD standards with n=5 for each level.

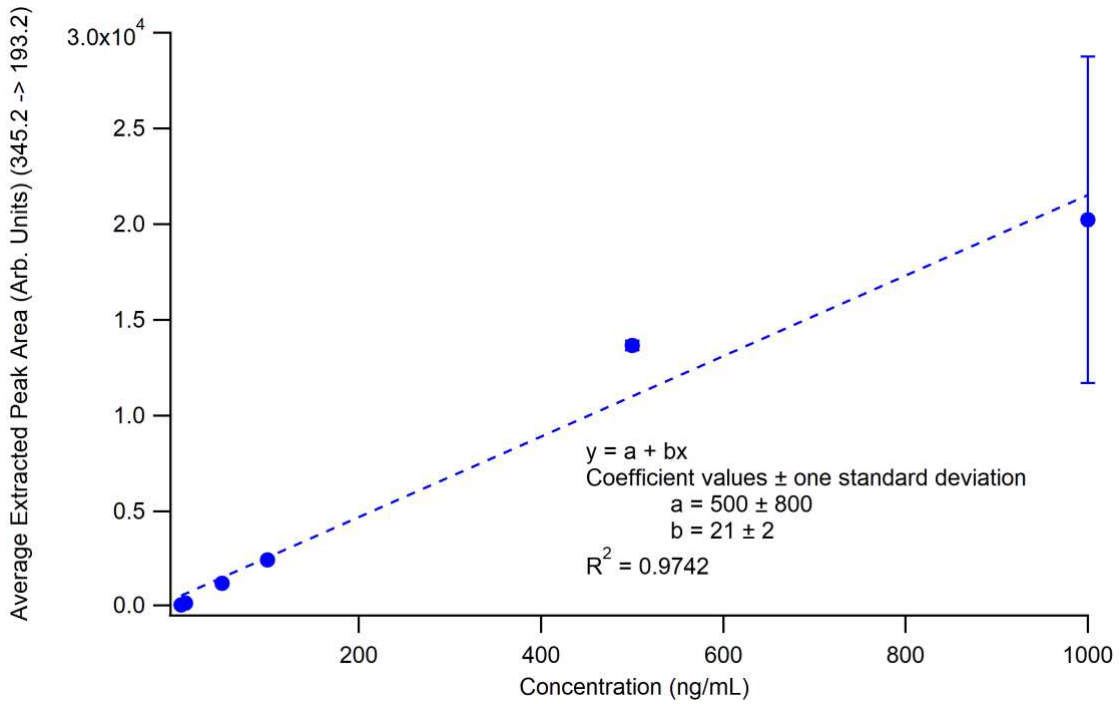

Figure SI45: Calibration curve generated from neat THC-COOH standards with n=5 for each level.

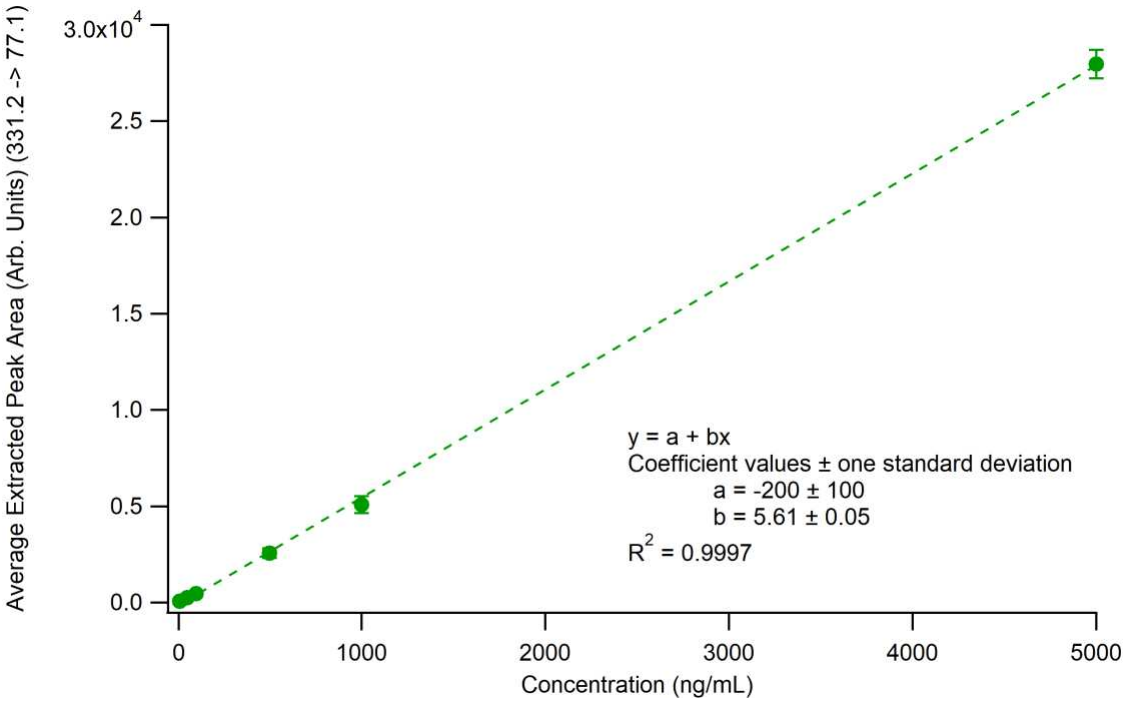

Figure SI46: Calibration curve generated from neat 11-OH-THC standards with n=5 for each level.